Dottorato di Ricerca in Ingegneria dei Prodotti e dei Processi Industriali – 30° Ciclo

UNIVERSITÀ DEGLI STUDI DI NAPOLI FEDERICO II
SCUOLA POLITECNICA E DELLE SCIENZE DI BASE

Ph.D thesis

DEVELOPMENT OF A FUEL FLEXIBLE, HIGH EFFICIENCY COMBUSTION UNIT

by

Pio Bozza

TUTOR
Professor Antonio Cavaliere

COTUTORS
Dr. Mara de Joannon
Dr. Raffaele Ragucci
Dr. Pino Sabia
Dr. Giancarlo Sorrentino

2017

TABLE OF CONTENTS

ABSTRACT

The present work is aimed to develop a fuel flexible small-scale burner (1 - 10 kW) with high performance in terms of energy saving and pollutant reduction.
In this study the design, manufacturing and testing of a lab scale burner operated in highly diluted combustion processes, also known as MILD combustion, have been carried out. Firstly, a cyclonic flow-field configuration was chosen as the most valuable design solution because it allows to operate with very strong internal recirculation levels of the burned gases. This implies modest and uniform (no hot spots) temperatures, thus ensuring a significant reduction of pollutant emissions, while providing for long mixture residence times in small size systems to insure complete conversion. Then, the Laboratory Unit CYclonic flow-field (LUCY) burner has been constructed and tested.
The cyclonic flow has been achieved by two pairs of oxidant/fuel jets that feed the combustion chamber in an anti-symmetric configuration thus realizing a centripetal cyclonic flow field with a top-central gas outlet. Autoignition and stabilization of distributed combustion regimes have been proved to occur when a sufficient entrainment of hot species in the fresh oxidant and fuel jets, by means of an efficient turbulent mixing, is reached. The cyclonic burner has been designed to operate by varying the external operational parameters (inlet temperature of the main flow, equivalence ratio, external dilution of the mixture, residence time, nominal thermal power), which can be varied independently each other allowing to investigate a wide range of operative conditions.
Experimental campaigns has been performed in order to define the operational conditions which the cyclonic burner can stably operate in MILD combustion. In particular, it was possible to identify different working regimes of the system (No Combustion, Low Reactivity and Stable Combustion) and thus the operative conditions corresponding to stable working regime. Moreover, during the experimental campaigns it has been observed a hysteresis behavior of the system that allows to stabilize the process operating two different procedures, thus extending the operative range of the system. Then, a characterization of LUCY burner in terms of pollutants emission have been carried out and the main operational characteristics of the cyclonic combustion burner were investigated.
Temperature measurements inside the chamber and gas sampling analysis were carried out in order to evaluate the operability range of the cyclonic burner and its performance. It has been demonstrated that MILD Combustion can be achieved in a wide range of operating conditions and the lowering of the working temperatures inside the combustion chamber allows to obtain very low NOx and CO emissions in a whole range explored.
Finally, experimental campaigns have been operated in order to verify the performance of LUCY burner and to optimize it in terms of low pollutants emission

in the usual working conditions by varying the nominal thermal power, without external preheating and external dilution. In particular, slightly fuel-lean conditions seem to be the optimal working point in order to minimize CO and NOx, simultaneously. Furthermore, it has been showed that it is possible to achieve a complete fuel conversion and low pollutant emissions for nominal thermal powers up to 10 kW. Such condition ensures very good performance in terms of stable working conditions of the cyclonic burner, thermal efficiency and eco-compatibility. It has been shown that the cyclonic burner is fuel flexible, stable and efficient in a wide range of operative conditions.

INTRODUCTION

The environmental emergency has led to the development of new combustion technologies. The research in this field responds to the necessity of finding heat/electrical energy production systems by means of high efficiency, eco-friendly and flexible processes, by using alternative fuels. These necessities are related to the reduction of non-renewable energy sources (fossil fuels and petroleum), the diffusion of non-conventional fuels and the protection of the environment and human health. Indeed, the "energy and environment" union is one of the main priorities in the development of energy production systems that meet increasingly stringent emission standards for polluting substances such as nitrogen oxides, particulate carbon (fine and ultrafine) and dioxide carbon. Strategies to address these issues include both optimizing existing combustion processes and developing innovative processes that allow a strong pollutant reduction. The implementation of innovative technologies involves the identification of new fields of combustion functionality in terms of characteristic parameters such as pressure, temperature and mixture composition.

In this context, MILD or Flameless combustion offers the prospect of a less polluting and more efficient systems. In the field of innovative technologies currently under development, MILD combustion process is of particular interest. MILD is the acronym of "Moderate or Intense Low Oxygen Dilution", thus suggests the use of external dilution of the mixture with high preheating of the involved gases by means of internal or external recirculation of burned gas. High working temperatures ensure high thermal efficiency with high degree of fuel conversion to final combustion products, resulting in lower emissions of carbon dioxide in the atmosphere and fuel economy. The high degree of dilution of the mixture also implies high thermal capacity and therefore modest increases in temperature.

Therefore working temperatures are lower than the critical temperatures for the formation of pollutants such as nitrogen oxides and soot. On the other hand, the high dilution level of the mixture ensures that it could be out of flammability limits. As a result, the oxidation process can only be sustained if the temperature is higher than the auto-ignition one of the mixture. Therefore, exhaust gas recirculation is necessary in order to dilute and preheat the mixture until the achievement of the self-ignition conditions.

In this way, the result is a clean, stable combustion process, extended to the entire combustion chamber where temperature profiles and chemical species are uniform. Thus, the oxidation is uniform and the combustion process could be defined as "distributed". Furthermore, the process is very flexible with respect to the fuel can be used in the combustion chamber. In fact, high inlet temperatures allows a fast atomization and the vaporization processes of liquid fuels, and promote the volatilization of the volatile compounds in solid fuels. In addition, it is important to note that MILD combustion working conditions are suitable for the oxidation of low-

calorific fuels such as biogas and syngas containing high percentages of inert species. The high level of dilution and preheating also permit to reach a stable and noiseless process.
On the other hand, in the traditional systems periodic or non-stationary dynamic regimes can be the cause of low efficiency, emission of pollutants and also physical damage to the mechanical parts of the combustion units.
Some of the MILD combustion technology applications are systems where uniformity temperatures are required, for example in the metals, steel, glass and ceramics manufacturing and production industries. In addition, the stability of the process makes it very interesting for applications on gas turbines and external combustion engines.
In the industrial field, the systems using this technology work in a small range of operating conditions, due to the MILD combustion process requirements that are very strictly for the actual devices. In fact, the high level of dilution, coupled with strong preheating of the oxidizer flow, ensure that the reactive zone has different characteristics compared to traditional systems, by means of homogeneous, self-igniting structures.
In these working conditions, the kinetics and the characteristic time of the process (self-ignition and oxidation) are different compared to the working conditions of the conventional systems. In fact, high dilution levels, strong preheating and low temperature gradients of the oxidation process have a strong effect on the kinetic of the reaction. In addition, due to the exhaust/burned gas recirculation need to achieve MILD conditions, large amounts of carbon dioxide and steam recirculate the reaction zone, thus changing the oxidation time of the reactants.
As already mentioned, the achievement of the operating conditions that allow the stabilization of the process strongly depends on the recirculation of the gases inside the combustion chamber. Then, a strong turbulence it is necessary to obtain an efficient mixing between the mixture and the burned gases. This involves a strong interaction between kinetics and fluid dynamics, because the lower concentration of reactants means the lower chemical time. Thus, the oxidation time and fluid-dynamics time of the process become comparable. This means that in these conditions it is fundamental taking into account both the kinetic and the velocity of mixing.
The modeling of this kind of combustion technologies is therefore extremely difficult. In fact, models developed for the traditional combustion process applied to diluted and preheated working conditions, do not describe efficiency the oxidation process.
These considerations suggest that the process should be characterized with respect to both oxidation kinetics and turbulence levels, in order to develop valid kinetic and turbulence models. Actually, the scientific literature lacks of experimental data need for the development of kinetics and predictive tools. This because the difficulty of carrying out experimental campaigns on prototype systems due to the extreme working conditions of the MILD process, in particular for the high inlet

temperatures. In this context, it is challenging to adapt the traditional laboratory devices to MILD/Flameless working conditions. For this reason it is necessary to design an appropriate experimental apparatus.
The basic knowledge of the MILD/Flameless technology have been carried out by means of laboratory scale reactors, allowing to study separately several aspects of the combustion process. Hence, considering the wide perspectives of this technology, tools that simulate the behavior on an industrial scale in a simplified way are required.
For this purpose, it is worthwhile the evaluation of the working process parameters and the implementation of diagnostic techniques in the laboratory scale burners. This, in order to make useful the knowledge acquired from studies on elementary reactors and applicable in technologies. The limit of the actual laboratory scale burners is on the operative flexibility. In fact, given the importance to recirculate mass and heat to sustain the MILD combustion process, it is extremely important to varying the operating working parameters (preheating temperature, mix composition, average residence time, fuel type or diluent, etc.) in order to study the single effect on the combustion process.
Thus, the necessity to develop a burner that allow to varying the operating parameters such as the inlet temperature and the composition of the mixture independently of the recirculation, in order to study the influence of operational conditions on the stabilization of the process. This is useful to develop industrial systems based on the working conditions.

For these purposes, this work is aimed to develop a fuel flexible and high efficiency combustion unit working in MILD combustion conditions.

In particular the present work has been focused on:

- The design of a flexible, efficient and low pollutant burner operated in MILD combustion.
- The construction of the burner. It is explained the reason of the constructive choices and the realization of the burner.
- Experimental campaigns performed on the burner in order to evaluate its performance in terms of process stability and pollutant emissions.

In particular, in the present work the cyclonic burner was firstly performed to evaluating the range of operational parameters in which the MILD combustion occurs, by means of varying the main operational parameters such as equivalence ratio, dilution level of the mixture, inlet preheating temperature and average residence time. Then, it has been evaluated the operability range of the cyclonic burner in terms of fuel flexibility for different inlet nominal thermal power.

1. MILD COMBUSTION

1.1 Innovative Combustion Technologies

As well known, combustion of hydrocarbons involves the release of several pollutants into the atmosphere such as carbon dioxide (CO_2), nitrogen oxides (NO_x), carbon monoxide (CO), polycyclic aromatic hydrocarbons (PAH) and soot. As already introduced in the previous chapters, the growing attention to environmental issues focuses the research towards high efficiency and low pollutant emissions energy production systems. In this context, the burner efficiency has been improved by adopting regenerative or recuperative systems that preheat the reactants by means of the heat recovering in the exhaust gas. The temperature increase of the reactants allows to obtaining higher temperature in the combustion chamber, thus a better thermal exchange with an efficiency improvement [Weinberg, 1971]. In particular, regenerative systems recover the enthalpy of burned gases more efficiently than the recuperative systems, allowing to obtain preheating temperatures higher than 1500 K [Sato, 1997]. However, the higher temperatures in the combustion chamber are the higher production of pollutants is, such as the NO_x. Thus, if the preheating of the air improves the heat exchange, on the other hand it raise the maximum temperatures, increasing the nitrogen oxides thermal production [Flamme et al., 1991]. New combustion technologies have been developed to match the goals of improving the global efficiency and lowering the pollutant emission.
In the past years, German and Japanese researchers [Tsuji et al., 2003] unexpectedly measured low NO_x concentrations in a regenerative furnace. These concentrations further diminished when the air flow injected into the furnace increased. In particular, preheating the air up to about 1600 K and injecting it approximately 90 m/s, NO_x concentrations measured were extremely low ($\leq$ 80 ppm). Moreover, any flame was observed and the authors confirmed that under such operating conditions, the oxidation process occurred throughout the combustion volume. Then, many researchers focused their interest on operating systems with high reagent temperatures; In particular, attention has been focused on systems based on the pre-heating of air [Bolz et al., 1998; Katsuki et al., 1998; Yoshikawa, 2000]. In fact, the most widely used acronym, which is found in various works available in literature [Katsuki et al., 1998; Gupta, 2000], refers precisely to the air. This is the "High Temperature Air Combustion" (HiTAC) and refers to a strict definition first reported by Katsuki and Hasegawa [Katsuki et al., 1998], born of the concept of "excessive enthalpy" introduced by Weinberg [Hardesty, 1973; Weinberg, 1986]. In this process, the preheated air reaches very high values of temperature so that the inlet temperature is higher than the self-ignition temperature of the mixture. On the other hand, "High temperature COmbustion Technologies" (HiCOTs) refer broadly to all technologies that exploit the high temperature of reactants, so they do not limit the

use of air alone. In the last few years, other definitions have been given for such or similar technologies.
This thesis work is mainly focused on the technology known in the literature as "MILD Combustion" [Cavaliere et al., 2004].

1.2 MILD combustion process

In order to define the MILD combustion and the conditions under which this process evolves, differently from that of the standard combustion process, it is taken as example a Well Stirred Reactor (WSR) in which a stoichiometric mixture $CH_4\backslash O_2\backslash N_2$ react in a residence time of 1 s. In Figure 1.1 [Cavaliere et al., 2004], the operating temperatures (TWSR) are calculated in adiabatic conditions for three values of the oxygen molar fraction (XO_2) according to the inlet temperature (T_{in}). The calculation results for XO_2 = 0.2, represented by the dotted line, show the typical working temperature trend as function of the inlet temperature of the mixture.

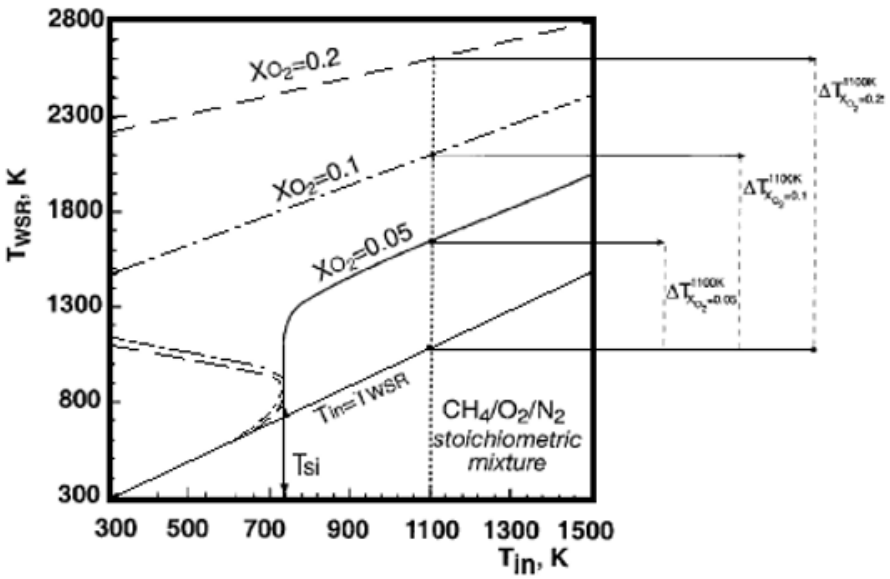

Figure 1.1 Working temperature in a WSR as function of the inlet temperature for a stoichiometric mixture of $CH_4/O_2/N_2$

In a WSR, the self-ignition temperature (T_{si}) is the inlet temperature for which, for any differential temperature increase, the system reaches the high branch of the S-curve and the oxidation process occurs. Thus, for $T_{in} \geq T_{si}$ the mixture ignites and burns and the system temperature increases. The maximum increment of the temperature (ΔT) is the difference between the maximum temperature inside the reactor and the temperature of inlet reactants. In this case, for T_{in} = 1100 K, the

resulting ΔT is about 1600 K and most of the mixture reacts in the residence time considered. By increasing the dilution level, at constant CH_4/O_2 ratio, the maximum temperature increment during the oxidation process is lower. For example, for $XO_2 = 0.1$ and $T_{in} = 1100$ K, the ΔT is about 1000 K and becomes 550 K for $XO_2 = 0.05$. The latter condition is an example of "MILD Combustion" conditions, because the temperature increment is very low, compared with that of conventional combustion processes.
A definition of MILD Combustion was given by A. Cavaliere and M. de Joannon [Cavaliere et al., 2004] as: "A combustion process is named MILD when the inlet temperature of the reactant mixture is higher than mixture self-ignition temperature whereas the maximum allowable temperature increase with respect to inlet temperature during combustion is lower than mixture self-ignition temperature (in Kelvin)".
The definition of MILD combustion is given for mainly two reasons:

- it is characterized by smooth changes of the temperature, unlike all other combustion processes that evolves in a much wider temperature range and where any temperature-dependent process can pass chaotically through different regimes;
- MILD stands for "Moderate or Intense Low-oxygen Dilution," which is one of the typical conditions that allows to reach such process.

Figure 1.2 well explains when MILD combustion conditions occurs. It shows the ΔT as function of ΔT_{in}, which is the difference between Tin and the minimum self-ignition temperature. It is remarkable that the minimum self-ignition temperature is not dependent from the dilution of the mixture [Zabetakis, 1965]. In fact, the self-ignition temperature of the reagent mixture depends on the inlet flow composition, the pressure and the residence time.
Moreover, Figure 1.2 shows even processes with a negative maximum temperature increase, the pyrolysis processes, and two categories are identified: "auto-incepted pyrolysis" and "assisted pyrolysis". The first process is located in the lower-right quadrant, where $\Delta T_{inlet} > 0$ and therefore no external source for sustenance is required. The second process is located in the lower left quadrant, where $\Delta T_{inlet} < 0$ is defined as "assisted pyrolysis" because it needs an external heating or a catalytic device to be sustained. The upper-left quadrant, on the other hand, identifies the "assisted ignited combustion region", where $\Delta T > 0$ and $\Delta T_{inlet} < 0$. This represents the standard combustion condition, where an external source ignites the mixture.

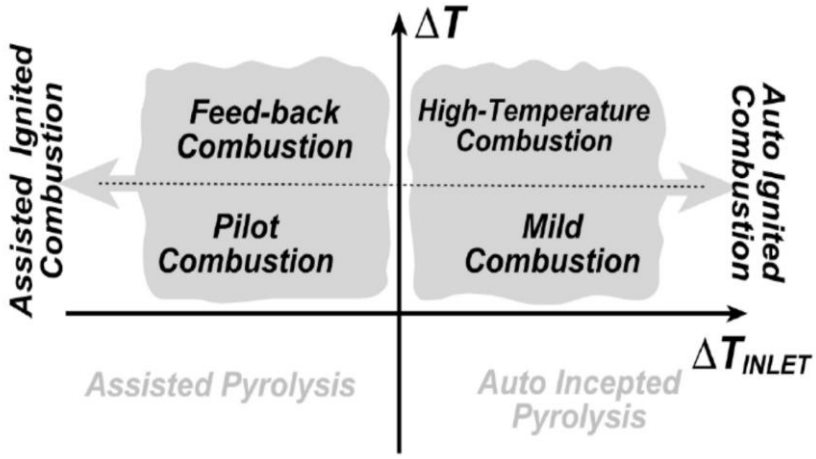

Figure 1.2 Combustion Regimes as function of ΔT and ΔT_{inlet}

It is well known in the literature [Zabetakis, 1965] that, under such conditions, the propagation of a deflagrative structure is allowed if the temperature is high enough ($\Delta T > T_{si}$) to provide a radicals feedback. Thus, the mixture can reach the ignition temperature and then self-ignite. This process can only occur if the mixture composition is internal to the flammability limits. Furthermore, two regions can be identified in the assisted ignited combustion area of the Figure 1.2: the feedback combustion and the pilot combustion.

In fact, for $T_{in} < T_{si}$ and XO_2 outside the flammability limits, as mentioned above, the deflagrative process can not be sustained and no combustion occurs without an external permanent source. On the other hand, spontaneous ignition occurs in the processes classified as "auto-ignited combustion". Even in this case, symmetrically, two regions can be identified. The first, known as high-temperature combustion, represents the region where the temperature increases according to the air/fuel ratio values. The second, in the region $\Delta T < T_{si}$ MILD combustion occurs as the definition given above. It differs from other combustion regimes because, under MILD combustion conditions, the process can not be self-sustained without the pre-heating of reactants.

It is worth pointing out that the Figure 1.2 is a qualitative map. In fact, as already mentioned, the self-ignition temperature of a fuel/air/diluent mixture depends on parameters such as mixture composition, pressure, residence time.

Moreover, Figure 1.2 has the purpose to show the MILD Combustion occurring range and, together with Figure 1.1, to clarify the basic concept of this combustion process.

Another key factor defining the MILD combustion process is the configuration of the system. For example, the maximum temperature reached in a non-premixed system corresponds to the adiabatic flame temperature associated with the

stoichiometric condition, which may also occur if the mixtures differs from stoichiometric.
On the other hand, the maximum temperature reached by a premixed inlet flow is fixed by the stoichiometry and by the dilution level [Cavaliere et al., 2004]. It should be noted that the maximum temperature depends on the highest level of oxidation and can be different from both the equilibrium temperature and that actually reached the reactor.
For instance, a methane/oxygen/nitrogen mixture that reacts in rich and diluted conditions can reach different temperatures depending on the different kinetic pathways followed in the chemical process. To support this claim, Figure 1.3 [de Joannon, 2000] shows the ΔT calculated in a WSR as function of T_{in} for a methane/oxygen/nitrogen mixture with carbon/oxygen ratio equal to 1, a dilution level of 85 % and a residence time of 1 s (continuous line). Dotted and dashed lines represent respectively the temperature increments at the equilibrium (ΔT_{eq}) and the theoretical adiabatic flame temperature (ΔT_{af}) of the system. In this case, ΔT_{af} is always higher than ΔT because, in diluted and rich conditions, the main oxidation product is the CO.
The trend of the continuous line is explained due to the different distributions of the products that are obtained by varying the inlet temperature. The arrows in Figure 1.3 mark the different output compositions of the different oxidation paths.

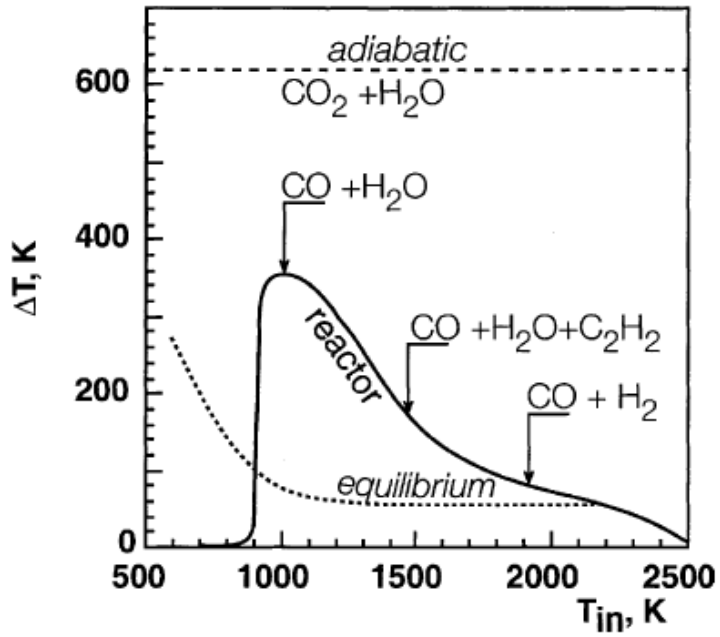

Figure 1.3 Temperature increment (ΔT) in a WSR as function of the inlet temperature in the working conditions, equilibrium and flame adiabatic for a methane/oxygen/nitrogen.

The previous classification places MILD combustion in an atypical temperature range with respect to the other combustion processes.
The high preheating temperatures of the mixture, which can be obtained by means of a burned gas recirculation, permits the lowering of the local oxygen concentration and simultaneously increases the temperature of the reagents. This, due to the lower reactions rate, leads to a distributed and homogeneous reactive zone, which means uniform concentrations and uniform temperature profiles in the combustion chamber, resulting in a higher efficiency of the oxidation process.
In addition, inlet temperatures higher than the self-ignition temperature allow the use of low calorific fuel such as biofuels, characterized by large quantities of inert species, and therefore suitable to perform MILD conditions. This means very high fuel flexibility.
Moreover, the high percentage of inert gases, which leads the mixture outside the flammability limits, increases the thermal capacity of the system, contains the maximum temperature and so the emission of pollutants such as NO_x and soot.
Figures 1.4, Figure 1.5, Figure 1.6 and Figure 1.7 provide the soot yield according to the temperatures, obtained from experiments performed in a shock tube under pyrolytic and oxidative conditions for several mixtures [Agafonov, 2011].

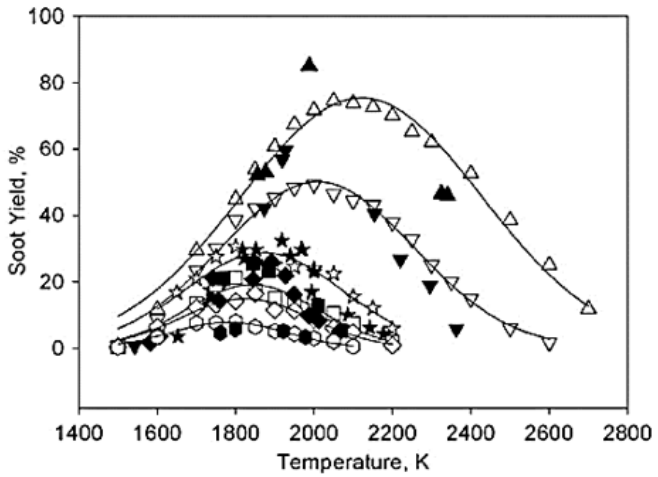

Figure 1.4 Numerical (continuous) and experimental (symbols) Soot Yield for toluene/Ar.

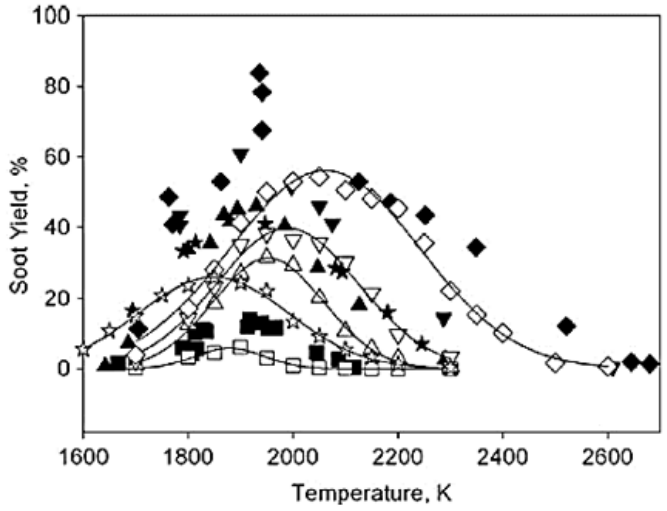

Figure 1.5 Numerical (continuous) and experimental (symbols) Soot Yield for benzene/Ar.

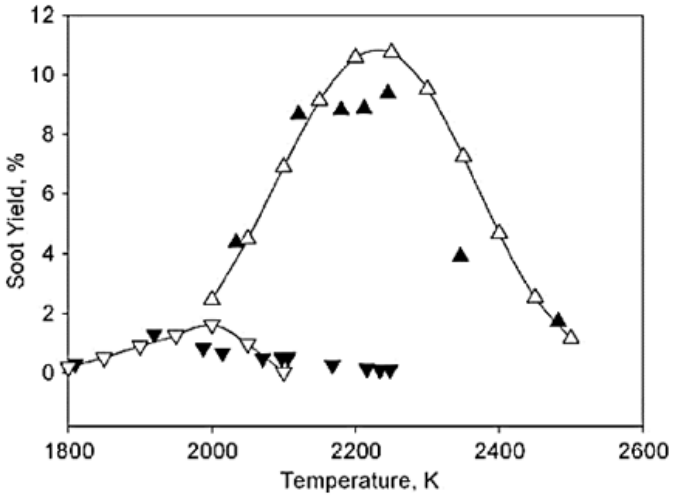

Figure 1.6 Numerical (continuous) and experimental (symbols) Soot Yield for methane/Ar.

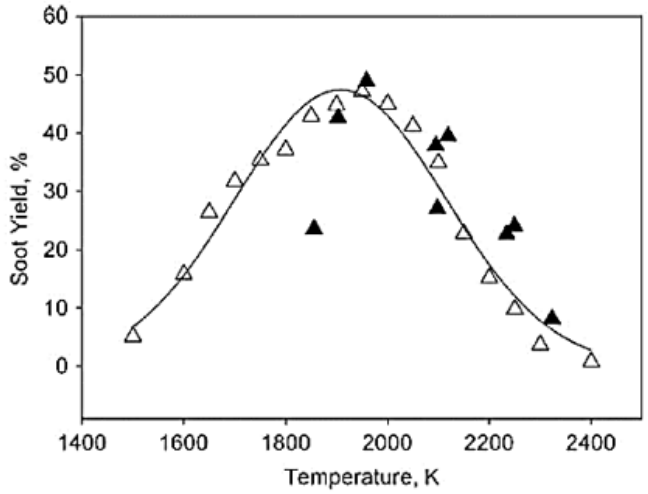

Figure 1.7 Numerical (continuous) and experimental (symbols) Soot Yield for ethylbenzene/Ar.

In that work several aromatic hydrocarbons (benzene, toluene, ethylbenzene) and aliphatics (methane, propane, propylene) have been studied. The results identify a temperature range in which soot production becomes relevant independently on the fuel. In particular, it has been observed the maximum soot production at 2100 K with toluene as fuel, while the lowest yield is obtained for temperatures lower than 1800 K or higher than 2400 K. The same trend can be observed for the other fuels. The results show that under MILD conditions the soot yield is reduced, due to the lower temperatures that inhibit the formation of soot.
The dilution level of the system can be increased by mixing inert species such as nitrogen, or by recirculating exhaust gases, which have a high water vapor content and carbon dioxide. The latter solution allows to preheat the reactants at temperatures higher than required to support the oxidation process, thus it is an interesting solution. In addition, CO_2 and H_2O recirculation can have benefits on the reaction kinetics. For example, when CO_2 concentration increase the equilibrium shift to the reactants [Zhang et al., 2007]:

$$CO + OH \leftrightarrow CO_2 + H \qquad (1)$$

There are two positive effect on soot formation. First, the reduction of radicals H reduces soot formation due to the key role of these radicals in the nucleation and particulate growth. Moreover, according to reaction 1, the reduction of hydrogen radical concentration leads to an increase in the concentration of the hydroxyl radicals, which are the major species responsible for the oxidation of soot in the flame.

Such effects are present when referring to water vapor as a diluent. In this case, the reduction of radicals H and the increase of OH radicals occurs due to the shifting of the following equilibrium to the products:

$H_2O + H \leftrightarrow OH + H_2$ (2)

The presence of H_2O can also limits the surface growth mechanism by disabling radical sites on the particles surface [Zhang et al., 2007]. Figure 1.8 shows the NO_x emission as function of the inlet temperature in a gas turbine. It is possible to evaluate strong effect of the temperature on the NO formation for T > 1000 K, while for T < 1000 K, NO_2 emission is higher and almost constant.

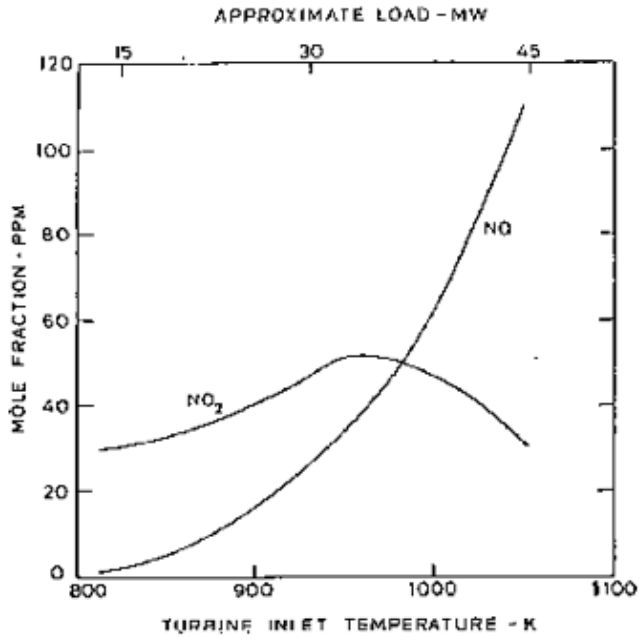

Figure 1.8 NO and NO_2 molar fraction as function of the inlet temperature in a gas turbine combustor

Nitrogen Oxides production can be evaluated through three kinetic mechanisms, among which the most important is Zeldovich's mechanism:

$O + N_2 \leftrightarrow NO + N$ (3)
$N + O_2 \leftrightarrow NO + O$ (4)
$N + OH \leftrightarrow NO + H$ (5)

These are the so-called “thermal NO_x”, because the reaction (3) has a very high activation energy (75250 cal/mol). Therefore, this reaction is fast enough only at

high temperatures and represents the limiting stage of the process, so that the stationary state hypothesis can be applied to radical N. By matching the result with the NO balance, the following equation is obtained:

$$\frac{D\,NO}{dt} = 2K_1[O][N_2] \qquad (6)$$

Equation (6) is the production of NO, where K_1 is the kinetic constant of the first reaction. According to (6), decreasing the temperature and the concentration of the O radicals, NO production decreases. The high dilution of in the combustion chamber, as well as lower the concentration of O radicals, results in an increased thermal capacity of the mixture and, consequently, lower temperature thus limiting the NO. Figure 1.9 shows the effect of the mixture composition and the dilution level on the NO_x emission in a premixed flame. According to the Zeldovich mechanism, NO concentration reach the maximum value at stoichiometric conditions (R = 1), coherently with the maximum temperature. Moreover, the increasing of the dilution level reduces NO_x emissions.

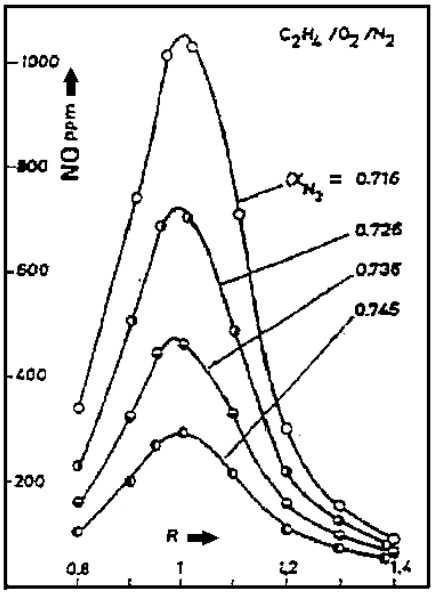

Figure 1.9 NO concentration in a premixed flame as function of the stoichiometry of the mixture for different dilution levels

As results, both the low temperatures and the low oxygen concentration have a positive effect on soot and NO_x emissions, so it can be stated that the MILD combustion is a "clean" process and therefore eco-friendly.
Another topical aspect of MILD combustion is the absence of a flame front. In the conventional burners, the combustion process evolves in a stationary flame front, a

surface stretched by turbulence where the typical reactions occur. Although the thickness of the flame front is very thin, the gradients of the temperature and concentration are very high. The position of the flame front and its stability in the combustion chamber depend even on fluid dynamics, thus a proper design of the combustion chamber is required. In MILD combustion processes, the reaction does not develop on a flame front, but in the whole volume of the combustion chamber, thus avoiding flame instabilities.

1.2 Burned gas recirculation

The burned gas recirculation, as already mentioned, is a strategical way to increase the dilution level and preheating of the reactants. Wünning J.A. and Wünning J.G. [Wünning et al., 1997] defined an internal recirculation rate, K_v, as the ratio between the mass flow of the recirculated gases (M_E) and the mass flow of the inlet mixture ($M_F + M_A$), that is:

$$K_v = \frac{M_E}{M_F + M_A} = \frac{M_J - M_F - M_A}{M_F + M_A}$$

Where $M_E = M_J - M_F - M_A$ and M_J is the total mass flow rate.
K_v is a crucial parameter to evaluate the influence of gas recirculation in MILD combustion. Figure 1.10 shows the axial and radial diffusion of the combustion-air jet in the burned gas of the combustion chamber. Reactants are gradually diluted by the burned gas (CO_2 and H_2O) and inert gas (N_2).

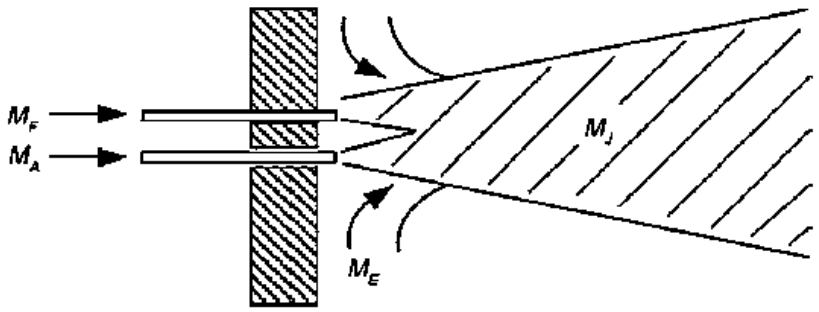

Figure 1.10 Stability of the MILD combustion of non-premixed methane/air mixture

Furthermore, Figure 1.11 shows the relationship between the K_v and the working temperatures and identify the areas in which MILD combustion occurs [Wünning et al., 1997].

Other works in literature have been focused on testing several fuels, including natural gas [Cavigiolo et al., 2003], Biogas [Derudi et al., 2007, a; Effuggi et al., 2008], hydrogen [Derudi et al., 2007; Wu et al., 2007; Wu et al., 2007], Biomass [Dally et al., 2002], diesel and coal [Zhang et al., 2007; Wu et al. Et al., 2007; Parelli et al., 2008; Galletti et al., 2009; Dally et al., 2002; Weber et al., 2005; Derudi et al. 2007, b; Stadler et al., 2009; Yu et al., 2010].
It has been found that the critical values of K_v and temperature could differ each other because of the differences between the heat values of the fuels. This distance has been found even when the oxy-combustion conditions occur, in which K_v required is much higher [Krishnamurthy et al., 2009].

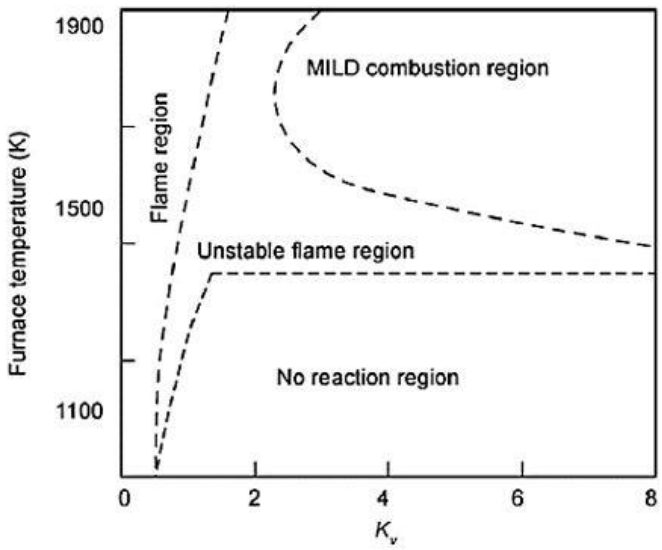

Figure 1.11 Combustion regimes as function of K_v and working temperatures for a methane/air mixture

In these studies, the influence of such parameter on the NO_x and CO emission was also evaluated. The lowering of reaction rates under MILD combustion can explain the low NO_x emissions, in addition to the decreasing of the 70% of thermal NO.
This suggests that MILD combustion is very flexible related to the type of gaseous, liquid, or solid fuel used. Even though the high dilution of mixtures in MILD combustion, the mass fraction of OH radicals in the reactive zone for MILD combustion is smaller and uniformly distributed than in the conventional case [Dally et al., 2002; Medwell et al., 2007].
Moreover, the homogeneity of the combustion zone, in addition to the advantages mentioned above, saves computational time for engineering applications, as described by Galletti et al. [Galletti et al., 2009], which found that differences between CFD simulations of MILD 3-D and 2-D combustion are negligible.

1.3 Light emission and radiative heat flux

Another aspect properly of MILD combustors is the light emission compared to traditional combustion processes. When the MILD combustion occurs, the whole oven becomes bright and any flame is visible [Tsuji et al., 2003; Katsuki et al., 1998; Cavaliere et al., 2004; Wünning et al ., 1997]. Thus, this process is often called Flameless Combustion or Flameless Oxidation (FLOX) [Wünning et al., 1997].
Figure 1.12 gives an example of a combustor performed in MILD combustion. The picture on the left represents a 40 MW natural gas burner under standard combustion conditions [Saponaro, 2009], where the fuel is fed by a central nozzle. In this case, it is possible to clearly observe the flame front and the light emission.

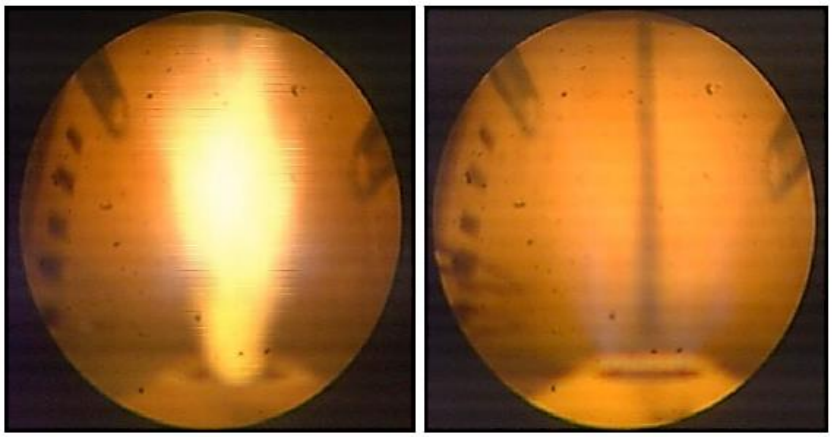

Figure 1.12 Pictures of the combustion chamber in presence of natural gas flame (left) and flameless oxidation (right)

On the other hand, the right picture in Figure 1.12 represent the same combustor performed in a MILD combustion condition. In this case, natural gas was injected in the chamber allowing the recirculation of the burned gas.
It is remarkable the light emission occurs by means of the walls radiative emission. Based on these observations it can be stated that MILD combustion can be defined as distributed combustion instead of a flame front combustion [Milani et al., 2001] and the system works almost in perfectly mixed conditions [Orsino et al. 2001]. The presence of radiating species such as H_2O and CO_2 lowers the thermal gradient and the maximum temperature.
Figure 1.13 shows the temperatures and the radiative flux profiles in an oven performed under MILD conditions. It is highlighted the homogeneity of the working temperature (1500 K) and the high radiative heat flux (300 - 350 kW/m2) due to the high CO_2 and H_2O concentration, which emits infrared radiation [Orsino et al.,

2001]. In this case, due to the homogenous distribution of the species inside the combustion chamber, the whole environment becomes more radiant than a traditional oven, thus improving the heat exchange.

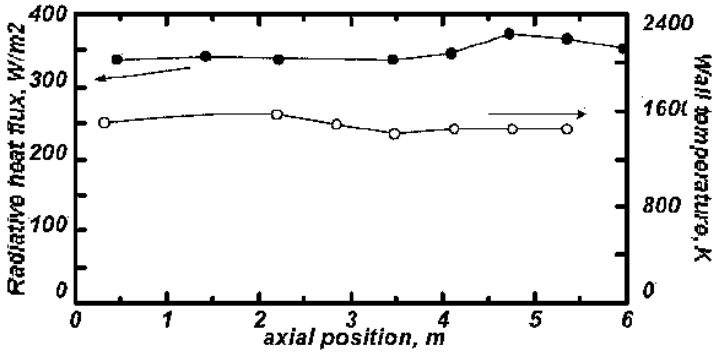

Figure 1.13 Radiative heat flux and Temperature profiles in a combustor performed in MILD combustion

Some applications on steel treatment prove the advantages on performing the devices under MILD combustion conditions [Yasuda, 1999; Masunaga, 2001].
Since the absence of a visible flame, some experiments have been conducted in order to characterize the MILD combustion process through optical analysis. For example, Gupta [Gupta, 2000] studied the light emission produced by flames obtained from various pre-heated fuels up to 900-1100 ° C and the O_2 fraction ranging from 5% to 21%. As results, the author shows that different colors of the flame depend on the dilution level of the mixture: from yellow, blue and green until any visible flame has been observed. Yasuda [Yasuda, 1999], on the other hand, observed an emission in the green spectrum for propane flames.
Furthermore, similar behavior have been reported by de Joannon [de Joannon, 2000] for the auto-ignition of tetradecane in diluted conditions, high temperature and high pressure, and Gaydon [Gaydon et al., 1955] for the auto-ignition of methane.
The shape and the color of flames depend on several parameters such as preheating temperature, oxygen concentration, fuel and diluent. In particular, for higher preheating temperature and lower oxygen concentration, the volume of reaction increases, while the radiative emission of the flame decreases.
Moreover, Shimo [Shimo, 2000] has shown that kerosene, for high preheating temperatures and low oxygen concentration (5%), emits a green flame if diluted in N_2, blue-orange if diluted in Ar and a different color diluted in CO_2. This difference is probably ascribable to the thermal capacities of the diluents and the different interaction they may have with the oxidation process.

It is known that, in the case of propane combustion, the the CO_2 as a diluent, which can thermally be converted at high temperatures, can allow the formation of CO and O_2 radicals involved in the oxidation, for example, of acetylene.
Similar considerations can be pointed out when considering H_2O as a diluent [Knight, 2000].

1.4 Microscopic and modelling aspects

Although MILD combustion systems have been successfully introduced in some industries, the diffusion in a large scale is still limited. A great amount of works on basic knowledge of MILD combustion process is available in the literature, which has been obtained through studies conducted on elementary reactors. In fact, the approach on studying model reactors can highlights particular features of the combustion process. Therefore, new studies are necessary to characterize MILD combustion in complex systems to allow a microscopic analysis of the process. In the recent years, the research has been focused on the modeling aspect of MILD combustion. In particular, low reactants concentration increases the chemical times while gas recirculation, which is fundamental for stabilizing the process as already discussed, reduces the fluid dynamics characteristic times. Thus, the chemical and turbulent time scales become comparable, according to the Damköhler number:

$$Da = \frac{\tau_t}{\tau_c}$$

Where τ_t corresponds to the turbulent time scale and τ_c corresponds to the chemical time scale.
Thus, the interaction between fluid dynamics and kinetics becomes extremely relevant. In particular, for Damköhler numbers close to Da = 1 [Parente et al., 2008] the mutual interaction among fluid dynamics (mixing) and chemistry must be considered with appropriate turbulent combustion models. This was studied by Parente [Parente et al., 2011], which analyzed MILD combustion data [Dally et al., 2002] using Principal Component Analysis (PCA). Results showed that the standard flamelet approach is not suitable for MILD combustion. Recently, successful predictions of MILD combustion conditions have been reported in the literature [Parente et al., 2008; Galletti et al., 2009; Parente et al., 2011, b; Parente et al., 2012] adopting the Reynolds-Average Navier-Stokes model (RANS) and the Eddy Dissipation Concept (EDC) [Magnussen et al., 1981].
However, numerical MILD combustion modeling for large-scale flows requires models that can predict complex auto-ignition.
In laboratory scale MILD burners, such as the JHC flames (Dally et al., 2002) or the cyclonic combustor here presented, auto-ignition typically occurs at very low mixture fractions due to the high dilution level of the oxidant current. Specifically, a

number of experimental analyzes have been carried out in order to study the flame JHC as a modeling system for MILD combustion [Dally et al., 2002; Oldenhof et al., 2010].
As results, a turbulent flame has been observed due the auto-ignition of the mixture in the hot-burned gases. In these experiments, the fuel was a CH_4/H_2 mixture, with H_2 varied from 0% to 25% by volume, and OH measurements highlighted that small amounts of hydrogen help the stabilization mechanism. In this case, the prediction of auto-ignition conditions strongly depends on the molecular diffusion model.
Moreover, a study on very low mixture fraction by means of Direct Numerical Simulations (DNS) of the CH_4/H_2 auto-igniting mixing layers with detailed chemical and transport models has been performed [Van Oijen, 2013].
It has been shown that auto-ignition occurs for very small mixture fractions (<0.02) near the oxidizer zone, due to the high dilution of the oxidant. It has been observed that, in this case, molecular diffusion becomes as important as the turbulent mixing in the auto-ignition, and the hydrogen supports the molecular diffusion due to its high diffusivity. Therefore, numerical MILD combustion models requires reduced mechanisms for turbulence and chemistry.
Successful models are mainly based on flamelet [Peters, 1984], such as FGM (Flamelet Generated Manifold) [Van Oijen et al., 2000], [De Swart et al., 2010], FPV (Flamhete Progress Variable) [Ihme et al. 2013] and REDIM (Reaction-Diffusion Manifolds) [Bykov et al., 2007]. Another issue regarding the numerical modeling of MILD combustion is the auto-ignition stabilization.
Although many studies have been focused on Reynolds-Averaged Navier-Stokes (RANS) simulations [Coelho et al., 2001; Christo et al., 2002], Large Eddy Simulation (LES) can be a useful tool to predict auto-ignition.. LES simulations based on PDFs and reduced chemistry [Pope, 1985; Hawarth, 2010] or based on flamelet [Peters, 1984], FGM [Van Oijen et al., 2000], FPV And FPI (Flame prolongation of ILDM) [Gicquel et al., 2000] have been performed.

1.5 Technological aspects

As already discussed, a combustion process has to satisfy several requirements in terms of pollutants emissions, energy efficiency and fuel flexibility. These constraints, imposed by the attention to the environmental safety, give the opportunity to define new technological solutions that support an eco-sustainable development by means of the efficiency improvement in power generation plants. In this context, the research is focused on fuel-flexible devices, which work with high or low-calorific fuels, biomasses or wastes (direct use or as gaseous or liquid biofuels).
Many aspects have to be taken into account. For instance, it is easier to use this kind of fuels in micro/small-scale energy production plants, due to the relative low availability, than in larger plants. On the other side, the main targets that guide the

development of energy production devices are the efficiency and the environmental impact. For this purpose, low-calorific fuels plays an important role in the development of new gas turbine technologies [el Hossaini, 2013; Ahmed et al., 2013; Pilavachi, 2002]. Even though natural gas is largely used for gas turbines, syngas produced by gasification plants (IGCCs) and low-calorific fuel can also be used in gas turbine combustors [Jones et al., 2011]. In this context, MILD combustion technology, by means of a strong exhaust gas recirculation and high dilution levels, is one of the most efficient way for using low calorific fuel [Kwiatkowski et al., 2016].

In particular, recirculation of exhaust gases in fresh reagents has two purposes:

- Increasing the reactants temperature (heat recovery)
- Reducing the local oxygen concentration (dilution)

As already discussed, the development of low-emission MILD/FLOX combustors is suitable for applications especially aimed at materials processing furnaces even though low power density available [Hasan, 2013]. Such plants can keep CO emissions lower than 10 ppm and NO_x less than 100 ppm. The process stability in these devices is reached by a first start-up phase, in which a conventional diffusion flame warm up the system until the achievement of MILD conditions by means of the mass/heat recirculation. In particular, a proper design of the combustion chamber is required allowing the exhausted gases recirculation by means of the "reverse flow" technique [Rafidi et al., 2006].
Over than furnaces, MILD combustion is also a suitable technology for Combined Heat and Power (CHP) systems [de Azavedo et al., 2015; Parente et al., 2012; Hosseini et al., 2015; Bianchi et al., 2012; Hosseini et al., 2014]. In this case, several requirements have to be taken into account such as compact size, high power density, high flexibility, and high process stability.
On the other side, one of the main constraints on the internal recirculation systems development is the high heat loss related to the small volume-surface ratio. This implies the difficult stabilization of the MILD combustion process due to the wall quenching effects in small-scale systems. In addition, for such devices, it is hard to obtain a complete oxidation due to the short residence times [Khalil et al., 2015].
The advantage of a CHP energy production system is the higher fuel saving compared to separate production, as summarized in Figure 1.14.

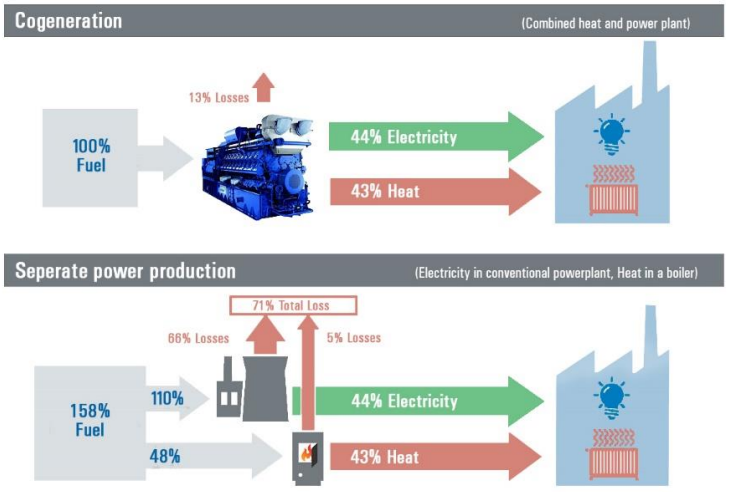

Figure 1.14 Fuel saving comparison between in CHP systems and separate power production

Generally, electrical energy is obtained by operating a thermodynamic cycle in thermoelectric power plants, thus there is part of heat, derived from the fuel, loss into the environment. On the other hand, the demand for thermal energy is provided by using boilers at low temperatures. Thus, the electrical energy demand and thermal energy demand can be met by operating a thermodynamic cycle for the production of both electricity and heat in the same thermodynamic cycle. Combined production of electricity and heat can be applied both in the industrial field and in the civil field. From this point of view, cogeneration is a valuable strategy, especially from biomasses [Maraver et al., 2013], to achieve the goal of a significant energy savings [Rosato et al. 2013].

2. HIGH EFFICIENCY BURNERS

The development of high-efficiency systems operating with low pollutants emissions respond to environmental policies and better management of energy resources. In particular, systems that allow the exhaust gas recirculation inside the combustion chamber are particularly promising. In fact, due to the internal recirculation of mass and enthalpy, the thermal capacity of the mixture increases and it is possible to lowering the operating temperatures of the system in order to contain NO_x emissions [Wünning et al., 1997; Plessing et, al., 1998; de Joannon et al., 1999; Ozdemir et al., 2001; Coelho et al., 2001; Bolz et al., 1999]. This strategy is one of the basic aspects for energy production processes, such as MILD combustion processes, oxy-fire and EGR engines.
Furthermore, MILD combustion processes allow to achieve a stable oxidation process even outside the flammability limits of the mixture, by means of high levels of recirculation of exhaust gases [Cavaliere et al., 2004]. As already mentioned, these working conditions result in operating temperatures lower than the critical temperatures for the production of thermal NO_x [Turns et al., 1995; Bowman et al., 1992].
The development of burners operated in MILD combustion involves several consideration about the design and the size of the combustion chambers [Li et al., 2011; Kumar et al., 2005]. In fact, the high dilution levels and low operating temperatures result in relatively slow oxidation kinetics compared to systems with premixed or diffusion flame. As a result, the kinetic oxidation times are long and a longer residence times, respect to the traditional systems, in the combustion chamber are required. This means that the combustion chamber volumes must be higher than for systems with a similar heat output.

2.1 High Efficiency Burners: State of Art

Due to the wide field of applications related to burners that operate in MILD combustion, a first classification on the basis of their size, thus in terms of thermal intensities, has been carried out. Table 2.1 shows the thermal intensities of some high efficiency burners experimental facilities present in the literature. It shows low thermal intensity (oven furnaces), high thermal intensities (gas turbines) systems and their properties [Arghode et al., 2013]. The table also shows the characteristic dimensions of the systems, the oxidizer and the fuel flow rates, the operating temperatures and pollutant emissions for each combustor. The burners are listed starting from large sizes with high thermal power to small size burners with high thermal intensity.

Refs.	*Intensity (MW/m³ -atm)*	*Heat load (kW)*	*Air vel. (m/s)*	*Fuel vel. (m/s)*	*Air temp. (K)*	*NO_x @15%O_2 ppm*	*CO @15%O_2 (ppm)*
Weber et al., 2005	0.02	580	85	100	1600	9 (Φ=1)	<10 (Φ=1)
Colorado et al., 2010	0.05	20	79	81	810	1 (Φ=0.8)	<10 (Φ=0.8)
Wünning et al., 1997	0.07	200	–	–	1100	11 (Φ=0.9)	–
Gupta et al., 2003	0.1	350	–	–	1400	9 (Φ=0.8)	<10 (Φ=0.8)
Sobiesiak et al., 1998	0.1	368	145	51	650	12 (Φ=0.8)	–
He, 2008	0.1	32	118	41	324	3 (Φ=0.6)	34 (Φ=0.6)
Yetter et al., 2000	0.1	0.54	17	1	300	5 (Φ=0.1)	225 (Φ=0.1)
Mi et al., 2009	0.2	10	21	10	723	1 (Φ=0.8)	<10 (Φ=0.8)
Dally et al., 2004	0.2	7	85	15	1352	7 (Φ=0.8)	–
Xing et al., 2007	0.3	1000	–	63	300	26 (Φ=0.9)	<10 (Φ=0.9)
Szego et al., 2009	0.3	15	20	40	723	14 (Φ=0.8)	<100 (Φ=0.8)
Verissimo et al., 2011	3.8	10	96	6.2	973	4 (Φ=0.9)	12 (Φ=0.9)
Kumar et al., 2005	5.6	150	95	243	300	7.5 (Φ=1)	2900 (Φ=1)
Kumar et al., 2002	10	3	79	60	300	4 (Φ=0.9)	2200 (Φ=0.9)
Lückerath et al., 2008	14	475	160	78	735	1 (Φ=0.4)	<10 (Φ=0.4)
Vandervort et al., 2001	15	46000	–		631	<9 (Φ=0.6)	<10 (Φ=0.6)
Bobba et al., 2008	20	20	110	30	450	1 (Φ=0.5)	<10 (Φ=0.5)
Straub et al., 2005	20	700	–	–	644	40 (Φ=0.5)	<10 (Φ=0.5)
Melo et al., 2009	25	32	75	83	300	6 (Φ=0.5)	500 (Φ=0.5)
Shuman, 2000	90	0.85	80	–	573	3 (Φ=0.6)	50 (Φ=0.6)
Hsu et al., 1998	144	30	48	17	300	52 (Φ=0.2)	520 (Φ=0.2)

Table 2.1 List of thermal intensities of some High Efficiency Burners present in literature.

For the most of the configurations here presented, NO_x emission is about 10 ppm, while significant changes in CO emissions have been observed.
Figure 2.1 shows the thermal intensities of the various burners shown in Table 2.1. Up to 1 MW/m^3-atm they are suitable for furnaces applications, while higher intensities apply to gas turbine applications [Arghode et al., 2013].

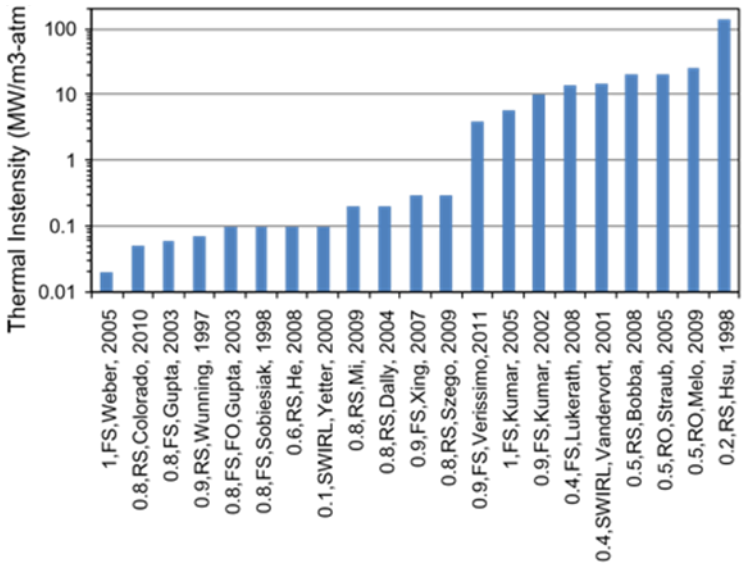

Figure 2.1 Thermal intensities of some combustors in literature

Several studies [Plessing et, al., 1998; Ozdemir et al., 2001; Coelho et al., 2001] showed that the opposite flow configuration is the most suitable for the application on gas turbines combustors. In this configuration, the combustion chamber inlet flows have not only an axial speed component, but also tangential and radial components. Therefore, large areas of hot gas recirculation and better mixing with reactants can be obtained [Gupta et al., 1984].
For instance, gas turbines for aircraft systems require higher thermal intensity in order to reduce the weight and volume of the combustor.
For small-scale systems in the range of 1-10 KW of thermal power, high power density systems is required. In such systems, pressure is not an exploitable parameter to increase the thermal density of the burner, as they work in atmospheric conditions. In order to ensure the high power density even to small-scale systems, the fluid dynamic plays a fundamental role and appropriate combustion chamber geometries must be designed. The necessity to ensure an efficient mixing between the fresh flows and the exhaust gases requires longer residence times inside the combustion chamber than the oxidation time of the mixture.
MILD combustion process occurs through highly turbulent motion fields in such a way as to mix the flows quickly and effectively, and inhibit oxidation reactions during the mixing process.

Below are examples of MILD burners with high power intensity and low thermal power, in order to show the strategies commonly adopted on small size and atmospheric pressure systems.

2.2 CDC (Colorless Distributed Combustion) Burner

An example of a small scale burner with high thermal intensity is the CDC system [Tsuji et al., 2013]. In Figure 2.2, a picture (a) and the system configurations of the CDC combustor (b, c, d) are shown. The heat output of the burner is 3.91-6.25 kW, thus the thermal intensity is much higher than the usual values in the traditional systems such as gas turbines.
The combustor is a rectangular chamber, with optical access on the vertical side for the implementation of optical diagnostics. The air is injected from the upper side of the chamber, where the exhaust gas outlet is also stored, as shown in Figure 2.2, while the fuel is injected on the side to the air flow (Figure 2.2c), or fed together with the air flow (Figure 2.2d). The inlet air can be preheated by an electric heater up to 600 K, while the fuel is injected at room temperature.
The NO_x concentration was measured using a chemiluminescence analyser, the CO concentration with an infrared detector, while the O_2 concentration (used to correct NO_x and CO emissions at a standard oxygen concentration of 15%) was measured with an analyser equipped with a galvanic cell.

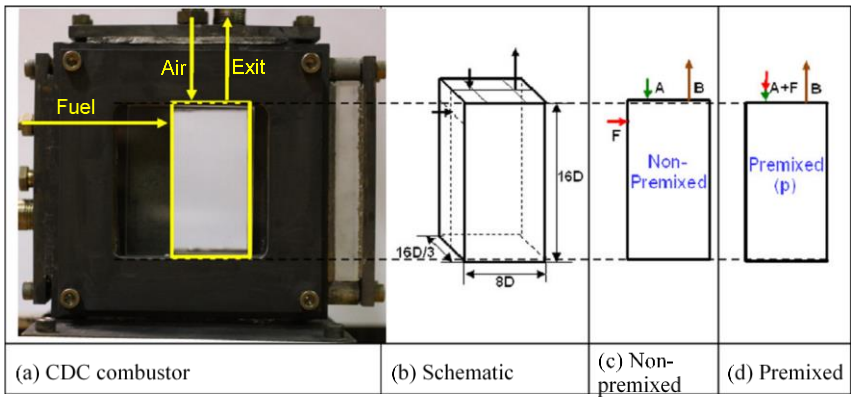

Figure 2.2 CDC squared burner: a picture (a) and sketches (b) in the standard configuration (c) and premixed configuration (d) of the system

The NO_x concentrations are low for the two configurations (pre-mixed flow NO_x = 1 ppm, flow through NO_x = 4 ppm) while the CO emissions are approximately 30 ppm for both configurations. The combustion is characterised by colourless reactive areas, pressure losses of less than 5%, heat losses of about 15%. In general, operation is very regular for both pre-mixed and non-premixed flow configurations

Figure 2.3 and Figure 2.4 show the diagram of a CDC cylindrical combustor with high thermal intensity [Kahili et al., 2011].

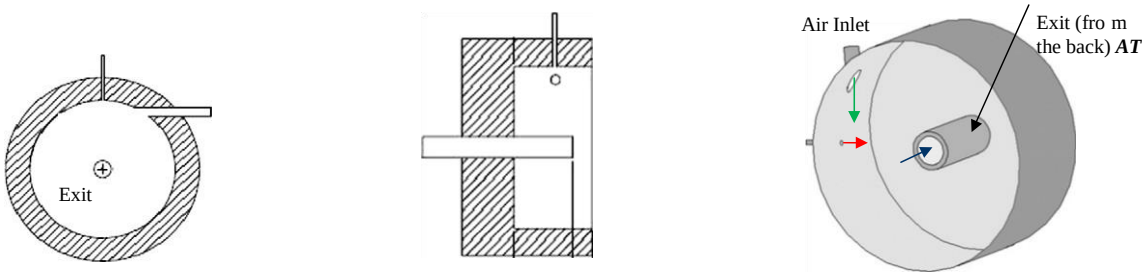

Figure 2.3 Sketch of the CDC cylindrical burner

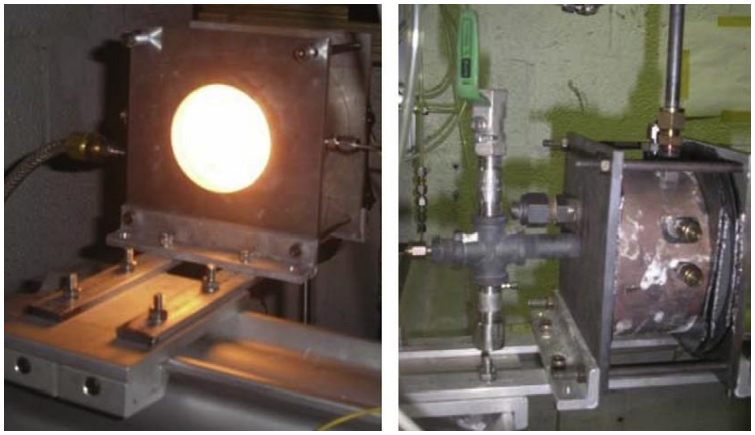

Figure 2.4 Optical (left) access and exhaust gas outlet (right) of the cylindrical CDC burner

In the cylindrical configuration of the CDC burner, the thermal intensity is 36 MW/m^3-atm while the thermal power is 6.25 kW. Three arrangements for the gas outlet were examined: the first (a) normal to the axis of the cylinder, the second (b) located on a wall at the axis of the cylinder and the third (c) outlet is also along the axis of the cylinder, but positioned inside the combustion chamber (called 'AT' in Figure 2.3). The change in the position of the outlet has a strong influence on the recirculation of exhaust gases, emissions and process stability.
In particular, very low emissions were detected for the 'AT' configuration. To simulate the usual operating conditions of gas turbines, the air injected into the combustion chamber is preheated to 600 K, which corresponds to the output temperature of the air from a characteristic compressor of a gas turbine system. There is also a valve at the exhaust that provide to increase the pressure inside the combustion chamber.

NO_x emissions are 3 ppm for non-premixed configuration and 2 ppm for premixed conditions. The experimental results obtained preheating the inlet air showed a drop of CO emissions increasing the inlet air temperature.
In general, very low NO_x and CO emissions (below 10 ppm of NO_x and CO) have been demonstrated at high temperatures and pressures with an equivalence ratio of 0.5. In conclusion, the results obtained in the experimental campaigns suggest the possibility of obtaining close to zero pollutant emissions for combustors operating in gas turbine plants, even at higher pressures and temperatures.

2.3 High-intensity and low-emission burner

A further example is the burner developed by Kumar and Mukunda at the Indian Institute of Science, Bangalore [Kumar et al., 2002]. Figures 2.5 (a) and 2.5 (b) show the geometry of the system. It consists of an insulating cylinder (25 mm ceramic fiber wool) with fuel and air injection from the holes around the perimeter of the base. The exhaust gas outlet is located at the top of the system. A thin truncated conical object is placed so that the fluid can move from region A to region C through region B (Figure 2.5a). The size and shape of the conical object have been designed using CFD simulations. Combustion air is fed through coplanar primary jets to feed jets, while excess air is fed into the upper part of the plant in order to burn the residual CO.

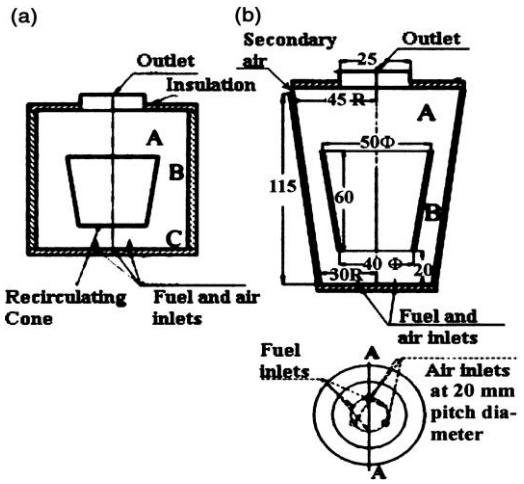

Figure 2.5 Schematic diagram of the heat-intensive and low-emission combustor system

The distribution of O_2 and temperature range vary in the ranges 0.002-0.007 and 1550-1900 K respectively. The occurrence of low oxidant concentrations and high temperatures in most of the volume is indicative of the operation of the burner in the

MILD combustion regime. The burner has a thermal power of 3 kW and a thermal intensity of 6 MW/m^3 with NO_x emissions lower than 10 ppm and CO lower than 5%. Low CO emissions has been achieved feeding the system with excess air. The low emissions, high heat intensity and particularly quiet operation of this type of burner, make it particularly suitable for applications for industrial furnaces.
Figure 2.6 shows the recirculation ratio values as function of the length of the cone.

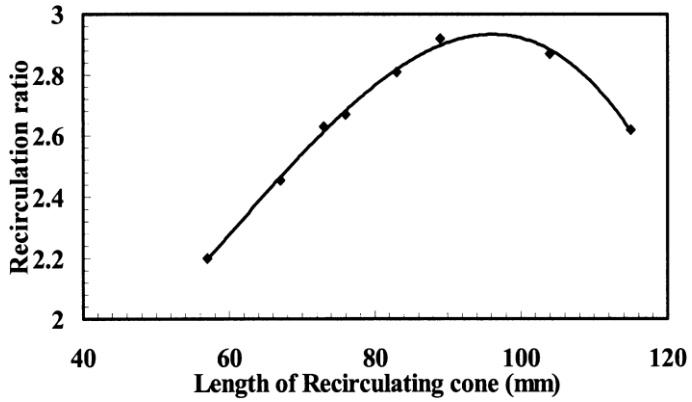

Figure 2.6 Recirculation ration as function of the length of the conical body.

A maximum value of the recirculation ratio has been obtained for a length of 90 mm of the conical body and rapidly decrease up to 60 mm.
The burner has been performed in lean conditions (limited to 10% excess air of the total) to reduce CO emissions. For this purpose, the 75% of the air has been supplied through the primary air jet in the bottom, while remaining air has been released from the upper region, allowing to burn the residual CO.
Lastly, similar trend of the velocity field has been observed for a different size of the conical body, as shown in Figure 1.13 [Kumar et al., 2002].

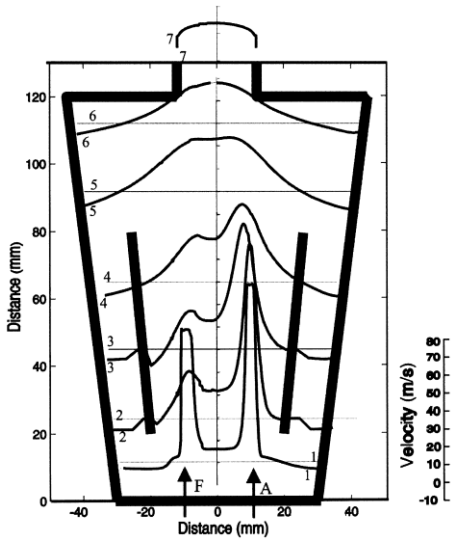

Figure 1.13 Velocity field in the combustor for a different size (80 mm) of the conical body

2.4 JHC Burner

The experimental apparatus performed at the University of Adelaide in Australia by the group of Prof. Dally gives an example of high efficiency burner [Dally et al., 2002].
The JHC (Jet in Hot Coflow) shown in Figure 2.6 is made by an 82 mm diameter annular tube isolated by a ceramic fiber layer in order to minimize the heat losses. As shown in Figure 2.1, it consists of a single fuel nozzle, positioned on the mid of the inlet duct, surrounded by four symmetrically secondary burner inlets.
Tests performed on the JHC showed significant changes on the reactive zone inside the combustion chamber compared to a conventional flame when the oxygen concentration is low. The temperature was measured by means of a type R thermocouple (platinum - 13% rodio (+) / platinum (-)), while the temperatures on the preheating line and on the exhaust were measured by K thermocouples (Chromel (Ni-Cr) (+) / Alumel (Ni-Al) (-)). Average temperatures values on 5 min running were considered. Total uncertainty after correction is ± 1.2%. NO_x, CO and CO_2 concentrations measurements at the exhaust have been obtained.

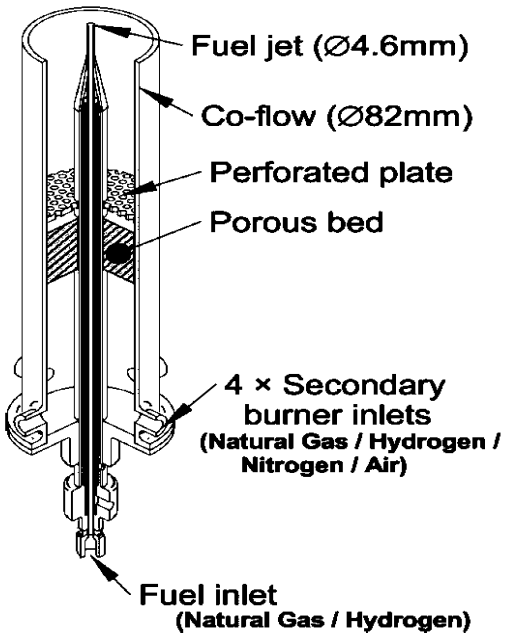

Figure 2.6 Jet in Hot Coflow

Natural gas/H_2 mixture has been used as fuel and coflow air/secondary burner inlet air ratio was varied from stoichiometric to lean conditions. H_2 addition has been used to reduce the soot formation so as the dilution level, while not significantly changes the flame structure. Figure 2.7 shows flame images presented by Dally [Dally et al., 2002] and two detection points placed at 35 mm and 125 mm from the inlet, for three values of the Reynolds number. The detection points have been chosen to represent two oxidation regimes. Furthermore, Temperatures, OH concentration and H_2CO concentration have been evaluated as a function of the radial coordinate by fixing the axial dimension respectively to 35 mm and 125 mm, for three values of the Reynolds numbers as shown in Figure 1.3.

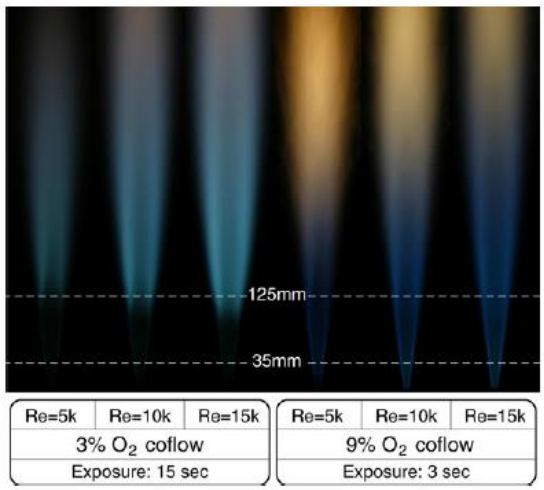

Figure 2.7 A picture of flames lift off as function of Reynolds number

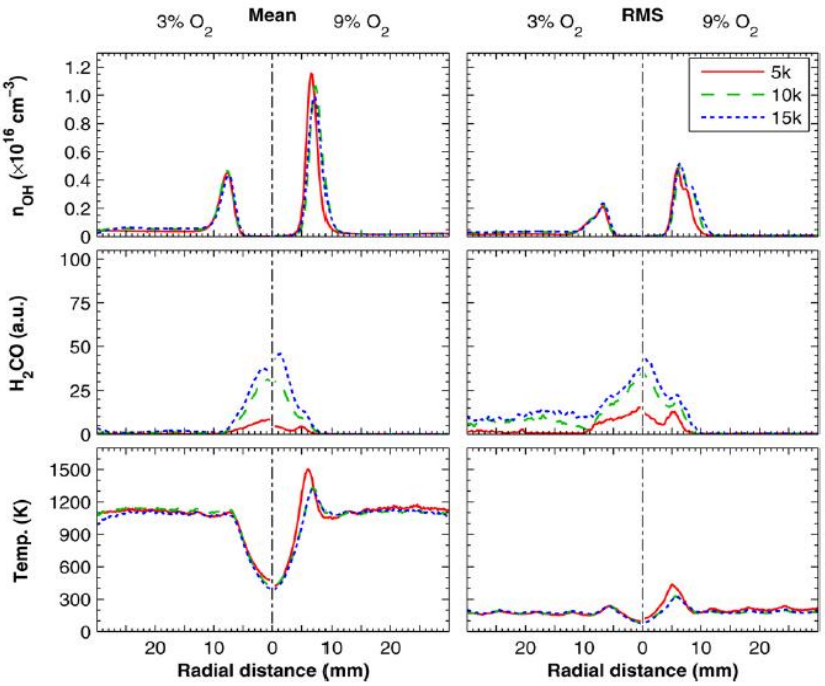

Figure 2.8 OH, H_2CO, Temperature as function of the radial distance for Re=5000, Re=10000, Re=15000

A second test has been performed varying the dilution of the mixture by air, N_2 and H_2.

Figure 2.9 shows some pictures of the flame front obtained in the tests. For all the tests the flame presents a lower brightness varying the oxygen level from 9% to 3%. This can be explained due to the reduced temperatures and the formation of intermediate species at high-diluted conditions. Furthermore, at 9% of O_2, the flames appear visibly detached from nozzle (lifted flames). In this study, the length of the lift-off has been evaluated and the results show that when the jet velocity outflow is increased, the lift-off decreases. Thus improves the stabilization of the process [Dally et al., 2002]. This trend highlights the differences in the stabilization mechanisms of the oxidation process in diluted conditions compared with conventional ones.
A further contribution on the stabilization may be related to the increased mixing, which reduces the ignition delay.

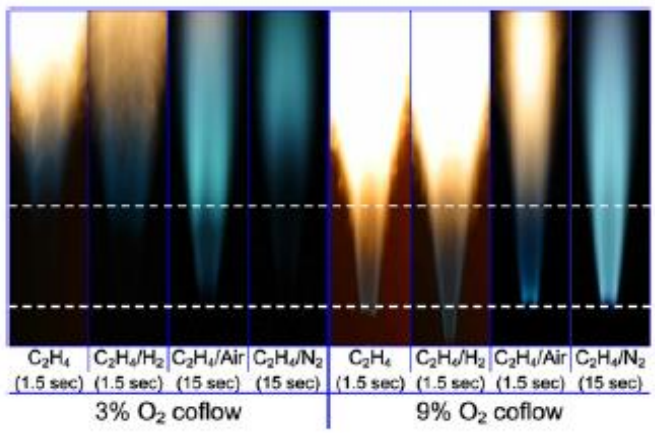

Figure 2.9 A Picture of flames lift off for different fuels at 9% O_2 and 9% O_2 dilution level

2.5 FLOX Burners

A valid strategy to reduce NO_x emissions and to achieve a high global efficiency is the FLOX technology developed at WS – Wärmeprozesstecnik. FLOX® is the acronym of FLameless OXidation and it is a trademark of WS GmbH, Renningen GERMANY.
Differently from the standard combustion processes, which the flame can be stabilized within or close to the burner, FLOX technology allows to control the process without a visible flame front.
In fact, the different methods for flame stabilization play an important role in the field of burner development, in particular for the optical and electrical features of flames that allows using UV or ionization detectors for automatic flame safety systems. Thus, in the absence of a flame signal, it is possible to turn off the burner

in a safety way. As consequence, it is important to highlights the benefits that a flame provides in terms of stabilization and signals for safety systems.
On the other side, it is worthwhile to reach the lowest pollutant emissions and the highest global efficiency in terms of fuel saving. Thus, the heat recovery from the exhaust for preheating the combustion air, with consequent energy savings, is a useful strategy extensively implemented in high temperature furnaces for the steel industry. FLOX combustion allow to obtain very low NO_x emissions [Cresci et al., 2012; Wünning et al., 2012; Baukal, 2010]. For instance, Figure 2.10 and Figure 2.11 show two configuration of FLOX® burners. The former is a Rekumat configuration, in which the heat recovery from the exhaust gases occurs by means of a steel/ceramic heat exchanger. The latter is a Regemat, that is a regenerative burner in which a heat storage from the exhaust occurs by means of coupled regenerators.

Figure 2.10 Self recuperative FLOX® burner: Rekumat CX200

Figure 2.11 Self regenerative FLOX® burner: Regemat® M250

In addition, in the Figure 2.12 is represented a panoramic of the improvements in the performance of FLOX burners. The last technologies regarding the heat exchangers for self-recuperative burners are described in terms of NTU (number of transfer

units) index, that is around equal to 1. Depict to that, the regenerative and gap-flow recuperative heat exchangers can reach NTU values up to 5.

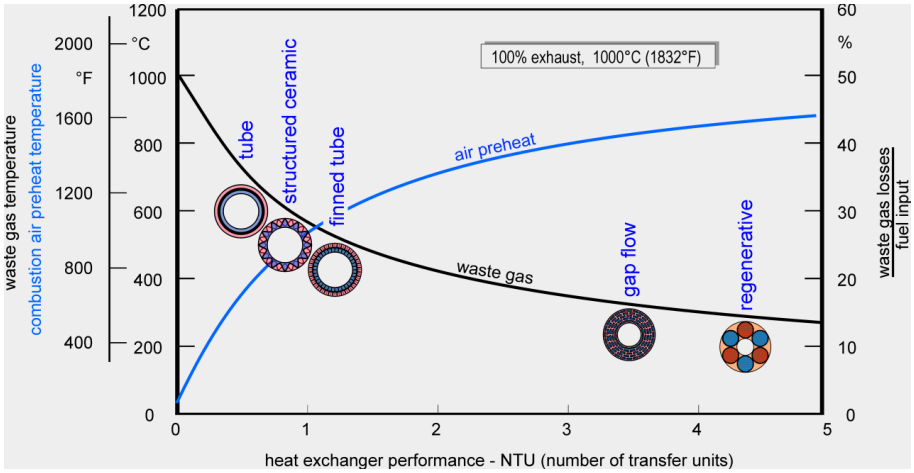

Figure 2.12 Effect of heat exchanger design on air preheating and exhaust gas losses

2.6 Flameless Burner

This burner was developed at the Technical University of Lisbon from the group of Prof. Mario Costa. The combustion chamber is shown in Figure 2.13 [Verissimo et al., 2013 a]. It is a quartz with an internal diameter of 100 mm and length of 340 mm, isolated by a 30 mm layer of ceramic fiber. The burner is fed by a central inlet of 10 mm diameter, from which the combustion air is supplied, surrounded by 16 fuel inlets of 2 mm diameter, positioned on a circle with a radius of 15 mm. The air is preheated by means of electrical heaters that allow to reach an inlet air temperature up to 700 ° C. The temperature is monitored with a K thermocouple positioned at the burner inlet. A water cooled stainless steel probe provide the gas sampling to measure the O_2, CO_2, CO, HC and NO_x concentrations [Verissimo et al., 2011].

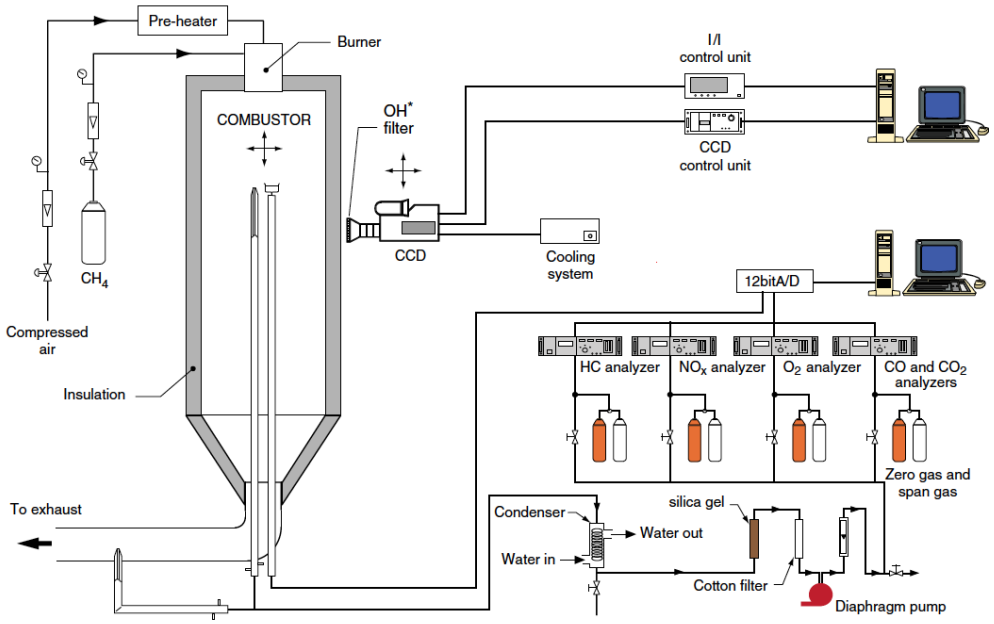

Figure 2.13 Flameless Burner

The experimental campaign was performed varying the thermal power of the flameless burner [Verissimo et al., 2013 a]. As it can be seen from the Figure 2.14 at the thermal power of 7 kW, the reaction zone is between z ≈ 70 and 160 mm.
When the thermal power of the fuel increases it can be two remarks: first of all, the enlargement of the reaction zone, in the region where OH is detected, and secondly, the area of the reaction moves progressively closer to the exit of the combustion (exhaust), and this is due to the increase in the amount of motion.
For thermal power between 8 and 13 kW, as shown in Fig.2.14, the OH * distributions reveal that reactive areas develop between z ≈ 75 and 175 mm; Z ≈ 80 and 190 mm; Z ≈ 100 and 220 mm; Z ≈ 110 and 225 mm; Z ≈ 120 e 230 mm, and z ≈ 125 and 235 mm, respectively.

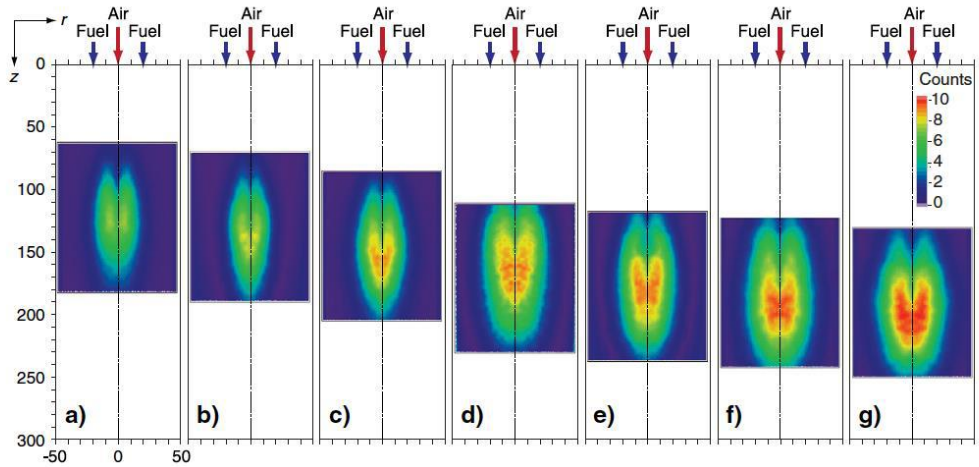

Figure 2.14 Position of the reactive zone long z, detected by the OH radical

Excess air, in this study, is low enough to ensure a stable flameless combustion regime in the whole range of thermal power investigated, with very low emissions of NO_x and CO. As shown in Fig. 2.15 the low emissions of NOx, are almost independent of the input thermal power [Verissimo et al., 2013].

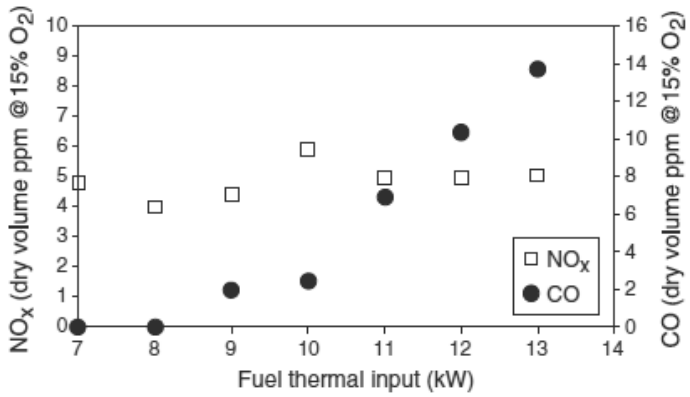

Figure 2.15 CO and NOx emissions as a function of the thermal input power

In other experimental campaigns carried out on the same experimental apparatus, the performance of the flameless combustor has been evaluated [Rebola et al., 2013].
It has been found that it is possible to obtain a stable flameless oxidation process in a wide range of operating conditions. In particular, it is possible to operate the flameless burner from stoichiometric to lean conditions up to $\lambda = 2$, for thermal loads of 10 kW and 13 kW, limiting the working temperatures and thus obtaining very low NOx and CO emissions.

Figure 2.16 shows NO_x and CO emissions as a function of V_{air}. HC emissions were not detected for any of the conditions of test. NO_x emissions are less than 7 ppm and CO emissions are below 21 ppm and, CO emissions are less than 21 ppm in the whole range of V_{air} considered. Also in Figure 2.16 it can be observed that NO_x emissions decrease when V_{air} increase while CO increases when increases V_{air} [Verissimo et al., 2013 b].

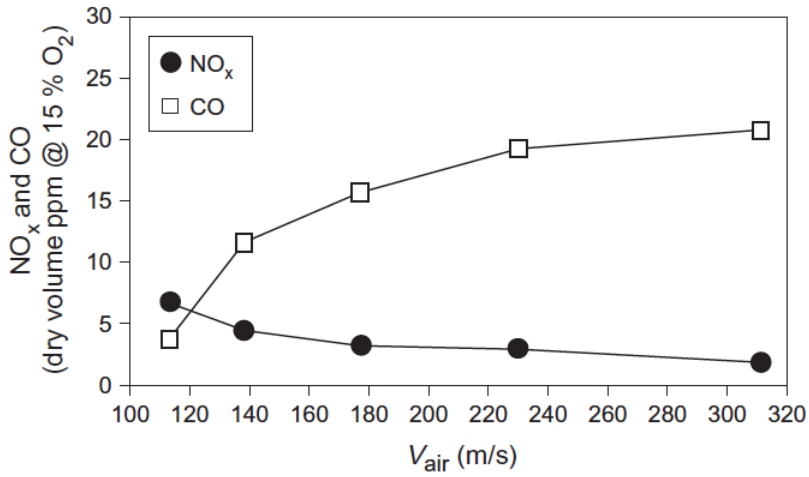

Figure 2.16 NO_x and CO trend as a function of V_{air}

3. CYCLONIC BURNER (LUCY)

Existing industrial MILD combustion systems usually reach the auto-ignition conditions by efficiently recirculating the product gases into the incoming fresh reactants [Rafidi et al., 2006; Zhang et al., 2000; Abtahizadeh et al., 2012; Arrieta et al., 2014].

The exhausted gas recirculation serves two purposes:

(i) to raise the reactant temperature (heat recovery)
(ii) to reduce the oxygen concentration (dilution).

To achieve an efficient MILD combustion process, the establishment of an effective mixing process between the recycled gases and the fresh reactant jets plays an important role. This in turn produces locally high turbulent mixing rates to avert the insurgence of oxidation reactions before reaching diluted conditions [Tsuji et al., 2002; Abtahizadeh et al., 2012; Kahlil et al., 2011]. Thus, the entrainment of products with either fuel or air and the mixing between fresh reactants [Sidey et al., 2014; Li et al., 2014] are essential processes. Another key point for MILD systems is the achievement of relatively long residence time within the combustion chamber because dilution levels imply longer kinetic characteristic times with respect to traditional systems [Sabia et al., 2014; Sabia et al., 2013; Sabia et al., 2014].
In summary, the entity of recycled heat and mass, the efficiency of mixing and the relatively long residence times are key factors in the establishment of MILD combustion regimes.
The recirculation of hot reactive species into the fresh stream can be achieved through a proper design of the combustor flow-field. Flow entrainment can be obtained with different flow arrangements. It can be achieved through internal or external recirculation; however, internal recirculation is favourable for many applications.
This technology was further investigated even for applications to high thermal intensity (higher than 15 MW/m3-atm) (gas turbine) [Lückerath et al., 2008; Arghode et al., 2011]. Such systems provided ultra-low NO_x and CO emissions only in some operational points. In particular, one of the main limitations to the large deployment of internal recirculation based combustion devices is the difficulty in stabilizing the oxidation in small-scale systems due to the high heat losses and very low flow residence times inside the combustor.
Such considerations poses the problem of identifying suitable configurations and geometries capable of realizing stable, efficient and clean combustion processes on small scale preserving the fuel flexibility needed and a reasonable degree of simplicity.

Hence, attention should be paid to the engineering of the flow field inside the combustor and the design of chamber geometry; it has to promote the aerodynamic features controlling the rate of internal recirculation and the size of the generated recirculation zone. In this context several configuration were considered based on fluid-dynamic stabilization by swirling or other convoluted flow fields [Khdir et al., 2017].
An effective method to create recirculation zone involves the use of cyclone like configuration. Cyclone or vortex combustion chambers have been reported in many forms for gaseous [Gupta et al., 1984] or solid fuels [Duan et al., 2013].
The key factors associated with such an arrangement can be summarized as follows:

(1) Longer residence time inside the combustor.
(2) Recirculation zones and turbulence generated internally by shear between differing fluid.
(3) Large toroidal recirculation zone with high level of turbulence generated for the central exit configuration.

In these arrangements, the recirculation of hot active species is achieved through two key features. The first is the main jet entrainment, and the second is the recirculated gases imposed by the geometry of the combustor itself.

3.1 LUCY Burner: Design and Configuration

At the IRC-CNR in Italy, a burner was conceived under the idea to stabilize a cyclonic flow-field. LUCY burner (Laboratory Unit CYclonic flow-field) was designed to operate at a nominal thermal power of 2 kW under the constraint of lab-scale dimensions. Briefly, it consists in a prismatic chamber with a square section of 20x20 cm and a height equal to 5 cm as shown in Figure 3.1.
As showed in the figure, the non-premixed feeding configuration consists in a couple of injectors located at two opposite walls of the burner in an asymmetric way. Both of them are composed by a main injector (D_i = 0.8 mm) to feed the main flow, composed by oxygen and a diluent species, and a smaller one (d_i = 0.08 mm) to inject the fuel.

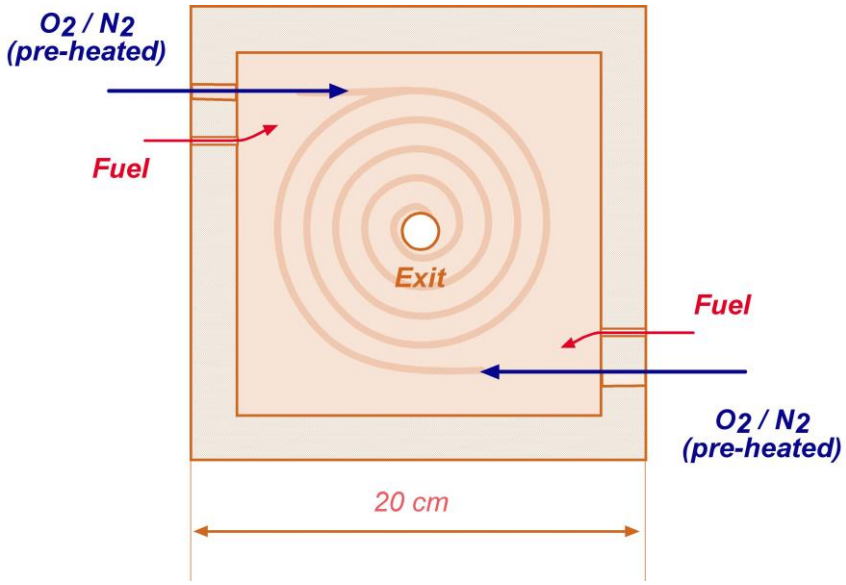

Figure 3.1 Sketch of the section of the burner with the reactants feeding configuration.

Oxidant jets are adjacent to the combustor wall (the distance between the wall and the oxidant jet is 0.02 m) and fuel is injected between the oxidant jet and centerline of the combustor (the distance of the fuel jet from the oxidant one is 0.025 m). The combustion product gas exit is from the top side with a diameter of 0.025 m. The gas exit is located on the top of the chamber. As a consequence, the flow injection configuration and the exit location induce a cyclonic flow field inside the combustion chamber.
Given these geometrical features, CFD simulations were realized to characterize the cyclonic flow field in terms of gas residence time distribution, mixing between fluxes and local turbulent intensities. The next paragraph is dedicated to this numerical analysis.

3.2 Numerical Characterization of the Cyclonic flow-field

In order to verify the establishment of a cyclonic pattern within the combustion chamber and to characterize the residence time distribution, non-reacting flow simulations were performed using a commercial CFD software (Fluent 6.3.26). The system volume was meshed with a full hexahedral grid using the Gambit software with an appropriate refinement in the region with high geometrical gradients. It

contained 850,000 hexahedral cells. The grid refinement effects on calculations showed negligible effect on the results for the conditions examined here.
The mixing field was solved using a steady state, implicit, finite-volume-based compressible solver, and the Reynolds Stress Model (RSM) with non-equilibrium wall functions was used to model turbulence in highly swirling flow conditions. RSM provides a more accurate prediction of the mixing pattern for swirling flow-fields than standard two-equation turbulence models (k-ε and k-ω based models) [Arghode et al., 2010]. The turbulence intensities of the mass flow inlets and pressure outlet were set equal to 0.05, and the SIMPLE algorithm was used for the pressure-velocity coupling. A second-order upwind discretization scheme was used to solve all governing equations.
Convergence was obtained when the residuals for all the variables were less than 10−5. Figure 3.2a shows the (mean) velocity vectors in the burner mid-plane. The fuel flow was injected at 50 m/s and 300 K, with the main flow at 39 m/s and 1045 K. The fuel flow is partially diluted to keep its velocity independent of the carbon/oxygen feed ratio. The global mixture dilution level is 94%, and the inlet equivalence ratio is 1 (stoichiometric mixture). The operating pressure is 1 Atm, and the average residence time is 0.5 s.
Figure 3.2a and Figure 3.2b show the establishment of a cyclonic pattern within the reactor. Figure 3.2a reports the velocity field at the mid-plane of the reactor, which shows that the high-speed oxidizer jet induces a strong swirl within the reactor and that the fuel jet is strongly bent by the recirculated gases, assuring an efficient mixing between flows.
The pathline plot (Figure 3.2b) confirms the presence of a strong recirculation of gases inside the combustor, ensuring high residence times.
Such an arrangement is characterized by long residence times inside the combustor with recirculation zones and turbulence generated internally by shear between differing flows. Moreover large toroidal recirculation zone with a high level of turbulence are established inside the combustor and the high gas recirculation rates promote the attainment of the high temperature, low oxygen concentration conditions required for the stable autoignition of the MILD mixture [de Joannon et al., 2012].
For this purpose, the average residence time value $\tau = 0.5$ s (calculated as the ratio between the combustor volume and the volume flow rate of reactants) was identified as the optimal value to achieve a good compromise between mixing times, the gas recirculation levels and the kinetics times.

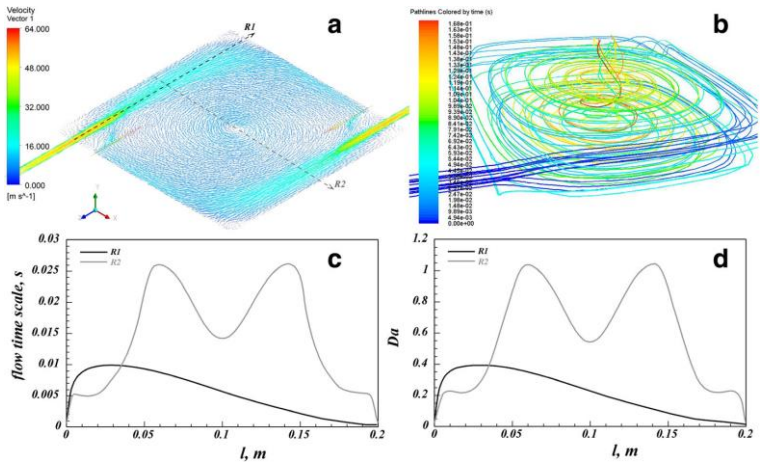

Figure 3.2 Numerical computations of the velocity field (a) and pathline plots colored by residence time (b) for non-reacting conditions. Local flow time scale (c) and local Damköhler number (d) profiles are reported along two selected lines

In order to elucidate the microscopic characteristics of MILD Combustion in the present system, further simulations were used to confirm that the MILD combustion regime was characterized by low Damköhler numbers with the enhancement of internal flue gas recirculation. The Damköhler number, as already mentioned, is defined as the ratio between a characteristic flow time τ_{flow} and a characteristic chemical time scale τ_{chem}.

Thus, it is a widespread opinion that for such a combustion regime the Damköhler number approaches unity [Isaac et al., 2013]. The chemical time scale τ_{chem} is based on the ignition delay time τ_{ign} for the homogeneous reactant mixture at the inlet temperature (T_{in}). The ignition delay value for $C_3H_8/O_2/N_2$ mixtures was evaluated on the basis of the external operating conditions of the numerical simulations reported in Figures 3.2a and 3.2b ($XN_2 = 0.94$, $\Phi = 1$, $T_{in} = 1045$ K, P = 1 atm). For such conditions, the ignition delay was evaluated as 0.025 s. It was computed using the PLUG application of the commercial software ChemKin 3.7 [Rupley et al., 2013].

The evaluated value of τ_{ign} is consistent with the typical ignition-delay time values for propane/oxygen mixtures highly diluted in nitrogen obtained in previous studies by the same research group [Sabia et al., 2014].

The local characteristic flow time τ_{flow} is defined as the flow time based on the integral scale of large eddies in turbulent reacting flow,

$$\tau_{flow} = \frac{l_0}{u'(l_0)}$$

where l_0 is the integral scale of large eddies in turbulent flow and $u'(l_0)$ is the turbulent velocity fluctuation. Local values of l_0 and $u'(l_0)$ were evaluated on the basis of the quantitative information obtained from the non-reacting simulations with

the RSM model. The flow-time scale and Damköhler number distribution were locally evaluated for the cyclonic reactor along two selected lines R1 and R2 (see Figure 3.2a) and they are reported in Figure 3.2c and Figure 3.2d, respectively.
The results indicate that the characteristic flow time scale becomes short along R1 because of strong mixing and entrainment of the fuel jet (Figure 3.2c). The toroidal flow-field involves a decreasing of the velocity magnitude along the R2 line and thus mixing time scales become longer toward the center of the reactor. Figure 3.2d shows Damköhler number distributions along R1 and R2.
It is found that the Damköhler number value is lower than 10 and is near unity in the central reaction region (see profiles along R2), which proves that both chemical reaction and turbulent mixing control the finite reaction rate.
Therefore, the overall effect is to obtain a Damköhler number as small as possible confirming that the combustion characteristics of the present cyclonic burner are in the well-stirred reactor regime.

Further analyses were realized in order to characterize the effect of the flow velocities (thus the thermal power) on the establishment of the cyclonic flow-field. The nominal power of the experimental test rig was varied between 0.5 and 5 KW (by varying the average residence time). Considering a $C_3H_8/O_2/N_2$ mixture at stoichiometric conditions, with an overall nitrogen dilution equal to 90 % and an inlet oxidizer temperature of 1045 K, the total flow rate is changed by varying the average residence time (τ) values from 0.2 to 1. The inlet fuel temperature is 300K.
In Tab. 3.1 the different configurations are reported along the inlet oxidizer jet velocity (diluent/oxygen) that was calculated on the basis of the declared average residence time while keeping constant the fuel jet velocity at 50 m/s.

Case	Configuration	J	Nominal heat load (kW)	Average Residence time (s)	Oxidizer Velocity (m/s)
1	A1	382	4	0.2	98
2	A2	58	1.6	0.5	38
3	A3	16	0.9	0.9	20

Table 3.1 Summary of the investigated configurations

Figure 3.3 shows the tangential velocity profiles for the configurations reported in Table 3.1 along the burner centerline (Z coordinate). A recirculation flow zone and a strong swirl covering the entire combustion chamber are observed inside the combustor for low residence times. Due to the higher oxidizer injection momentum than the fuel injection momentum (see Table 3.1) and due to the position of the exit on the top, the strong swirl is mainly induced by the high speed oxidizer jet, which induces entrainment and recirculation. Moreover, because the fuel flows at the inlet is in the same direction as the oxidant stream, the high-speed fuel jet also enhances the oxidant jet dominated flow field. As reflected by the profiles of Figure 3.3,

stronger swirl is observed for configuration A1 and A2 with maximum tangential velocity of 22 and 8 m/s respectively. This is attributed to the higher oxidizer injection velocity. It can be observed that for the preheating and dilution effect of recirculated combustion products, high gas recirculation rates promote the attainment of high temperature low oxygen concentration condition required for the stable autoignition of MILD mixture [de Joannon et al., 2012]. In this sense the average residence time inside the burner cannot be too low because mixing characteristic times have to be comparable with chemical ones that in MILD cases are longer than traditional combustion systems [Sabia et al., 2014].

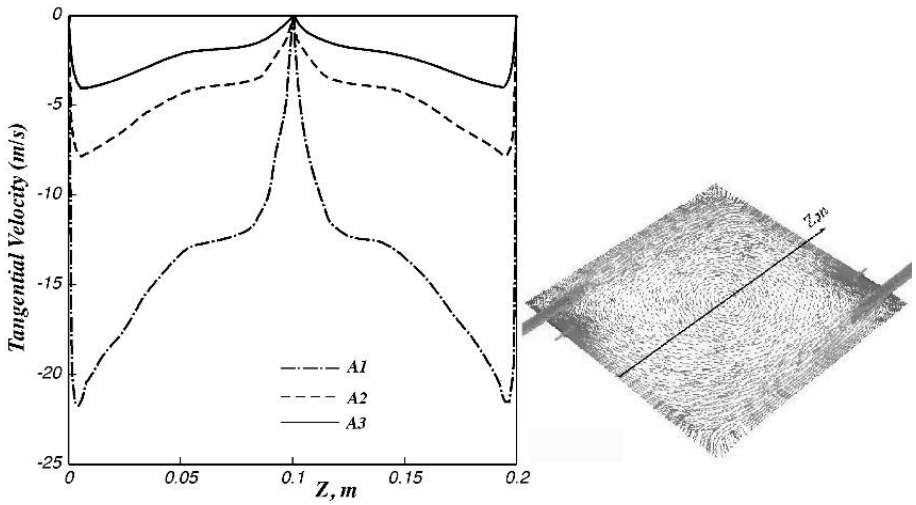

Figure 3.3 Tangential velocity along the burner centerline for the different configurations of Table 3.1.

It is recognized that the flow field and mixing behaviour will be different under reacting flow conditions; however, comparative study of the non-reacting condition among various configurations provides important insights into the effect of oxidizer/fuel momentum flux ratio on the jet profile and gas recirculation characteristics. In this sense, the configuration A2 (τ = 0.5 s) was chosen as the reference one for this study because it represents a good trade-off between mixing time and recirculation pattern. Lower residence time values, in fact, involve high swirl with mixing times that are no more comparable with the chemical ones for stabilization of MILD/Flameless combustion conditions.

3.3 Cyclonic Burner and Experimental facility

Figure 3.4 shows a picture (a) of the reactor and a sketch of the section (b) of LUCY burner constructed and performed to investigate the MILD/flameless combustion process [Sorrentino et al., 2015].

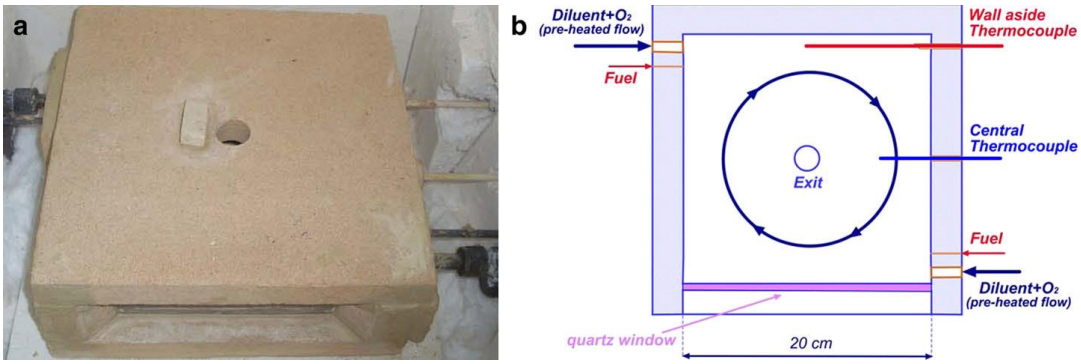

Figure 3.4 Photograph (a) and sketch of a section (b) of the cyclonic combustion chamber

The combustion chamber is made of vermiculite that is an easily machinable refractory material thus allowing for the realization of different geometries. It has an excellent resistance to high temperatures and excellent insulating capacity to reduce heat losses from the combustor to the surroundings. Moreover, the combustion chamber is well insulated from the external ambient by means of refractory ceramic fiber boards and electrical heaters (Figures 3.5a and 3.5b). The main flow passes through heat exchangers located within the electrical ceramic fiber heaters to raise the temperature to the desired values, while the fuel is injected at environmental temperature (Figure 3.5b). Temperatures are controlled and monitored by dedicated programs developed by means of LABVIEW. The set-point value of such electrical heaters is adjusted as a function of the inlet preheating temperature of the oxidizer in order to keep the system almost isothermal before the fuel injection. The fuel jet is partially diluted with N_2/CO_2 in order to keep its velocity independent of the equivalent ratio. The cyclonic burner is equipped with a set of thermocouples (type Nisil - NiCroSil) (Figure 3.5b) and an optical access with a quartz window on the front side (Figure 3.5c). Two movable thermocouples are located at the mid-plane of the reactor. The former is placed near the wall (0.02 m from the wall) and the latter is placed at the centerline of the combustion chamber (Figure 3.5d). The thermocouples can be moved across the reactor. A further thermocouple is placed at the outlet of the combustion chamber to monitor the exhaust gas temperature. Thermocouples have an accuracy of +/- 2.2 K in the range 300-1500 K with a good resistance to oxidation at high temperatures. The temperature measurement

uncertainty due to thermocouple heat exchange mechanisms was estimated to be less than 0.5 % by considering the heat transfer by convection and radiation towards the surroundings. The quartz window allows to visual observations of the combustion process on the side-view (Figure 3.5c). Given the nature of the design, there were practical limitations to the implementation of a top-view window. The exhaust is sampled by a GC analyzer, averaged over a 5-min duration for each operating condition studied. The concentrations of O_2, CO, CH_4 and C_2-species are measured. NO and NO_2 (NO_x) are measured through an ABB flue gas analyzer. The estimated error for NO_x emission is ±2 ppm in the range of 0–99.9 ppm, and ±5% in the range of 100–500 ppm.

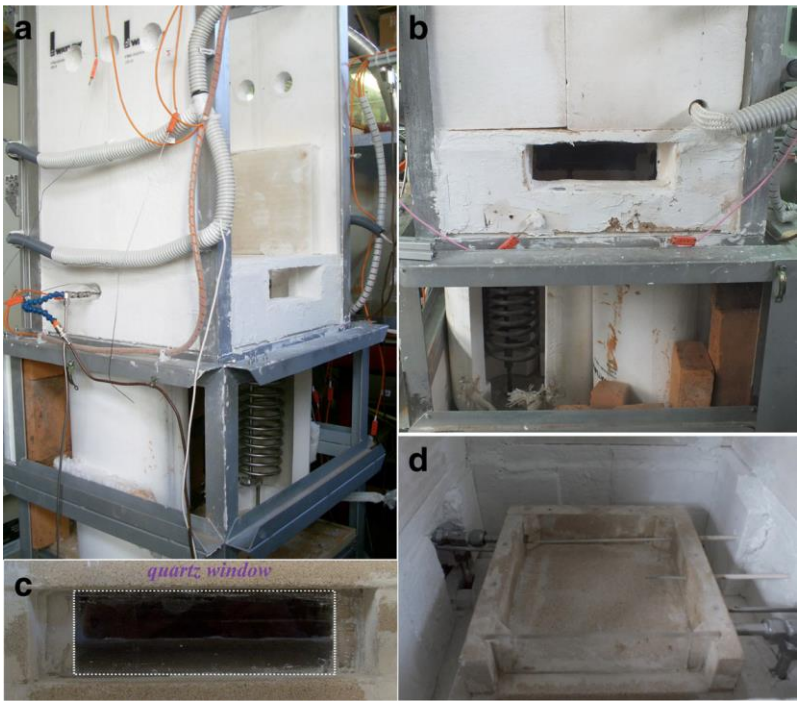

Figure 3.5 Picture of the plant

LUCY burner have been designed to be performed with several fuels at micro scale (P = 0.5 ÷ 15 kW) thermal power level. For this purpose, it is necessary a very high flexibility of the whole system. In order to characterize the cyclonic burner and define its operative conditions, five operational controlling parameters have been defined. Furthermore, in order to verify the high flexibility of the system, the external operational parameters, can be varied independently each other allowing to investigate a wide range of operative conditions.

The operational parameters that were varied in the experimental campaigns are reported in table 3.2:

	PARAMETER	OPERATIVE RANGE
$\mathbf{T_{in}}$	Preheating Temperature	Room Temperature ÷ 1300 K
$\mathbf{XN_2}$	External Dilution	AIR ÷ 0.99
Φ	Equivalence Ratio	0.05 ÷ 5
τ	Residence Time	0.1 ÷ 8 s
P	Thermal Power	0.5 ÷ 15 kW

Table 3.2 List of the external operational parameters and the operative ranges

- The inlet preheating temperature T_{in} ,

is the temperature of the main flow, the oxidizer one, at the inlet of the combustion chamber. It is possible to fix the value of the inlet temperature by regulating the heaters set-point temperatures of the experimental facility.

- The dilution level XN_2, $XN_2 = \frac{n_{N2}}{n_{tot}}$

where n_{N2} are the moles of N_2 and n_{tot} are the total moles, defines the inlet molar fraction of the external diluent (N_2) of the mixture.

- The equivalence ratio, $\Phi = \frac{{n_{fuel}}/{n_{ox}}}{\left({n_{fuel}}/{n_{ox}}\right)_{st}}$

is the ratio between the fuel-to-oxidizer molar ratio n_{fuel}/n_{ox} and the stoichiometric value of the fuel-to-oxidizer molar ratio $\left(n_{fuel}/n_{ox}\right)_{st}$. Thus, it is an index of the inlet mixture composition and it is not a function of the fuel nature.

- The residence time, $\tau = \frac{V}{Q_v}$,

is the average residence time of the reactants flow in the volume of the cyclonic burner, where V is the volume of the combustion chamber and Q_v is the volumetric flow rate of the mixture,

- The nominal thermal power, $P_{th} = \dot{m}_{fuel} H_i$,

where $\dot{m}_{fuel}$ is the mass flow rate of the fuel and H_i is the lower heating value.

3.4 Investigation on Process Stability

In order to verify the stabilization of the combustion process by means of the cyclonic flow field configuration, a preliminary experimental campaign has been performed. For this purpose, it was worthwhile starting to investigate the process stability in strong diluted conditions (94 %) at low thermal Power (P = 1 kW) for mainly two reasons:

- the stabilization at high dilution and low thermal power is critical, thus it is possible to predict the wide range of operative conditions in which LUCY can be performed
- the lower thermal power for the preliminary tests allow to perform the burner in safety conditions

Thus, experimental tests have been performed for C_3H_8/O_2 mixtures diluted in N_2 and CO_2 by varying the equivalence ratio (Φ) from 0.05 to 3.3.

The investigation on the process stability in CO_2 as a diluent is a key aspect to understand the role of the recirculation in the MILD combustion process. In fact, as a combustion product, the dilution of the mixture in CO_2 permits to study the stability of the oxidation process when the dilution of the system is obtained by means of the internal recirculation of the burned gases.

During the experimental tests, the inlet temperature of the main flow (T_{in}) has been varied from 850 to 1250 K. The equivalence ratio, defined as the ratio between fuel-to-oxidizer molar ratio and the stoichiometric value of the fuel-to-oxidizer molar ratio, defines the conditions of the inlet mixture. On the basis of such a definition, Φ = 1 is the stoichiometric value for propane/oxygen mixtures. Thus Φ values lower than 1 corresponds to fuel lean mixtures while rich fuel mixtures are characterized by Φ values higher than 1. The mixture was diluted in N_2 or CO_2 to 94 %. The mixture dilution level is the overall percentage molar fraction of the diluent species in the mixture. On the basis of the definition of Φ, CO_2 content does not alter the equivalence ratio value and the inlet oxygen content is not included in the mixture dilution level. The initial overall mixture dilution level was 94 %. Experiments were run at environmental pressure, and the average residence time was fixed at 0.5 s. The evaluation of the system behaviour was based on the systematic analysis of the temperature profiles in time with varying initial operating conditions. Several different behaviours were encountered during the experimental tests due to the different combustion regimes. Ignition conditions were identified with an ignition criterion which is satisfied when the working temperatures are at least 10 K higher than T_{in} [Abtahizadeh et al., 2012] [Sabia et al., 2014].

3.4.1 Mixtures diluted in N_2

The temperature profiles reported in Figure 3.5 are examples of the reaction modes experimentally detected for N_2-diluted mixtures. The figure refers to a $C_3H_8/O_2/N_2$ mixture for XN_2 = 0.94 and Φ =1.7. In the figure, the increase of temperatures obtained by monitoring both thermocouples located inside the burner is reported. For these tests, the thermocouples were positioned at a fixed location, namely the lateral one at 0.1 m within the reactor while the central one at 0.05 m. For T_{in} = 940 K, the temperature increases slowly in time, and the maximum increment of temperature ($T = T_{max} - T_{in}$) is lower than 10 K. Such a behaviour was associated with a "Low Reactivity" condition. In this combustion mode, the ignition criterion (T > 10 K) is not satisfied. For T_{in} = 1035 K, the temperature profile shows an initial abrupt jump followed by periodic temperature oscillations over time. Such behaviour was identified as the "Dynamic" regime. This regime encloses several temperature profiles characterized by regular, irregular or damped oscillations. For the sake of conciseness, they have been identified under the same regime. The T profile shown in Figure 3.5 for T_{in} = 1135 K corresponds to a "MILD Combustion" condition. The reactor temperature increases and reaches a stationary value. In this case, the thermal field in the combustion chamber is uniform and homogeneous. The uniformity at 94 % of dilution and Φ = 1 of the temperature distribution inside the combustor was demonstrated by moving the two thermocouples (lateral and central) inside the burner and measuring the temperature profile along the axis.

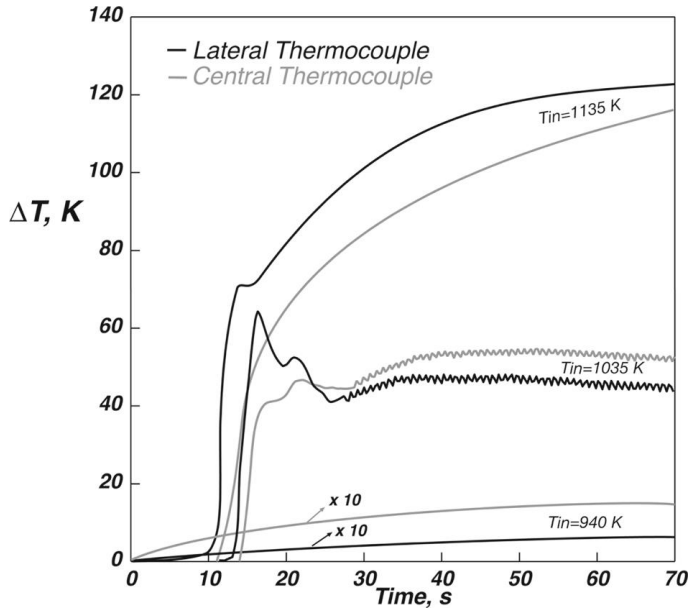

Figure 3.5 Temporal temperature profiles reported under different operating conditions for N_2-diluted systems

Figure 3.6 shows in-furnace images in nitrogen-diluted cases. The images are associated with several combustion modes. The effect of the inlet preheating temperature on the luminosity of the system is as follows: as T_{in} increases, the flame becomes less visible and finally invisible (Figure 3.6d).

In particular, for inlet temperatures lower than 1000 K, the system presents low heat release with a slight level of luminosity inside the combustor (Figure 3.6a), indicating a low reactivity regime.

By increasing the preheating level, the system approaches the dynamic condition with the occurrence of unstable behaviours due to the insufficient amount of enthalpy for the establishment of stable combustion conditions. In such conditions, the system is far from a distributed and flameless regime due to the presence of a non-premixed flame. Figure 5b and c show instantaneous images of the combustion chamber during the oscillating phenomenologies in the dynamic regime.

In particular, Figure 3.6b shows a homogeneous, bluish-colored flame inside the burner, whereas Figure 3.6c shows non-premixed diffusion flames attached to the fuel nozzle. In both cases, these spontaneous light emissions are repeated in time with the same frequency of the temperature oscillations shown in Figure 3.5.

After increasing the inlet preheating temperature, the amount of recirculated gases and the enthalpy are sufficient to stabilize MILD combustion conditions, thus the combustion becomes invisible. When MILD combustion is established (Figure 3.6d), the thermal field becomes more uniform, and flameless conditions are achieved inside the chamber.

MILD combustion in the present experiments is defined as the combustion regime where there is no visible flame front with a uniform thermal field.

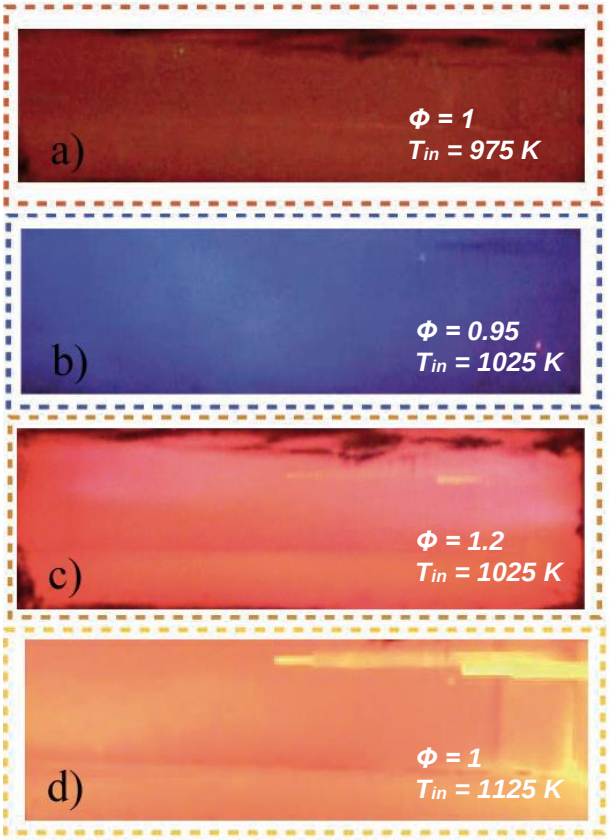

Figure 3.6 Images showing the in-furnace appearance of propane combustion for mixtures diluted up to $XN_2 = 0.94$ for different operating conditions

Several main typologies of the temperature profiles were recognized and associated with the characteristic combustion regimes. Briefly, it was possible to identify the following combustion regimes:
– "No Combustion": no temperature increase occurs, and the temperature maintains its inlet value.
– "Low Reactivity": the temperature profiles show a modest temperature increase that does not exceed 10 K.
– "MILD Combustion": the system approaches a stable combustion condition, and the working temperatures are at least 10 K higher than T_{in}.
– "Dynamic": the system is characterized by dynamic behaviour with regular, irregular or damped temperature oscillations.
On the basis of this classification, a map of the behaviour on a Φ–T_{in} plane was built and reported in Figure 3.7 for mixtures diluted in N_2 for a temperature range between 850 K and 1250 K and a Φ from 0.025 to 1 (i.e., from lean to fuel-rich conditions). The inlet temperature was varied with steps of 20 K, which were decreased in areas where transitions among combustion regimes were observed.

In Figure 3.7, it is possible to distinguish several areas that are related to different typical temporal profiles. For inlet temperatures lower than approximately 935 K, the mixture does not ignite across the entire investigated Φ range. This area is indicated as "No-Combustion". After increasing the inlet temperature, the "Low Reactivity" regime occurs, and the temperatures reach a steady value with an increment lower than 10 K. For higher T_{in} (>1000 K), the MILD combustion regime is established for inlet temperature with dependence on the equivalence ratio. In particular, the greater equivalence ratio is, the higher inlet temperature is required to pass from the "Low Reactivity" to the "MILD" regime. Such a transition passes through the "Dynamic" behaviour for $0.6 < \Phi < 1.5$ and for $1000 < T_{in} < 1050$ K.

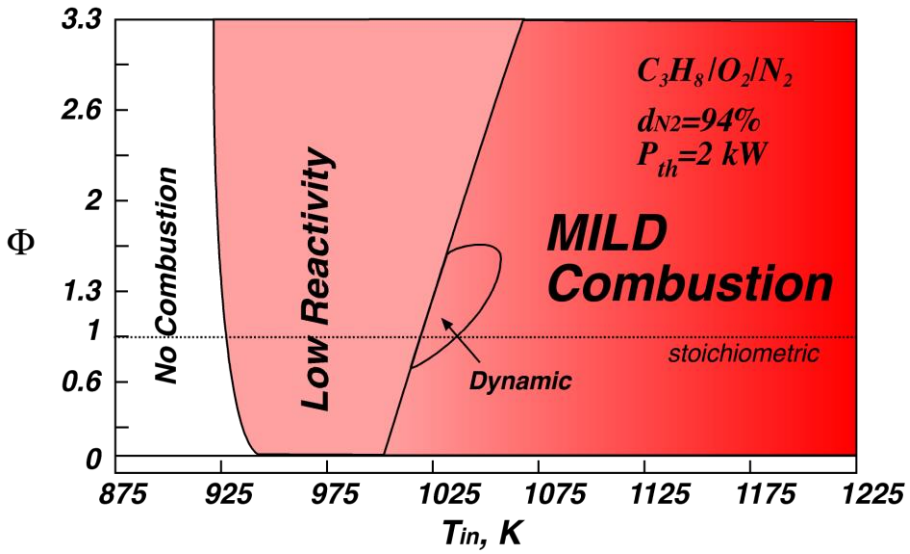

Figure 3.7 Experimental map of the behaviour for mixtures diluted up to 94% in N_2

Figure 3.8 confirms the MILD combustion operative condition of the cyclonic burner. In fact, it shows the temperature axial profiles inside the combustion chamber acquired by the central thermocouple at $X_{N_2} = 0.94$, $\tau = 0.5$ s, for two values of the equivalence ratio ($\Phi = 0.3$, $\Phi = 1$). It is highlighted from Figure 3.8 that the oxidation process is stable at uniform temperature inside the chamber even for different values of the equivalence ratio. Thus, it is possible to achieve stable regimes and to perform the cyclonic burner in MILD combustion in a wide range of operative conditions.

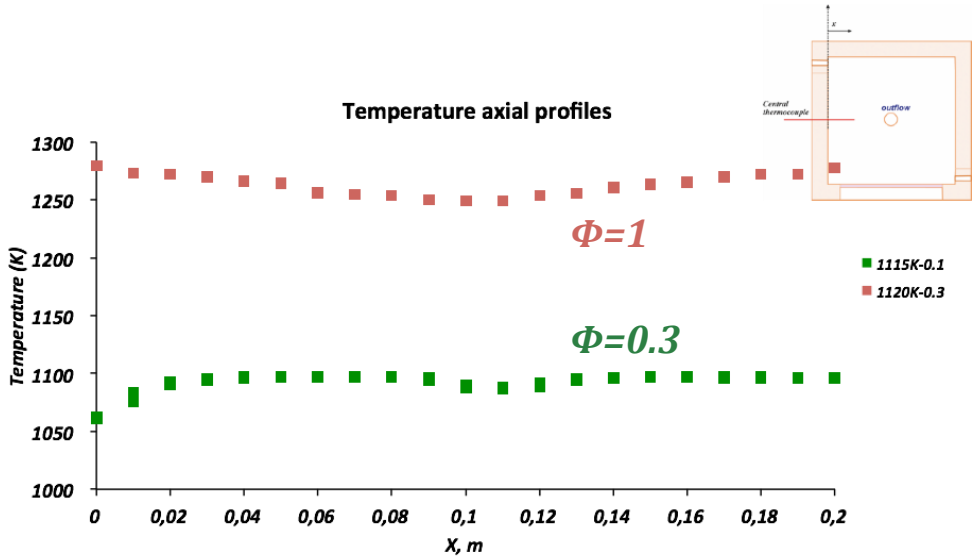

Figure 3.8 Temperature axial profiles inside the combustion chamber. $XN_2 = 0.94$, $\tau = 0.5$ s

3.4.2 Mixtures diluted in CO_2

Similar experimental tests were conducted for mixtures of C_3H_8/O_2 diluted in CO_2 at 94%. The experimental results showed the occurrence of the same combustion regimes identified on the basis of the temporal profiles for the mixtures diluted in N_2.

Thus, following the same analytical approach used for the mixtures diluted in N_2, a Φ-Tin map was drawn, as reported in Figure 3.9. The map shows that for low inlet temperatures, the transition from "No combustion" to "Low reactivity" depends on the mixture composition. In particular, the reactivity of the fuel-rich mixtures is higher than for mixtures with an equivalence ratio Φ lower than the stoichiometric ratio.

Therefore, for rich mixtures, the transition occurs at $T_{in} > 900$ K, whereas for lean mixtures, T_{in} increases. For instance, at $\Phi = 0.17$, T_{in} is 950 K. For $T_{in} > 1000$ K, the "MILD Combustion" regime is observed independently of the mixture composition. For $0.6 < \Phi < 1.3$ and $1000 < T_{in} < 1055$ K, the map shows "Dynamic" behaviour.

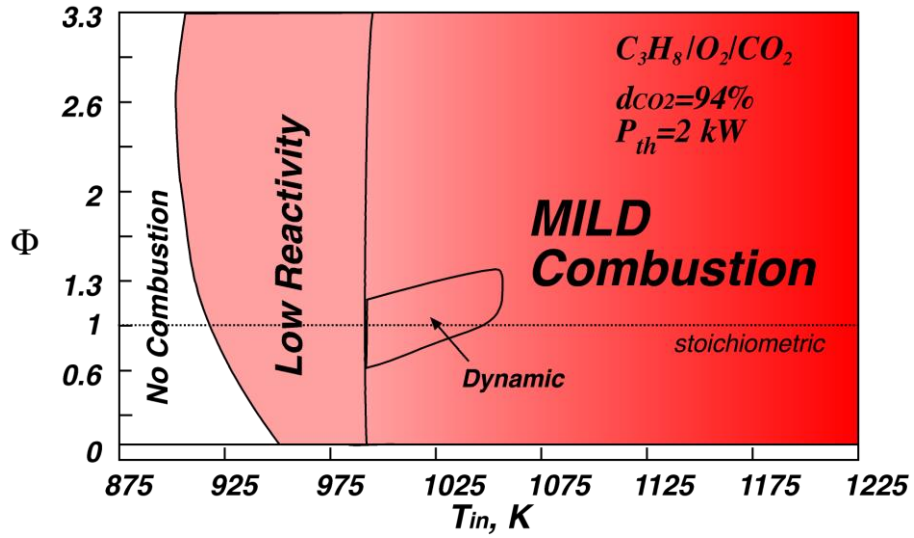

Figure 3.9 Experimental map of the behavior for mixtures diluted up to 94% in CO_2

3.4.3 Effect of diluent nature

To evaluate the effect of the diluent nature on the propane combustion process, it is useful to compare the experimental results in terms of the temperature increase. Figure 3.10 shows the T observed in the experimental tests for propane/oxygen mixtures diluted up to 94% in N_2 and CO_2. The experimental data show that in the case of N_2, the increase of temperature is higher than for CO_2 for all conditions analyzed, except the first condition (T_{in} = 975 K).

In all cases, the maximum T is close to the stoichiometric condition (Φ = 1). The description of the figures suggests that the oxidation pathways are significantly modified by the nature of the considered diluent species with complex interactions that depend on T_{in}. These results are explainable on the basis of previous works [Sabia et al., 2014] [Sabia et al., 2005] dealing with the chemical kinetic aspects of the CO_2 effects on the propane oxidation process under MILD conditions.

Briefly, because of the higher CO_2 collisional efficiencies in third molecular reactions with respect to N_2, CO_2 promotes the low temperature radical branching mechanism.

When increasing the initial temperatures, CO_2 decreases the reactivity of the system because it inhibits the faster high temperature branching mechanisms by promoting third molecular/recombination reactions. The higher heat capacity of CO_2 with respect to N_2 depresses the aiding chemical effect of CO_2 on system reactivity at low temperatures while emphasizing the inhibiting effect at high intermediate-high temperatures.

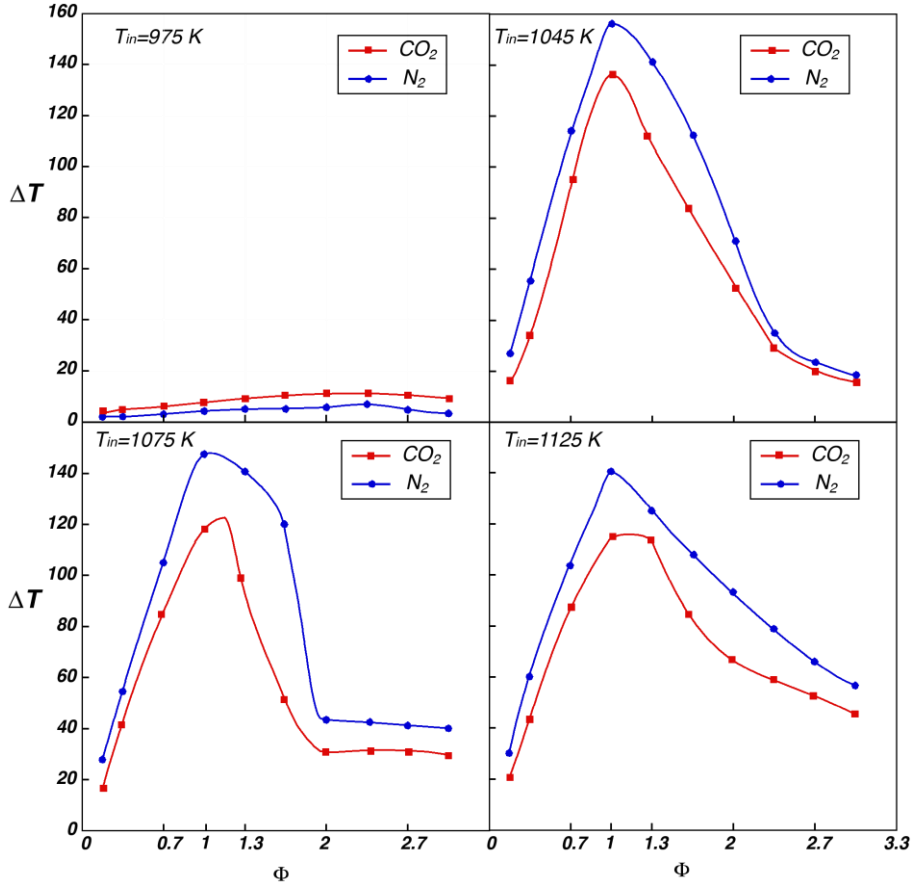

Figure 3.10 Experimental T as a function of Φ at different T_{in}. Comparison between systems diluted in N_2 and CO_2

3.4.4 Comparison between Experimental and Numerical Results for mixtures diluted in N_2 and CO_2

The aforementioned experimental conditions were simulated by PSR computations to assess the well-stirred reactor assumption based on the distributed characteristics of MILD combustion. Numerical simulations were performed using the AURORA module of ChemKin 3.7 [Rupley et al., 2003]. The "C1C3" [Ranzi et al., 2012] mechanism was chosen after evaluating its performance for predicting the main features of the oxidation process under MILD conditions in previous works [Sabia et al., 2014 a; Sabia et al., 2013; Sabia et al., 2014 b]. The overall heat transfer coefficient of the reactor was calculated using the thermal resistances in series concept based on the system boundary conditions, namely, the oven temperature in which the cyclonic chamber is located and the inlet flow temperature and velocity,

considering a non-reactive case. The calculated heat transfer overall coefficient value is 10 cal/m2 s K.

Figure 3.11 shows the increase of temperature ($\Delta T = T_{max}-T_{in}$) for propane/oxygen mixtures diluted in N_2 at 94% for four values of T_{in} (975 K, 1045 K, 1075 K and 1125 K) as a function of the Φ feed ratio. The numerical predictions are shown as blue lines, whereas the experimental results are in red. For T_{in} = 975 K, the numerical T increases with Φ from 10 K for Φ = 0.17 to 50 K for Φ = 1.7; then, it remains constant. For Φ > 2.7, the temperature increment slightly decreases. Although the experimental data confirm the trend of T with Φ, the values are significantly lower than the numerical ones. For T_{in} = 1045 K, the numerical temperature increase reach a maximum value (about 175 K) in correspondence of the stoichiometric condition (Φ = 1), then it diminishes and for Φ > 1.7 it slightly decreases.

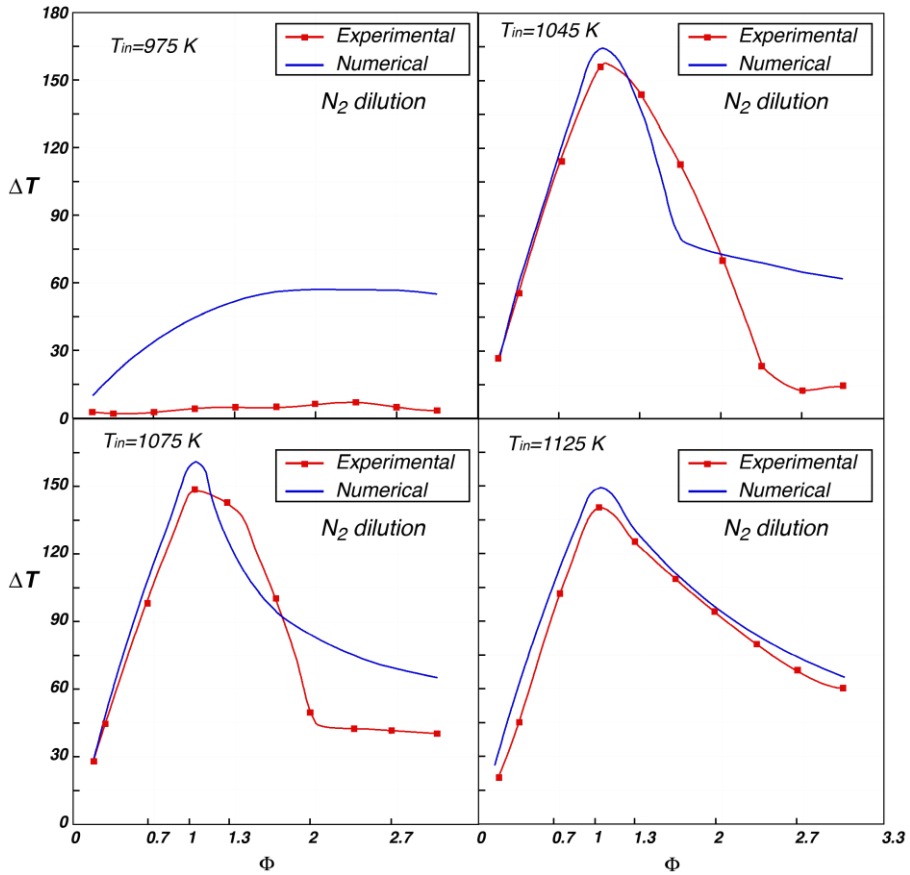

Figure 3.11 Comparison between the experimental and numerical T as a function of Φ for different T_{in} and N_2 dilutions

The experimental results confirm the trend depicted by the numerical simulations. For $0.1 < \Phi < 1$, the experimental data are well predicted by the integration. Some discrepancies occur for $\Phi > 1$, and in particular, for very rich fuel mixtures, the experimental results are lower than the numerical results. The difference between data is approximately 60 K. Similar considerations apply for T_{in} = 1075 K, even though for this inlet temperature, the difference between data is 30 K for fuel-rich conditions. For T_{in} = 1125K, the agreement between simulations and test data is very good over the whole equivalence ratio range.

In general, the comparison between the experimental data and predictions is good, except for low temperatures and, in the case of intermediate temperatures, for fuel-rich mixtures. A possible explanation for the discrepancy between results is the relative importance of the fluid dynamics (turbulent mixing) and chemical kinetic times. Chemical times depend on the local mixture composition and temperature.

At low inlet temperature (T_{in} < 1000 K) and for a fixed average residence time, the local strain rate induced by the strong interaction between flows promotes the quenching of ignition/oxidation reactions, causing a disagreement between the experimental and numerical results in the low reactivity region.

The chemical times are long for low temperatures and, at intermediate temperatures, for fuel-rich mixtures. For high temperatures, the chemical times are short enough to be comparable with the fluid-dynamic times; thus, the approach of a stirred reactor may work properly.

In this case, under MILD combustion conditions, quenching effects are not present, even at very high strain rates, and this finding is consistent with previous theoretical works [de Joannon et al., 2012] [Sidey et al., 2014] [Sorrentino et al., 2013].

On the basis of the comparison between the numerical and experimental temperature increase, the results imply that the system approaches the well-stirred reactor regime, dependent on T_{in} and the mixture composition.

Figure 3.12 shows the T for a propane/oxygen mixture diluted in CO_2 at 94% as a function of Φ for the same T_{in} considered in the N_2-diluted case.

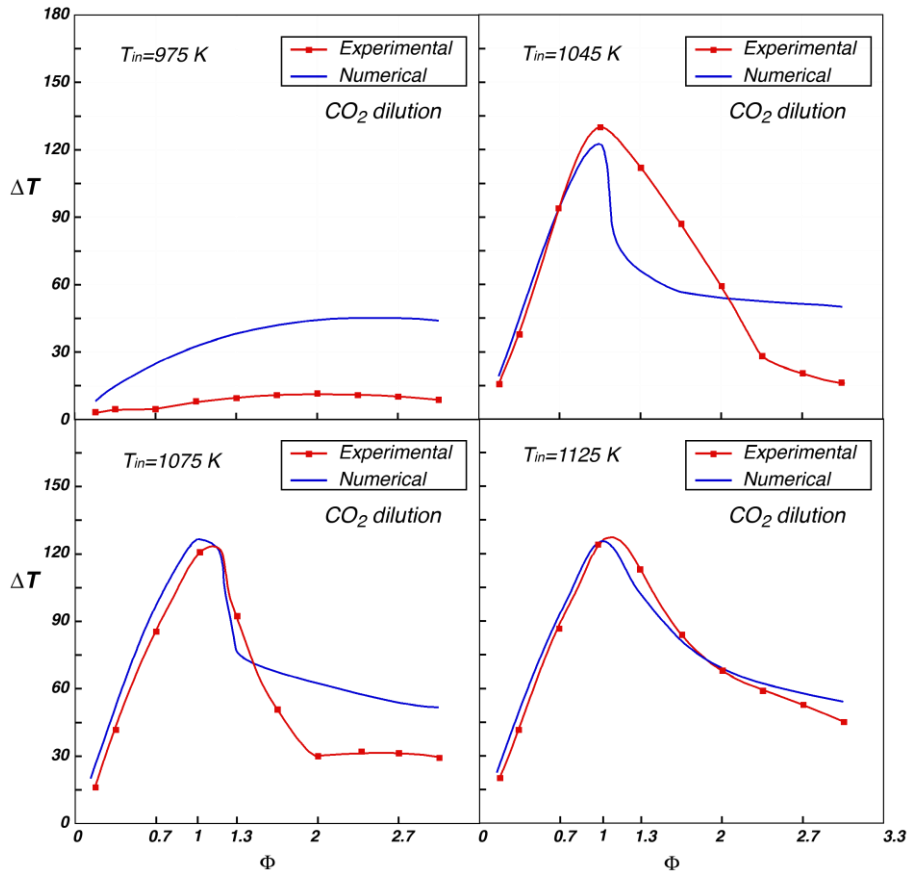

Figure 3.12 Comparison between the experimental and numerical T as a function of Φ for different T_{in} for the CO_2 dilution

In general, the agreement between the experimental data and the numerical results is similar to the case described in the previous section. For T_{in} = 975 K, the numerical and experimental results show the same trend of the temperature increase with Φ, but the simulated one are overestimated. In particular, the maximum numerical T is approximately 50 K, whereas the experimental value is 10 K. For T_{in} = 1045 K and 1075 K, the comparison between the experimental and numerical data is good for lean and stoichiometric mixtures but not for fuel-rich conditions, where for T_{in} = 1045 K the discrepancy is approximately 40 K, and for T_{in} = 1075 K, it is approximately 30 K. For T_{in} = 1125 K, the agreement is very good for any considered equivalence ratio.

The effect of the diluent nature on the ignition process can be emphasized by comparing the different T_{in}-Φ maps observed for N_2 and CO_2, reported in Figure 3.13. On the same graph, the dashed white line delimits the initial operating conditions where the reactor could be treated as a PSR. For temperatures below approximately 900 K and for fuel-rich mixtures, the “No Combustion” regime is

identified for both diluent species. As the fuel molar fraction is decreased, this area extends to slightly higher temperatures. The transition between the "No Combustion" and "Low Reactivity" area occurs at higher T_{in} when the diluent is N_2. This effect is due to the higher reactivity of CO_2 than N_2 at low temperatures, as previously explained. For T_{in} higher than approximately 1000 K, MILD combustion occurs with different features with respect to the nature of the diluent. In particular, MILD combustion is established for slightly lower inlet temperatures in the case of CO_2-diluted mixtures than for N_2-diluted mixtures. Furthermore, the transition from "Low reactivity" to MILD depends on the mixture composition, whereas for CO_2-diluted mixtures, the transition is not dependent on the equivalence ratio. These characteristics are due to the slightly higher reactivity of mixtures diluted in CO_2 and to the independence of the auto-ignition delay times with Φ for mixtures diluted in CO_2 [Sabia et al., 2014] at low-intermediate temperatures.

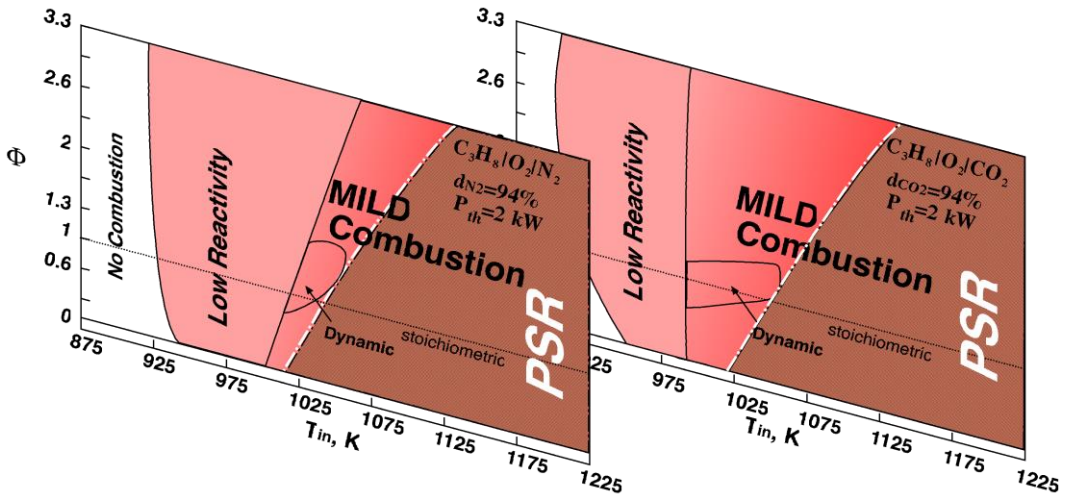

Figure 3.13 Comparison between the T_{in}- Φ maps obtained for propane/oxygen mixtures diluted in N_2 and CO_2 at 94% with the identification of the PSR-like region

The transition between the "Low reactivity" and "MILD Combustion" regimes for mixtures with compositions in proximity of the stoichiometric value occurs across the "Dynamic" behaviour. In agreement with previous works [Sabia et al. 2013], the onset of dynamic phenomenologies is related to the kinetics aspects of propane oxidation under diluted conditions. In particular, for lean fuel mixtures, propane oxidation occurs mainly through oxidative pathways, whereas for fuel-rich conditions, pyrolytic reactions are dominant [de Joannon et al., 2005]. In the proximity of the stoichiometric mixture, these kinetic routes compete with each other, promoting temperature oscillations. More specifically, for non-adiabatic systems, heat loss mechanisms from the reactor to the surroundings strongly interact

with this kinetic mechanism and emphasize the establishment of dynamic behaviour (thermo-kinetic oscillations) [de Joannon et al., 2004; Sabia et al., 2005].
In such a context, the dynamic region in the map for CO_2 is more extended with respect to the that obtained for mixtures diluted in N_2, suggesting an active role of CO_2 in the oxidation pathways [Sabia et al., 2014]. Nevertheless, some differences were recognized in the establishment of the different combustion regimes with dependence on the system external parameters for the two diluents; the Mild combustion regimes was established although the extreme mixture external/internal dilution levels for flow pre-heating temperatures was higher than approximately 1000 K for both the diluent species.
The stabilization process of MILD combustion is ensured by the strong heat/mass internal recirculation and the long residence times induced by the cyclonic flow pattern. Therefore, this configuration is a successful strategy to study MILD combustion features and represents a powerful tool to obtain important information on the complex, multi-dimensional interactions between fluid mechanics and chemical kinetics with the implementation of real-time optical and chemical measurements. The MILD combustion regime is characterized by a strong coupling between turbulence and chemistry because of the slower reaction rates (due to the dilution of reactants) with respect to conventional combustion [Galletti et al., 2007; Isaac et al., 2013].
Furthermore, the numerical simulations indicated that the PSR-like assumption was valid for a wide sub-set of the MILD region for both diluents. These results indicate that the cyclonic burner would serve, under the hypothesis of a well-stirred reactor, as a good canonical model for the optimization of kinetics under MILD conditions. The results are in accordance with several recent studies on the basic structure of the MILD combustion regime involving distributed reaction zones [Minamoto et al., 2015].
In particular, both the RANS and sub-grid PDFs studies suggest that the MILD combustion conditions involve distributed reaction zones regime combustion. This regime for MILD combustion is not because of idealized homogeneous reactive mixture but due to interacting flamelets having common features of conventional combustion and some distinctive characteristics of their own. These physical processes result in small scalar gradients, which are not the usual signature of typical flamelet combustion. Based on these observations, a PSR having a residence time representative of the local fluid-dynamic conditions is a suitable candidate for MILD Combustion.
In this context, PSR computations highlighted that the combustion characteristics of the cyclonic chamber are attributable to the achievement of a well-stirred reactor regime only for a sub-set of operating conditions. Therefore, novel turbulent combustion models have to be studied for MILD Combustion conditions in order to validate in a proper way the experimental data. For this purpose, recent studies pointed out that tabulated chemistry approaches involving a PSR could represent an

important solution for diluted combustion regimes with internal recirculation [Lamouroux et al., 2014].

3.5 Process Stabilization for Lower External dilution

A further step was, in order to characterize the stability of the oxidation process, to perform experimental tests at lower external dilution level. To evaluate the effect of mixture compositions and inlet temperatures on the combustion regimes established inside the chamber, experimental tests were carried out varying the equivalence ratio from 0.1 (fuel-lean conditions) up to 3.3 (fuel ultra-rich condition) and inlet oxidant temperatures (T_{in}) from 800 to 1000 K. At the same time, the mixture was diluted in nitrogen up to 90%. The average residence time (τ) was fixed to 0.5 s (configuration A3 as reported in Table 3.1). The inlet fuel injection velocity was fixed to 50 m/s and the oxidizer injection velocity was 38 m/s.
The combustor was allowed to run for about 2 min in each experimental test before taking the data. Temperature profiles were measured inside the reactor by means of two movable thermocouples. The first one is placed aside the wall and the other at the centerline of the combustion chamber. Another thermocouple is placed at the outlet of the combustion chamber. A 16-Channel thermocouple module, supplied by National Instruments, was installed and interfaced to a PC to monitor and store temperature data.
The evaluation of system behaviour was carried out on the systematic analysis of temperature profiles as a function of inlet pre-heating temperatures and mixture compositions (Φ). A first fundamental information on chemical evolution of the system came from the analysis of the shapes and trends of the axial temperature profiles measured in the different experimental conditions. More specifically, several main typologies of temperature profiles were recognized and associated to characteristic system behaviours.
The temperature profiles reported in Figure 3.14 are exemplifications of the several reaction modes experimentally detected.

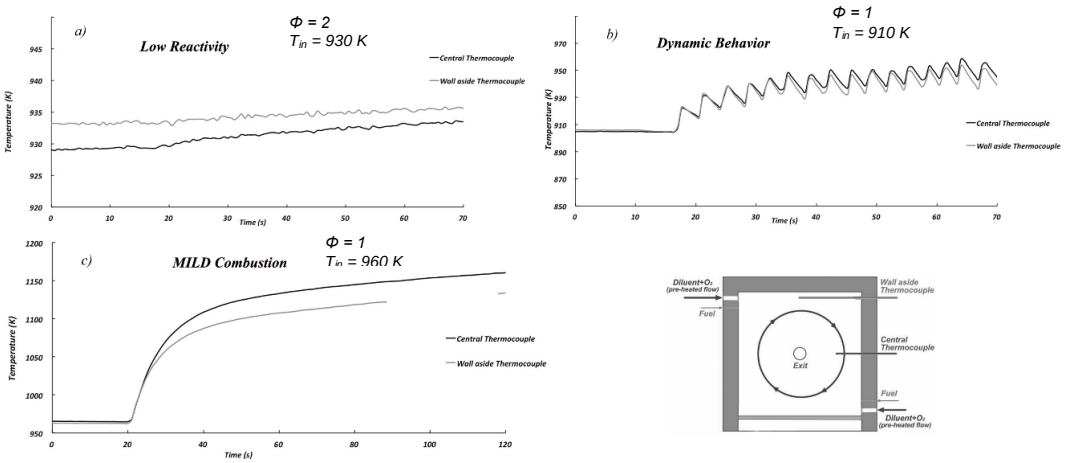

Figure 3.14 Temporal temperature profiles reported for different operative conditions

The profile corresponding Figure 3.14a) refers to a condition where the reactivity of the system is slow and the maximum temperature increase ($\Delta T = T_{max} - T_{in}$) is lower than 10 K. Such a behaviour was associated to a "Low Reactivity" condition. The temperature profile in Figure 3.14b) is representative by a dynamic phenomenology with ignition/extinction phenomena, characterized by temperature oscillations. Such behaviour was named "Dynamic Behaviour" regime. These flames were unstable and had the marks of a non-premixed flame, which appeared blue in colour close to the jet exit turning yellow further downstream. Closer observation revealed some downstream propagation from an upstream location toward the fuel exit. The temperature profile in Figure 3.13c) shows that T slowly increases reaching a maximum value. This profile corresponds to a "MILD Combustion" condition. In this case the thermal field in the combustion chamber is uniform and homogeneous [de Joannon et al., 2012].

On the basis of such a classification of temperature profiles, a map of behavior on a $\Phi - T_{in}$ plane was built up and reported in Figure 3.14 for N_2 dilution of 90% for the configuration A2. In particular, it refers to a temperature range between 800 and 1000 K and a Φ from 0.1 up to 3.3.

It is possible to distinguish several areas that were related to different typical temporal profiles. For low inlet temperatures (from temperatures up to about 890 K) the system does not ignite in the whole range of Φ investigated.

The area is indicated as "No-Combustion" and temperature profiles acquired for such conditions show no temperature increase and remain equal to the inlet value.

For temperature higher than 890 K and $\Phi > 1.3$ the mixtures ignite and then stabilize with a typical "Low reactivity" regime.

The latter establishes for with a temperature gradient lower than 10 K with respect to the isothermal inlet condition. For Φ lower than 1.3 and $890 < T_{in} < 940$ K the

"Dynamic Behavior" regime is identified. For temperature higher than 940 K the system shows different phenomenologies. For high Φ, low reactivity is still observed. For $\Phi < 2$ it is possible to recognize the "MILD combustion" regime. Increasing T_{in}, it enlarges up to cover the whole range of the equivalence ratio. In MILD combustion regime the system reaches the distributed combustion conditions and the temperatures in the combustion chamber become uniform.

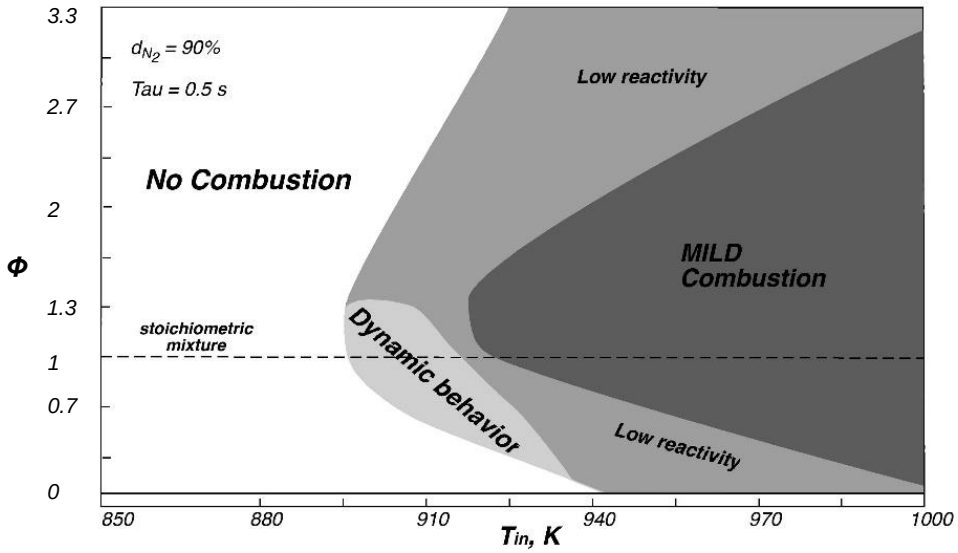

Figure 3.14 Experimental map of behaviour for mixtures diluted up to 90% in nitrogen.

3.6 Summary

After previous considerations about the requirements that an efficient burner has to satisfy, LUCY burner has been designed, installed and performed. It is possible to highlight that:

- in a first step, a numerical design of the cyclonic burner has been performed. It allowed to evaluate the geometrical and fluid-dynamic configuration that stabilize the cyclonic flow-field inside the combustion chamber
- LUCY burner has been installed and an experimental device has been built up
- Preliminary experimental tests have been performed in order to verify the stabilization of the MILD combustion process
- Further tests have been performed in N_2 an CO_2 as diluent, varying the equivalence ratio and the external dilution level: maps of combustion regimes have been obtained

4. STABILITY

In order to evaluate the optimal working conditions and the best performance of the combustor, several experimental campaigns have been performed. When the cyclonic burner here presented has been operated, the external parameters, as previously introduced, can be varied independently from each other. This is a very important feature because it means that it is possible to perform a parametric analysis and so evaluating the effect of the single parameter on the stability of the combustion process. Firstly, it was evaluated the stability of the process by means of the cyclonic flow and the range of operative conditions has been explored. Then, the performance of the system in terms process stability and pollutants emissions have been evaluated in order to identify the burner optimal operational range.
The operational parameters that were varied in the experimental campaigns are reported in the Table 4.1:

τ	XN_2	Φ	T_{in}
0.5 s	*AIR; 0.88; 0.94*	*0.17; 0.67; 1; 1.33*	***325 K – 1025 K***
0.5 s	*0.88*	***0.17 - 2***	*900 K*
0.5 s	***AIR – 0.94***	*1*	*900 K*
0.2 s – 5 s	*0.88*	*1*	*900 K*

Table 4.1 Overview of the operational parameters and working range investigated during the experimental campaigns

Such operational parameters were varied parametrically in order to investigate the combustion behavior of the system by monitoring the temperature profiles and the gas composition at the exit.
Detailed information of the investigated experimental conditions varying the residence time (τ), the external dilution (XN_2) and the equivalence ratio (Φ) are summarized in Table 4.1. In particular the dilution level is ranged from air conditions ($XN_2 = 0.76$) to $XN_2 = 0.9$ for $\tau = 0.5$ s and $\Phi = 1$. On the other hand the equivalence ratio is varied from ultra-lean ($\Phi = 0.1$) to fuel-rich conditions ($\Phi = 2$) at $\tau = 0.5$ and $XN_2 = 0.88$. Finally the average residence time τ is increased from 0.1 to 5 at $\Phi = 1$ and $XN_2 = 0.88$.
Experimental tests were carried out for C_3H_8/O_2 mixtures diluted in N_2 varying the external operating parameters of the system at environmental pressure. The

evaluation of the system performance was based on a systematic analysis of temperature profiles and emissions at the exit of the burner varying the operating conditions.

4.1 Sustainability evaluation

A further step toward the characterization of the cyclonic burner was the evaluation of its performance in terms of stabilization of the oxidation process in a range of operative conditions. The system was firstly schematized (see the scheme in upper right corner of Figure 4.1) as a non-adiabatic constant-volume CSTR reactor.
Part of the exit gases are recirculated back to the reactor to consider the mass and sensible enthalpy feedback mechanisms provided by the recycled exhausted gases to stabilize the oxidation process. Numerical integrations were performed using the ChemKin software [Rupley et al., 2013] and the C1C3 kinetic mechanisms [Ranzi et al., 2012] for a stoichiometric $C_3H_8/O_2/N_2$ mixture.
Pre-heating temperatures T_{in} was changed from 300 K up to 2000 K and the nitrogen contents from $XN_2 = 0.758$ (which corresponds to the nitrogen content in Air at an equivalence ratio $\Phi = 1$) up to $XN_2 = 0.98$. The reference mixture is a stoichiometric $C_3H_8/O_2/N_2$. The mass recirculation ratio K_v was fixed at a value of 5 that correspond to the average value of K_v for existing practical devices.
The chamber volume ($V_o = 2000$ cm^3) was adjusted to keep constant the averaged initial residence time τ at a value of 0.5 s.
The numerical results were reported in Figure 4.1 in a dilution level – thermal power plane, where the iso-preheating temperature lines are reported. As expected, thermal power diminishes both increasing the inlet temperature (due to the reduced gas density in the reactor) and the dilution level of the mixture (due to the higher inert gases concentration in the reactor).

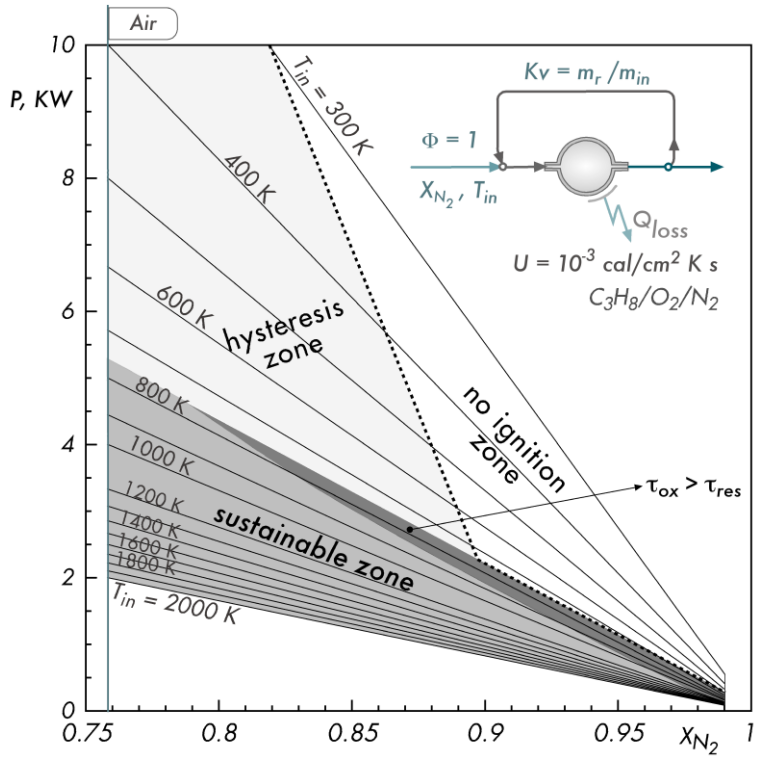

Figure 4.1 Numerical identification of the mixture "pre-heating temperatures-dilution level" values to sustain the oxidation process in a constant volume non-adiabatic system with a fixed recirculation ratio and identification of relative thermal power.

In Figure 4.1 it is clearly observable that for low T_{in} and for high XN_2, a "no ignition" zone can be numerically identified. In contrast, at pre-heating temperatures higher than a threshold value, ignition and oxidation processes take place in a stable and sustainable manner. Temperature threshold value increases passing from T_{in} = 785 K for air (XN_2 = 0.758 at Φ =1) to 950 K for XN_2 = 0.98. The "sustainable" zone enlarges with the pre-heating temperature while narrows with the mixture dilution level.

At temperature lower than the threshold level but outside the "no-ignition zone" there are two possible conditions. In a first zone, the residence time is not long enough to have a complete oxidation of the reactants within the chosen residence time. In this case the actual flow residence time (τ_{res}), induced by the gas volumetric expansion for the oxidation process is lower than the oxidation time (τ_{ox}), i.e. of the time required to achieve a complete oxidation of the reactants. This incomplete oxidation zone enlarges at higher dilution levels. Finally, a fourth zone can be identified above the incomplete oxidation one and on the left side of the plane. In this zone a "hysteresis" behavior can be found. As the dilution level increases, the hysteresis behavior is observable at higher T_{in} and completely disappear at XN_2 = 0.9.

In summary, it is possible to define the following zones:
I) “no ignition”: T_{in} and XN_2 delineate operating conditions for which no ignition occurs;
II) “incomplete combustion”: the ignition/oxidation process occurs but $\tau_{res} < \tau_{ox}$.
III) “sustainable”: the ignition/oxidation process occurs and $\tau_{res} > \tau_{ox}$.
IV) “hysteresis”: a second stationary steady state for the same operating conditions was numerically predicted.

In order to better explain the main features of the combustion process in the four zones, in Figure 4.2 the temperature increment as a function of T_{in} for Air, XN_2 = 0.88 and XN_2 = 0.94 are reported.
For the Air case (XN_2 = 0.758) the reactor working temperature (T) remains equal to the inlet one up to 785 K, then the mixture ignites (dotted-dashed line) and T becomes equal to about 1480 K. As T_{in} is increased, the temperature increment diminishes (continuous line). For T_{in} < 785 K, a secondary solution was predicted (dashed line). By lowering T_{in}, it is possible to note that the temperature increment increases, because of the mixture thermal power increase.

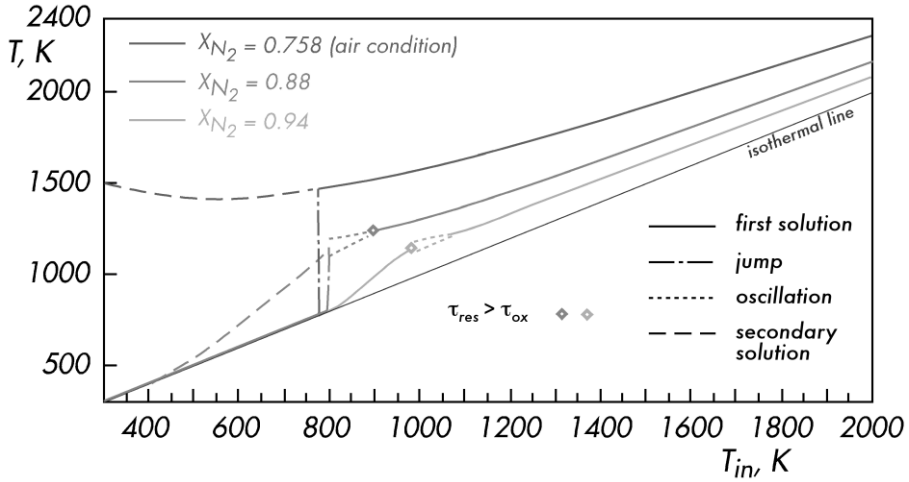

Figure 4.2 Numerical temperature increment as a function of T_{in} for air and two mixture dilution levels (XN_2 = 0.88, 0.94).

For XN_2 = 0.88, the mixture ignition temperature (T_{in} = 800 K) is slightly higher than in the previous case, while the temperature increment is less pronounced, because of the higher dilution level. At T_{in} > 800 K, periodic temperature oscillations are predicted up to T_{in} = 900 K. Then one steady state solution is obtained. In the figure the sustainability of the oxidation process is identified by the grey rhombus. For T_{in} > 900 K, the criterion is satisfied. For T_{in} < 800 K a secondary steady state is identified. In contrast with the previous case, the T diminishes as T_{in} decreases. The

system is not able to sustain the oxidation process because the low heat release rate does not compensate heat losses. In the last case, (XN_2 = 0.94), the reactor temperature increases with T_{in} smoothly without temperature jumps. Also for this condition, periodic temperature oscillations are detected.
Later on, a stationary steady solution is obtained. For low temperatures, no double solutions were predicted, resembling a typical condition of MILD combustion processes [Sabia et al., 2015; de Joannon et al., 2012].

4.2 Operational procedures: "Upward" and "Downward"

Moreover, further experimental tests were carried out for $C_3H_8/O_2/N_2$ mixtures varying the inlet temperatures of the main flow (T_{in}) from 500 K to 1100 K and the initial nitrogen mole fraction (XN_2) from air to XN_2 = 0.94. The mixture equivalence ratio (Φ) was changed from fuel lean to rich values. The flow average residence time was fixed at 0.5 s.
The results were obtained by using two different operative procedures, that are schematized in the sketch reported in the top right of Figure 4.3. The upward procedure allows to achieve the reactive conditions by increasing the inlet temperature of the oxidizer from a chemically frozen state by means of an external preheating systems, while the downward procedure performed to achieve the reactive conditions from a partially or fully burned state by decreasing the inlet temperature of the oxidizer.

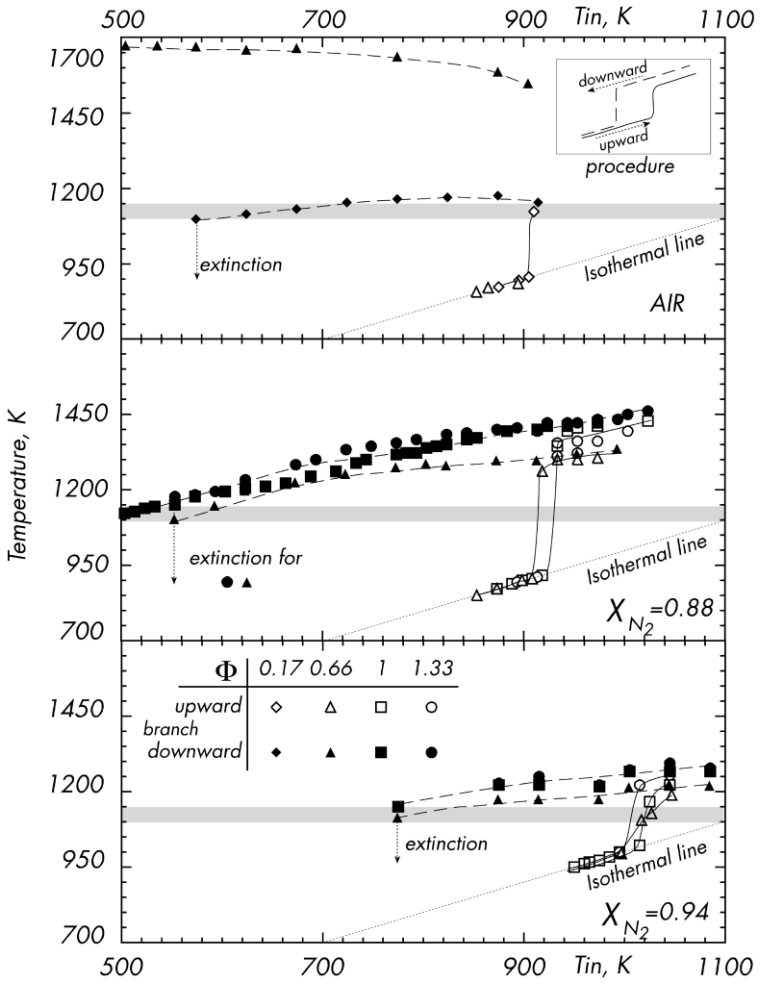

Figure 4.3 Experimental temperature increment as a function of T_{in} for three $C_3H_8/O_2/N_2$ mixtures (with oxidizer stream composed by air or diluted air with XN_2 = 0.88 and 0.94) and for fuel lean, stoichiometric and rich conditions.

Such procedures permitted to identify a hysteresis behavior, corresponding to different working temperature for the same external parameter. It is worth to note that the downward procedure allows for reaching reactive conditions not achievable with the upward procedure, increasing the working range of the burner even for lower external dilution of the system.

Figure 4.3 reports the maximum values of the temperatures inside the burner (T) as a function of T_{in}, and equivalence ratios (Φ) at three XN_2. The open and closed symbols correspond to results obtained with the upward and downward procedures respectively.

As shown in Figure 4.3, the minimum oxidizer T_{in} useful to achieve the reactive condition varies from T_{in} = 910 K to T_{in} = 1010 K, testifying that the ignition occurs in a range of 100 K for all the conditions considered. These temperature values

correspond to the lowest (air) and the highest (XN_2 = 0.94) value of the nitrogen molar fraction respectively, at the lowest Φ used. It is evident that for a fixed Φ, T measured for air are higher than temperatures achieved for XN_2 = 0.88 and XN_2 = 0.94 within T_{in} range here considered, for both the operational used procedures.
In the upper part of Figure 4.3, T measured with air for Φ = 0.17 and Φ = 0.67 were reported.
At Φ = 0.17, the upward procedure leads to a stable working condition for T_{in} = 910 K reaching a working temperature of about 1150 K. Starting from this condition, following the downward procedure, the burner temperature decreases down to reach the extinction temperature limit of T = 1100 K at T_{in} = 580 K.
No extinction limit has been reached at Φ = 0.67 in air down to T_{in} = 500 K.
The extinction temperature limit of T = 1100 K falls in the gray band reported in the figure, from 1100 K and 1150 K. This band highlights the working temperature region at which extinction occurs for most of the experimental tests here considered. This is confirmed by the temperature profiles reported in Figure 4.3 for higher XN_2. At XN_2 = 0.88, for Φ = 0.67 and 1.33 the extinction occurs for T = 1100 K and 1150 K respectively for T_{in} = 580 K.
Also in this case, no extinction limit has been reached at Φ = 0.67 in air up to T_{in} = 500 K. For XN_2 = 0.94 the extinction temperature limit has been reached for all the three Φ considered at about T_{in} = 760 K. Also in this case, the extinction occurs at T between 1100 K and 1150 K. These temperatures in the chemical kinetics of combustion processes represent noticeable values, because they are typical values for the onset of the high temperature branching mechanism [Sabia et al., 2014a].
It is worth noting that the upward procedure makes the burner reach the stable condition with a sudden increase of temperature from low to upper branch of the working temperature curve, as it occurs in a typical ignition process.
In contrast, at XN_2 = 0.94 and Φ = 0.66 and 1, the upward procedure allows for stabilizing working conditions characterized by a limited temperature increase and the burner reaches the upper branch of working temperature in a smooth way. It is remarkable that a flameless combustion has been observed in all the tested working conditions. This observation is also supported by the substantial uniformity of the temperature profiles inside the reactor measured by means of the mobile thermocouples.

In particular, the hysteresis behaviour shows the presence of two possible working regimes for a fixed inlet temperature, corresponding to a low and high fuel conversion respectively, for a certain range of inlet conditions. The transition from chemically frozen to fully burning states are crucial to understand ignition and extinction behaviours in combustion systems. Therefore, the analysis of these phenomena appears to be essential.
Furthermore, the minimum preheating temperature that led to reactive conditions is about 900 K for the upward procedure showing a transition between the chemically frozen and the fully burning states. In this case the transition between the low

reactivity and high reactivity branch is characterized by instability behaviours where unstable diffusion flames occurs during the time before the stabilization of MILD combustion conditions with homogeneous thermal fields. For the upward mode, a sudden increase of temperature corresponding to a nearly complete fuel conversion. On the other hand, the downward procedure has allowed to stabilize MILD combustion regimes not achievable from frozen conditions, thus extending the range of operative conditions of interest from a practical point of view.
It is worthwhile to note that during the downward procedure extinction phenomena can occur because of heat removal or quenching reactions. Therefore, sudden extinction behaviours are absent in such operating conditions. This result is of particular interest for the application of MILD technology to real systems. In fact, from a technological point of view, the cyclonic burner can reach self-sustaining conditions as a function of the external parameters when a stable MILD combustion is reached [Sorrentino et al., 2017].
Moreover, the occurrence of a hysteresis behavior, over the entire pre-heating temperature range, potentially increases the operability range of the system by using a suitable ignition strategy. It permits to stabilize MILD Combustion also with very low preheating levels. In such conditions radical pools seems to play a key role in the absence of extinction behaviours [Coriton et al., 2013].

4.3 Stability limits

The extension of the stability range goes beyond the conditions characterized so far. As a matter of a fact the cyclonic burner is stable in a range of parameters very wide with respect to the one of a standard burner as already discussed so far. This is further testified by the curves reported in Figure 4.4 where the extinction Φ, corresponding to the lowest possible Φ, for a fixed Φ, where stable working conditions could be established, is reported as a function of X_{N_2} at three inlet temperatures.

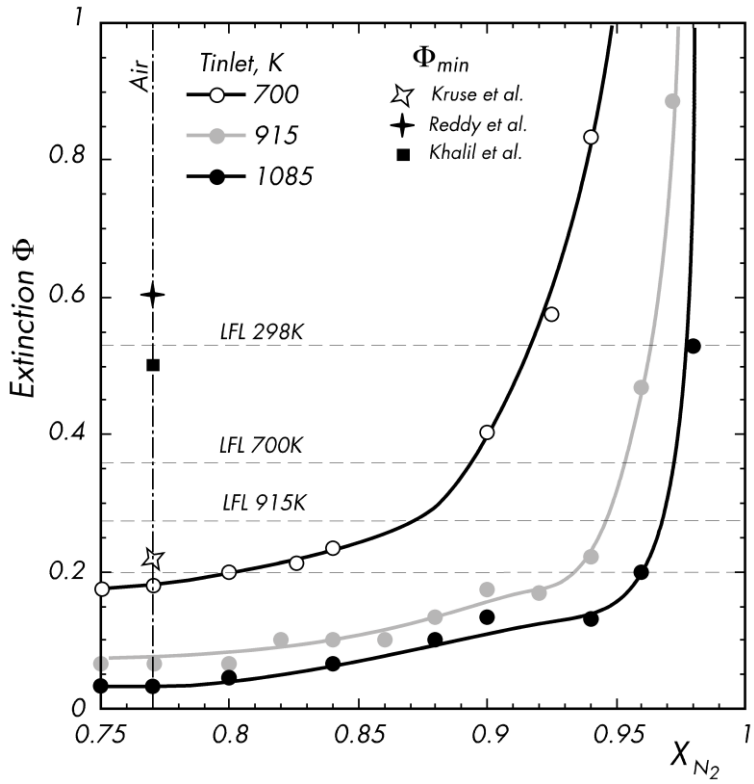

Fig. 4.4 Experimental identification of Φ_{ext} as a function of $C_3H_8/O_2/N_2$ mixture dilution levels on curves parametric in T_{in}.

On the same diagram also the Φ corresponding to the low flammability limit (Φ_{LFL}) were reported for the three considered temperatures. The dependence on temperature of Φ_{LFL} was evaluated according to the indication reported in Zabetakis [1965] and in Bolshova et al [2012]. On the other hand, the dependence of Φ_{LFL} was disregarded in this evaluation because it is well known that the dependence on diluent concentration is not high enough to affect the results presented here [Zabetakis, 1965].

The region above each curve identifies stable working conditions. It is possible to see that for a fixed T_{in} the extinction Φ decreases with a dilution decrease up to reach a nearly constant value. As expected, for a fixed XN_2, extinction Φ decreases by increasing the temperature. It has to be noted that the cyclonic burner is able to operate in stable conditions for Φ lower than the Φ_{LFL}. It is noteworthy to underline that the working temperature corresponding to the falls between 1000 K and 1100 K independently on the T_{in} and considered.

For comparison, on the same diagram, the lowest Φ used as working conditions of some advanced, new generation burners were reported [Reddy et al., 2013; Kruse et al., 2015]. As it is evident, the widest range of working conditions compete to the cyclonic burner.

4.4 Low Emissions Burner

Furthermore, in order to evaluate the system performance in terms of CO and NO_x emissions at environmental pressure, the impact of global equivalence ratio (Φ), external dilution level in terms of nitrogen content (XN_2) and average residence time (τ) on pollutants formation and process stability were analyzed.
In fact, results obtained as a function of a single parameter of the system (T_{in}), keeping fixed the others (Φ, XN_2, τ), do not allow to detect regions of jointly low NO_x and CO emissions and they do not permit to characterize the system performance for small-scale applications and its flexibility for wide ranges of working parameters. In this case experimental measurements were performed for a fixed value of the pre-heating temperature (T_{in} = 900 K) that serves as a reference value to investigate the effect of the other system parameters. Propane is used as fuel and the oxidizer stream is oxygen diluted with nitrogen.
When the equivalence ratio Φ is varied, the fuel and oxidizer flow rates remain constant (to keep constant the jets velocity and momentum) and the nitrogen content in each stream is adjusted to match the required equivalence ratio. Afterwards, the dilution level (XN_2) is increased from air conditions to XN_2 = 0.9 in order to decrease the inlet oxygen level. In this case the equivalence ratio is set to the stoichiometric value (Φ = 1) while τ = 0.5 s.
Finally, the average residence time of the chamber (τ) is varied from 0.1 to 5 s while the dilution level and the equivalence ratio remained constant to XN_2 = 0.88 and Φ = 1, respectively.
The residence time (τ), as already mentioned, is an average value (space-time of the system) calculated as the ratio between the volume of the combustion chamber (V) and the total volume flow rate of fresh gases. Such operating parameter affects both the gas recirculation level and the thermal power of the system. Short residence times improve burnt gas recirculation therefore affecting the fluid-dynamic of the system and the inlet fuel mass flow rate (nominal thermal load).

4.4.1 Effect of the equivalence ratio (Φ)

The performances of the cyclonic burner have been evaluated even in terms of pollutant emissions and maximum temperature inside the chamber by varying the equivalence ratio. In particular, carbon monoxide (CO) and nitrogen oxides (NO_x) concentrations in the exhaust gases were acquired at the exit. CO and NO_x emissions have been measured for the whole range of the operational conditions. Measured emissions are normalized to 15% O_2 in the exhaust gas [Baukal et al., 2001] according to:

$$X_{15,i} = X_i \left[\frac{(20.9 - 15)}{(20.9 - XO_2)}\right]$$

where X_i is the measured mole fraction of species i; $X_{15,i}$ is the normalized species mole fraction at 15%, and XO_2 is the measured O_2 mole fraction in percent in the exhaust gas.

The maximum temperature inside the reactor T_{max}, NO_x and CO emissions were reported in Figure 4.5, varying the mixture equivalence ratio Φ from 0.17 to 2 for a fixed external dilution level (XN_2 = 0.88) and a fixed residence time (τ = 0.5 s).

The main flow rate temperature T_{in} was set equal to 900 K. T_{max} inside the reactor (Figure 4.5a) is equal to 1150 K at Φ = 0.3, then it increases with Φ reaching its highest value (1400 K) for the stoichiometric mixture composition (Φ = 1).

Afterwards, for fuel rich conditions it decreases reaching 1300 K for Φ = 1.7. In this respect it is worth noting that the maximum allowable temperature is lower than the adiabatic flame one due to heat loss effects. Figure 4.5b reports the CO (empty square) and NO_x (triangle symbols) emissions in the exhaust gas as a function of Φ. NO_x emissions depict a non-monotonous profile and they are remarkably lower than single-digit limit (< 10 ppm) throughout the examined range of Φ.

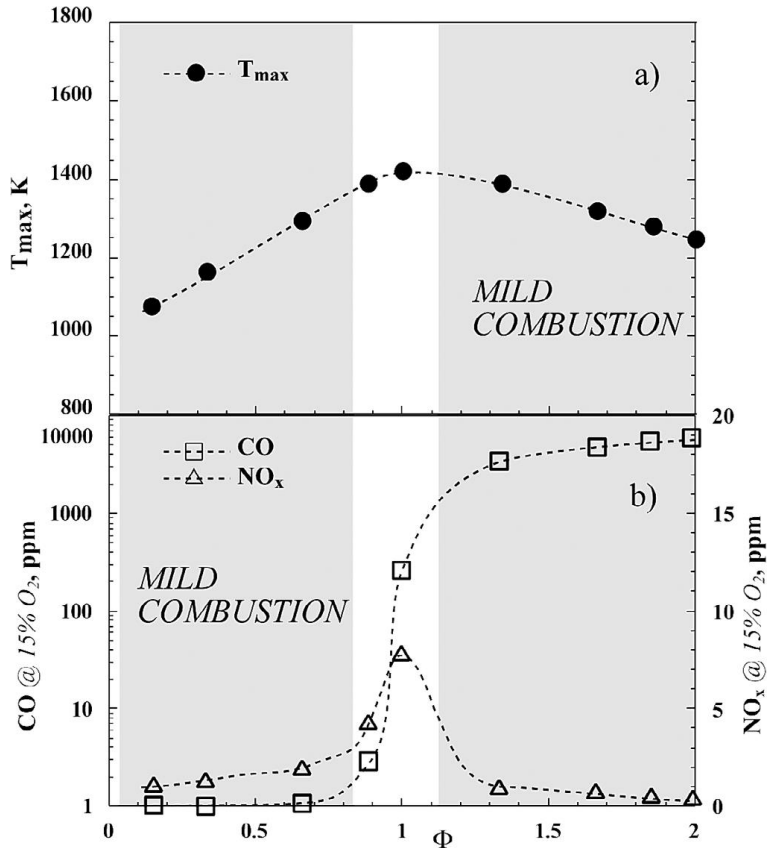

Figure 4.5 T_{max} (a), CO (square symbol) and NO_x (triangle symbol) emissions values (b) at $\tau = 0.5$, $XN_2 = 0.88$, varying the equivalence ratio (Φ)

In particular, at $\Phi = 1$, NO_x emissions reach their maximum concentration of 9 ppm. It is here important to note that the main effect of the equivalence ratio is to increase the NO_x emissions for stoichiometric mixture compositions and such maximum values are envisioned to be related to NO_x formation with the thermal route [Kahlil et al., 2015].
The distributed reactive regions mostly suppress the formation of NO through thermal mechanism due to uniform thermal field in the entire combustion zone and avoidance of high temperature regions ($T_{max} < 1500$ K).
Differently from NO_x emissions, CO depicts a rising trend with the equivalence ratio, for the whole range of Φ here considered. CO emissions rapidly increase from 1 ppm to 200 ppm by increasing the equivalence ratio from 0.17 to 1. Then, for $\Phi > 1$, the CO emissions rapidly increase to values higher than 3000 ppm. Such a behavior is related to the partial oxidation of the fuel in rich conditions with the occurrence of fuel pyrolysis conditions and the lowering of temperatures inside the reactor [Sabia et al., 2016].
In Figure 4.5 the nominal MILD Combustion region was reported. It depicts conditions were the maximum allowable temperature is lower than the auto-ignition one.
It is worthwhile to note that the combustor efficiency, in terms of pollutant emissions, is very high also outside the grey areas.
Such a result is amenable to the effect of the burned gas recirculation that locally provides for dilution and sensible enthalpy to the fresh gases. The obtained results for NO_x and CO emissions have clearly shown that ultra-low pollutant emissions were obtained for equivalence ratio lower than 0.95.
It is remarkable that it is possible to operate the cyclonic burner in a wide range of fuel-lean conditions ($\Phi < 1$), up to the stoichiometric value, obtaining very low CO and NO_x emissions.

4.2.2 Effect of the External dilution level (X_{N_2})

The maximum system temperature T_{max} and the pollutant emissions, in terms of NO_x and CO, were obtained as a function of the overall dilution level (XN_2), while the mixture equivalence ratio was fixed at $\Phi = 1$, and the residence time was fixed at $\tau = 0.5$ s.
They are reported in Figure 4.6. As shown in Figure 4.6a, the maximum temperature inside the burner decreases almost linearly with XN_2 (i.e. it increases with XO_2). As expected, high values of XO_2 in the inlet flows lead to higher T_{max}.

For $XN_2 = 0.86$ the system maximum temperature is 1400 K, while for $XN_2 = 0.80$ the system attains $T_{max} = 1600$ K. Figure 4.6b reports NO_x and CO emissions as a function of the dilution level.

Figure 4.6b shows that NO_x emissions progressively decrease for higher dilution levels according to the lowering of the system temperature, as expected. For highly diluted systems ($XN_2 > 0.84$), they are lower than 10 ppm (single-digit). High inlet oxygen levels led to an increase of the system temperature and thus the thermal NO_x path is enhanced, implying NO_x emissions that exceed the single-digit threshold because the system approaches air combustion mode [He et al., 2016; Cao et al., 2015].

Despite that, it is worthwhile to note that globally NO_x emissions are always lower than 20 ppm, even operating the cyclonic burner close to air conditions. CO emissions (Figure 4.6b) show an opposite trend with respect to NO_x. They decrease from 900 ppm for $XN_2 = 0.9$ to 2 ppm for Air conditions. It is worth noting that CO emissions are lower than the single-digit level (< 10 ppm) for $XN_2 < 0.85$. Such a behavior is ascribable to the increasing of the maximum temperature, while diminishing XN2, thus to an increase of the system reactivity.

In particular, the strong influence of the system temperature on the CO/CO2 equilibrium [Wang et al., 2014] partially explains this trends. In fact, the CO concentration steeply decreases when the reactor temperature is higher than 1400 K as a consequence of the decrease of the mixture overall dilution level.

On the other hand, under highly diluted conditions ($XN_2 > 0.88$), the system reactivity decreases, along with working temperatures, and the fuel oxidation times becomes not compatible with the residence time, thus leading to an increase of CO [de Joannon et al., 2017; Kruse et al., 2015].

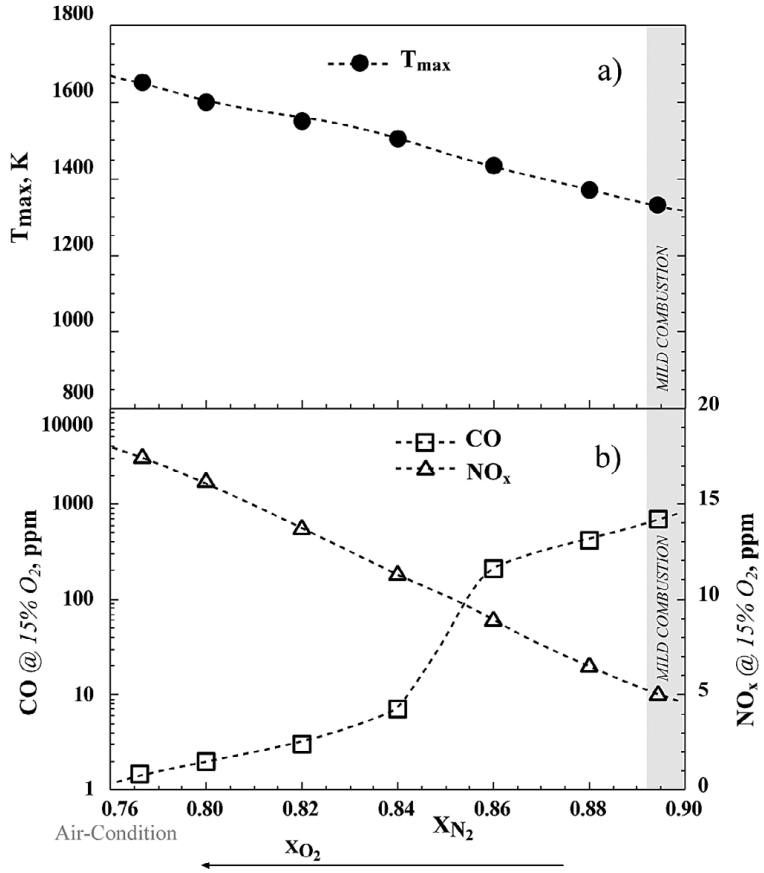

Figure 4.6 T_{max} (a), CO (square symbol) and NO_x (triangle symbol) emissions values (b) at $\tau = 0.5$, $XN_2 = 0.88$, varying the external dilution level (XN_2)

4.4.3 Effect of the average residence time (τ)

The residence time of the reactants within the combustion chamber is a significant parameter to achieve stable and complete combustion [Beer et al., 1965]. Mixture flow rate variations are strongly related to both the nominal thermal power and the velocity field (recirculation patterns) in the combustor, thus to the particle residence time distribution of fluid particles in the reactor [Doost et al, 2016].

Experimental tests were carried out to evaluate the performances of the cyclonic burner as a function of τ. Figure 4.7 shows the experimental results in terms of maximum system temperature T_{max}, nominal thermal power P_{th} (kW) and pollutant emissions as a function of τ for a stoichiometric condition ($\Phi = 1$), $XN_2 = 0.88$, $T_{in} = 900$ K.

The maximum temperature T_{max} inside the reactor and the nominal thermal power, as reported in Figure 4.7a, strongly depends on t. For $\tau = 0.2$ s, the nominal thermal

power is equal to 3.85 kW and for $\tau = 5$ s becomes 0.21 kW. For the former residence time, T_{max} is equal 1630 K while for the latter $T_{max} = 1060$ K. The strong decreasing of the system maximum temperature for very high τ values is mainly ascribable to the combined effect of the nominal thermal power and heat loss variation with the main flow rate.

Figure 4.7b reports the NO_x and CO. NO_x levels monotonously decrease with τ. They are lower than 10 ppm (single-digit) for $\tau > 0.3$ s and become also zero for $\tau > 3$ s. This result is due to the decreasing of system temperatures. Lower values of the mean residence time ($\tau < 0.3$ s) lead to NO_x emissions slightly higher than the single-digit threshold and they reach almost 14 ppm. The higher temperature conditions ($T_{max} >$ 1400 K) promote thermal NO_x routes. The CO emissions rapidly decrease from 2000 to 3 ppm when the mean residence time is increased from 0.2 s to 1.8 s, then they reach a minimum value for $\tau = 1.9$ s (CO < 10 ppm). Afterwards, for $2 < \tau < 4$ s CO emissions increase and for $\tau = 4.7$ s they are 500 ppm. It is still remarkable that both NO_x and CO emissions are very low in a wide range of operative conditions here investigated.

MILD Combustion region was also reported in Figure 4.7. It can be identified for $\tau > 0.8$ s. CO emission profiles are mainly associated with two asymptotic system behaviours: for very short residence time values ($\tau < 0.5$ s), the condition $\tau_{res} < \tau_{ox}$ occurs, which means that the residence time of the fluid particles (τ_{res}) in the combustion chamber is shorter than the oxidation time of the diluted mixture (τ_{ox}).

On the other hand, for long average residence times ($\tau > 2$ s) the flow velocities are very low, thus avoiding the formation of a cyclonic flow inside the combustion chamber. Specifically, the toroidal cyclonic structure for very low inlet jet velocity decreases its intensity and leads to an inadequate recirculation.

Therefore, such results are very important for scaling methodologies of this burner. In particular, high thermal power can be obtained for very short mean residence time values, implying higher CO emissions for a fixed system configuration.

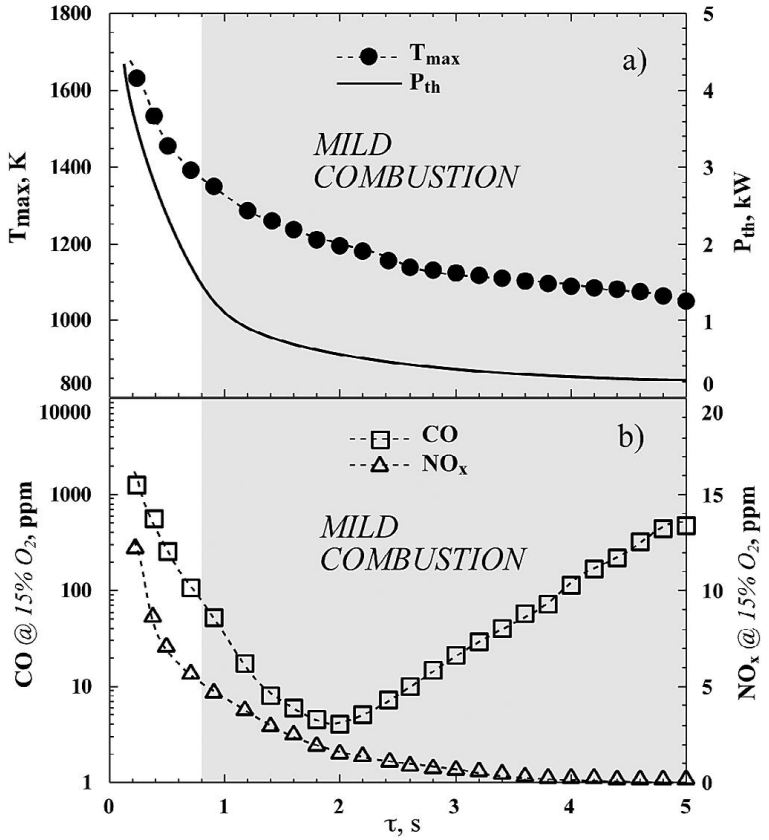

Figure 4.7 T_{max} (black filled symbol) and P_{th} (solid line) values (a), CO (square symbol) and NO_x (triangle symbol) emissions values (b) at $\Phi = 1$, $XN_2 = 0.88$, varying the residence time (τ)

4.5 Residence Time: cyclonic flow-field stability

In order to give an explanation of the pollutant emissions profiles depicted in Figure 4.7, flow field and vortex dynamics under non-reacting conditions are presented here for different values of τ (and therefore for different inlet velocity values). Moreover, tests for different values of τ permit to put in evidence the effects of the fluid-dynamics on the stirring/mixing phenomena and on the attainment of a stable vortex flow.

In the non-reacting flow, a helix shaped vortical mode is recognizable for low values of the average residence time (high velocities and Reynolds number) as shown in Figure 4.8. The results reported in Figure 4.8 were obtained by means of CFD simulations on a hexahedral grid of the cyclonic burner geometry and by means of Fluent 6.3 code to solve the cold flow-field. The oxidizer jet was considered as the

only stream that induce the cyclonic motion in the chamber, for the simplicity of cold flow simulations.
In particular, Figure 4.8 reports the iso-surfaces relative to the swirling strength of the vortex flows with a chosen threshold of 0.1% of the maximum value of the swirling strength for four selected values of τ.
The flow field is visualized by the 3D swirling strength (σ). The swirling strength is defined as the magnitude of the imaginary part of velocity gradient tensor eigenvalues, and represents the rate at which local streamlines spiral around a center point in a reference frame moving with the flow [Zhou et al., 1999]. It is noted that the exact definition of σ in terms of swirling rate is strictly valid only where the flow is locally isodense, which may be the case in the present reacting flows. However, it provides a good visualization of the flow and vortex structures.

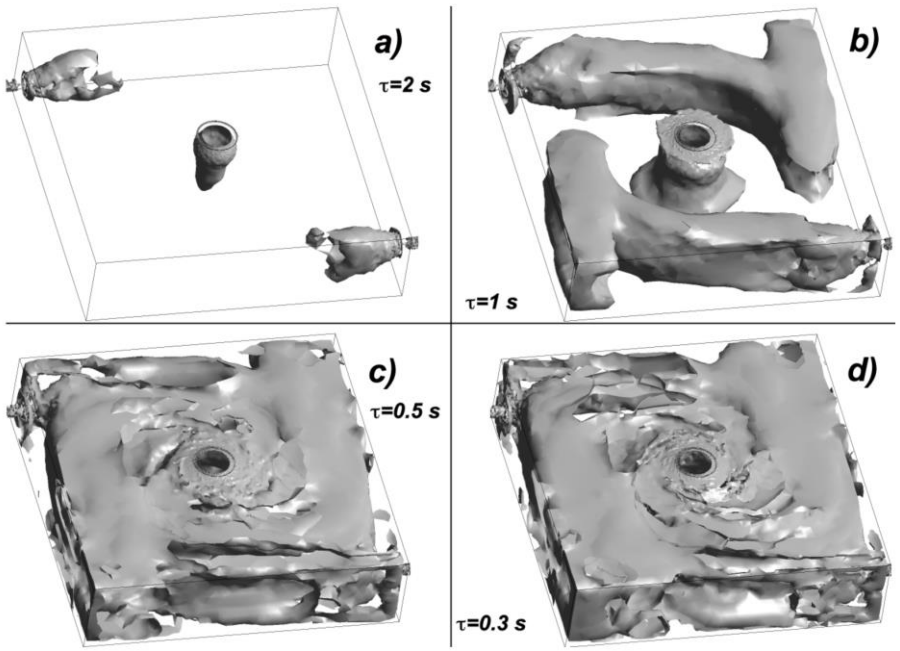

Figure 4.8 Isosurfaces of the Swirling Strength obtained by means of numerical simulations for LUCY burner for four selected values of the average residence time (τ)

For high inlet velocities (Figure 4.8c, 4.8d) and hence low τ values, the helical mode was present and it was stronger (higher vorticity and swirling strength) than in the lower velocity cases (Figure 4.8a, 4.8b) where the average residence time is higher than 1. The dominant dynamic flow structures in the cases at $\tau < 1$ were symmetric

(toroidal) vortices that were shed from the shear layers between in inflow and the central recirculation zones (CRZ).
Such a behavior partly justifies the trend of CO emissions for τ values higher than 2 s where they steeply increase up to 300 ppm for $\tau = 4$ s. In particular, at these conditions, the toroidal vortex structure steeply decreases its strength and intensity, due to the inlet Reynolds number diminishing (low inlet velocity of the jets) and therefore the internal recirculation/engulfment and the periodic mixing between fresh reactants and burned products get worsened.
The previous arguments provide a partial explanation of the main reasons behind the non-linear CO profiles as a function of the mean residence time of the flows inside the chamber. In fact, the toroidal vortex structure, due to the fluid-dynamics of the system, does not justify the very low CO levels when $1< \tau <2$ s.
In this respect, the Residence Time Distribution (RTD) of the fluid particles inside the combustor could help to provide a more complete explanation of the CO formation profiles. In particular, as well known the oxidation of CO is a slow process in all combustion systems so that lower residence time will result in higher CO emission levels at the exit of a combustor [Van Der Lans et al., 1997].
In this sense, an indication of the residence time distribution can provide important information about the fraction of gases in the reactor having low residence time, that leads to an increase of the CO emissions. Hence, with a favorable residence time distribution, giving minimal fraction of gases having low residence time, one can have higher conversion of CO and consequently lower CO emissions with the same nominal power and therefore the same average residence time.
Numerical calculations of residence time distribution were performed for the four cases already reported in Figure 4.8 ('case a-d'). First a steady state solution of non-reacting (only the oxidizer) flow field was obtained and then a passive tracer, having same property as that of the oxidizer was introduced from the injection location. Thereby, the surface-area averaged tracer concentration is monitored as a function of time at the outlet.
Residence time distribution calculations for the four conditions are shown in Figure 4.9 and they reported the exit age distribution E(t) that is a function that describes in a quantitative manner how much time different fluid elements have spent in the reactor. The average residence time for the four cases is reported on each profile in Figure 4.8.

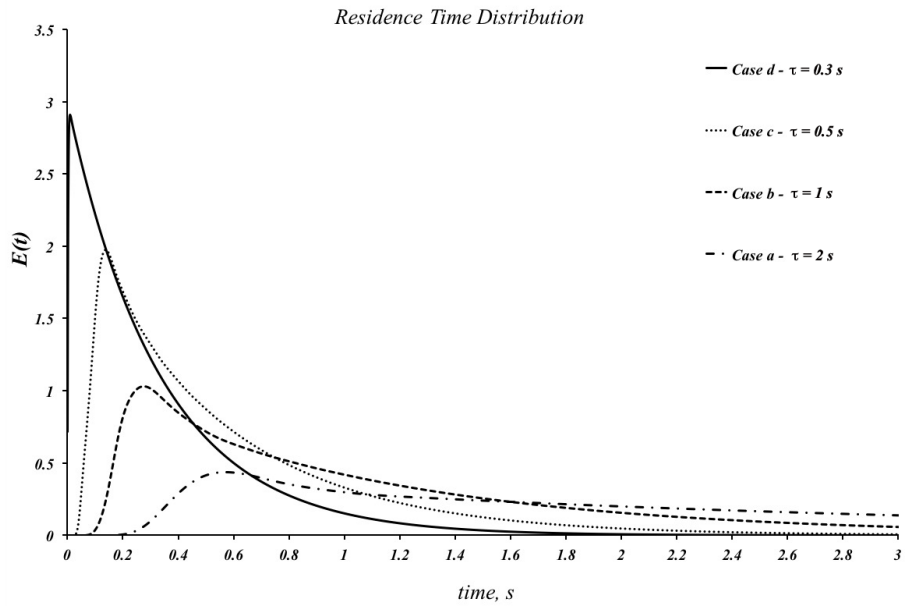

Figure 4.9 Residence Time Distribution of the cyclonic burner for four values of the average residence time (τ)

However, as observed from the frequency distribution, the 'case a' for $\tau = 2$ s has the lowest fraction of tracer particles having low residence time (t_{res}<0.2 s). This could also be observed from early inception of tracer at the exit for configuration 'c' (τ = 0.5 s) as compared to configuration 'd'. As previously said the cases with higher fraction of gases having lower residence time can lead to overall high emission of CO in the exhausts. Hence the residence time calculation suggests that the case 'd' can result in lowest CO emissions for the present case. This further implies that inlet flow velocities which will result in higher residence time can result in lower CO emissions. The figure also denotes that enhanced performance as compared to perfectly stirred reactor could be achieved by selectively choosing the flow configurations, as perfectly stirred reactor has higher fraction of gases having very low residence time as compared to other flow configurations.

These simple calculations also highlighted that one can have benefit of favorable residence time distribution by tailoring the flow field by operating optimal configurations even though the average residence time (τ) is the same for different configurations for a given volume.

This suggests that geometry and fluid-dynamics pattern have a strong influence on combustion characteristics and this factor needs to be considered while scaling MILD combustors [Arghode et al., 2013].

4.6 Summary

The sustainability of the combustion process, depending on inlet mixture preheating, the dilution level, the mixture composition in LUCY burner have been tested.
The analysis was also performed by means of numerical simulation on a simplified scheme of the burner. In this way it was possible to highlight the chemical/thermodynamic features of the process, while evidencing some discrepancies between experimental and numerical evidences that can be attributed either to the possible influence of fluid-dynamics on the process or to limitations/oversimplifications of the model.
Experimental results suggests that in any operating conditions, also for very diluted mixtures, the oxidation process remains stable when the temperature inside the reactor is above about 1050 K. Noticeably, this temperature corresponds to the activation temperature of the high temperature branching mechanism. Thus, even though these results are relative to propane mixtures and further investigations would be advisable, it can be stated in a first approximation that also for a large class of unconventional fuels, even if they have a lower calorific value being diluted by significant amounts of inert species, the oxidation process could be maintained if the working temperature exceeds such a threshold, as shown in the next.
However, LUCY burner performances in terms of measured CO and NO_x emissions are even better with respect to the ones predicted by the model also in conditions reached by igniting the system at high temperature and then reaching a stable burning regime, at lower inlet temperature, exploiting the observed hysteresis phenomenology.
In general, CO and NO_x production are remarkable limited in a wide range of operative conditions performed cyclonic burner. Such results have to be attributed to the flow residence time distribution induced by the cyclonic pattern with respect to the one typical of CSTR condition.
As matter of fact, the kinetic characteristic times (ignition, oxidation) become longer under diluted condition, because of low reactants concentration and mixture high thermal capacity that limits the temperature increase.
Therefore the prolongation of local residence times is beneficial for both the stability of the process and the full fuel conversion. Such aspect is confirmed by the comparison between the operational limits of the cyclonic burner with respect to the ones relative to literature burners with exhausted internal recycling.

5. PERFORMANCE

This chapter reports the performance of the cyclonic burner obtained through a deep experimental analysis. In particular, the investigation is a continuation of the previous chapter were external dilution and preheating were considered. The results will be presented by dividing them into paragraphs according to the different aspects of the process investigated. Thus, the first part of this chapter is related to the description of a new-release of the burner. Subsequently, results are reported for Air conditions with and without the external preheating. Finally, the effects of the thermal power and fuel nature are investigated.

In order to identify the optimal operative conditions of the cyclonic burner, the experimental campaigns previously explained suggest:

- MILD combustion is stabilized even for low dilution levels and air conditions, thanks to the internal recirculation of burned product by means of the cyclonic flow-field configuration
- The lowering of the mixture preheating level influences the sustainability of the process.

Further experimental campaigns have been performed to identify the optimal operating points for conditions close to real ones. First of all, some critical points emerged during the operation of the burner:

- The vermiculite has a low resistance to several thermal cycles and thermal shock, which could be cause of fractures and consequently compromises the burner seal.
- Volumetric shrinkage of the refractory cement during the sintering/drying occurring at higher temperatures results in the detachment of the various parts of vermiculite, with consequent sealing problems, and requires a new application of the adhesive material.
- The burner, assembled with refractory materials, is not physically accessible for inspection, maintenance (window cleaning for optical accesses) and/or replacement of fractured parts.

The problems reported above significantly reduce the operating period of LUCY burner and it needs to be entirely replaced in the event of a burner fracture.
As highlighted in the previous chapter, the cyclonic burner is able to stabilize MILD combustion conditions varying the external parameters (preheating temperature T_{in}, equivalence ratio Φ, total dilution of the mixture XN_2, average residence time τ). In this way, it is possible to study the transition to various combustion regimes.

The cyclonic flow induced by the geometric characteristics of the burner allowed the stabilization of the MILD combustion process by means of internal mass and heat recirculation. The experimental campaigns confirmed that the cyclonic burner could be operated without noise (noiseless), the temperatures in the combustion chamber were homogeneous, there was not a flame front and the CO and NO_x emissions were very low. As a result, the choices adopted for the design and construction of the cyclonic flow-field burner proved to be successful.

5.1 Upgrade of LUCY Burner

On the basis of the previous considerations, some modifications to the burner have been adopted in order to overcome the technological limits imposed by materials and to make the combustor optically accessible. Subsequently, the solutions implemented into the combustion chamber will be introduced.
In the previous chapter, the critical points that were found during the burner operation were essentially related to the characteristics of the materials used in the preliminary design of the reactor.
Thus, a new design has been realized in order to understand the sustainability of the process when operated with different thermal powers and different fuels. In addition, as already introduced, it was necessary to implement advanced diagnostic techniques, such as induced fluorescence, PIV and absorption, which involve the use of a light source (laser) for gas phase excitation in order to identify and quantify the major species involved during the process of fuel oxidation.
For this purpose, it was necessary to create a system with an input section and a beam output section, and a signal collection section (positioned at 90°) and thus optical accesses to the system have been made.
In addition, due to the high temperatures reached in low external dilution working conditions, N thermocouples had to be replaced with R thermocouples.
In the following, the critical aspects modified in the new configuration have been summarized, analyzed and discussed:

- Identification of materials:

    a. With high thermal resistance and thermal shock resistance;
    b. Mechanically easily machinable;
    c. Chemical inert materials.

At the end of the experimental campaigns performed with the cyclonic burner, it was found that the materials chosen for the design was not able to resist at working temperatures higher than 1300°C for continuous operation and were not resistant to thermal shock.

These problems were found when the experimental tests were performed with mixtures diluted in air or with low dilution levels. As a result, during the redesign of the new combustion chamber, a preliminary study was carried out for choosing suitable materials to overcome the technological limits imposed by the use of vermiculite, also considering the mechanical and chemical properties. In fact, they must be easily machinable and chemically inert in order not to catalyze or inhibit the chemical reactions involved during oxidation processes. Ceramic materials are chemically resistant and inert at high temperatures.

The material that completely satisfies the requirements listed above is the Ultraboard®1750/400 (www.schupp-ceramics.com). It is composed of polycrystalline alumina wool and special inorganic fibers, which resists to temperatures up to 2100 °C in continuous cycle. In addition, this material is easily machinable and it has excellent physical properties (low thermal conductivity, high resistance to thermal shock and high temperatures). It is available in the form of rigid slabs of different sizes.

The new cyclonic burner configuration has been designed for an easy access to the burner in order to carry out maintenance and inspection operations inside the combustion chamber. For this purpose, the cyclonic burner was installed in an external steel case. This case consists of a prismatic structure with a removable side and dimensions to accommodate the burner. The main structure is therefore equipped with a flanged side to be coupled to the surface of the removable case by bolting.

The case is made of AISI 310s steel. It is an austenitic stainless steel resistant up to 1400°C, particularly suitable for humid and corrosive environments. Finally, the upper wall is flanged and connected to the reactor by means of AISI 310s steel head bolts. WEICON nickel anti-sealing was applied to all the joints of the case to avoid any problems deriving from the oxidation of the components and to facilitate tightening and unscrewing of the threaded joints.

It is fundamental to avoid leakage of gases during the operations for safety reasons and to ensure the reliability of the initial conditions of the experimental tests. Since the reactor has been provided by a coupling of two flanged parts, it is necessary to apply seals suitable for working at high temperatures. In fact, although the operating pressure is atmospheric, the reactor case is stored between high temperature ceramic fiber-electric panels.

The seal is ensured by the use of ceramic fiber gaskets. This material is produced from alumina silicate fibers and binders (calcium oxide, iron, magnesium) which burn without residues at first heating. It has good tensile strength, low thermal conductivity, high resistance to thermal shock and high torsional resistance.

In addition, the ceramic panels placed in the steel chamber are cemented together by means of a specific refractory mortar, Blakite® (www.refrattarigenerali.com). It consists of finely ground alumino-silicate granules mixed with special binders, ensures a good grip after drying, forming a very strong joint and an almost monolithic structure of the masonry.

The bonding of refractory material slabs and steel slabs is achieved by means of a special binder with quick gripping in contact with air, the Belcolle MS, used mainly for aluminosilicate and insulating panels.
The burner is equipped with three different quartz windows: two of them are placed on the side and opposite sides of the case, to allow the light beam to pass through the control volume, and a third is placed on the upper wall to collect the output signal.
The windows are made of quartz HOQ 310. It has a high resistance to high temperatures, a very low thermal expansion coefficient, ability to resist at thermal stress without fractures and excellent optical properties due to the absence of defects.
The cyclonic burner performed with air/fuel mixtures and/or low dilution levels can reach working temperatures above 1600 K. Consequently, in order to evaluate the oxidation process in the whole combustion chamber, a new configuration of the thermocouples placement was adopted, as shown in Figure 5.1. The central (T_1), the intermediate (T_2) and the lateral (T_3) are located at 10 cm, 5cm and 2.5 cm from the lateral wall, with a respectively protrusion length of 5 cm, 7.5 cm and 10 cm within the combustion chamber from their insertion position.

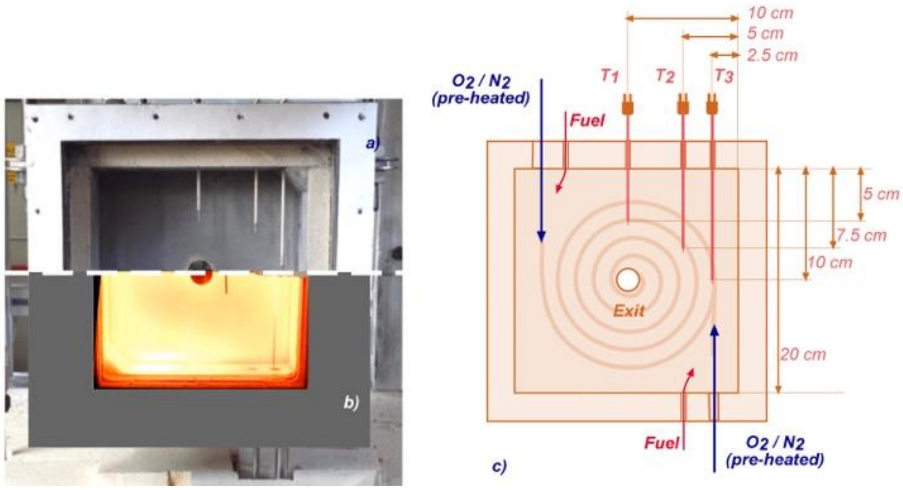

Figure 5.1 Top view of the reactor (a), picture of the burner under flameless combustion mode (b); mid-plane section sketch (c) of the cyclonic combustion chamber with geometrical features.

The result of the design is the new developed steel case for the cyclonic burner shown in the sketch in Figure 5.2. As it can be seen from the Figure 5.2, the geometry and internal dimensions of the combustion chamber are similar to those of the vermiculite-only reactor. Figure 5.3 shows the new version of the combustor assembled, while Figure 5.4 and Figure 5.5 show the cyclonic burner inside the experimental plant, at the laboratories of the IRC-CNR in Naples.

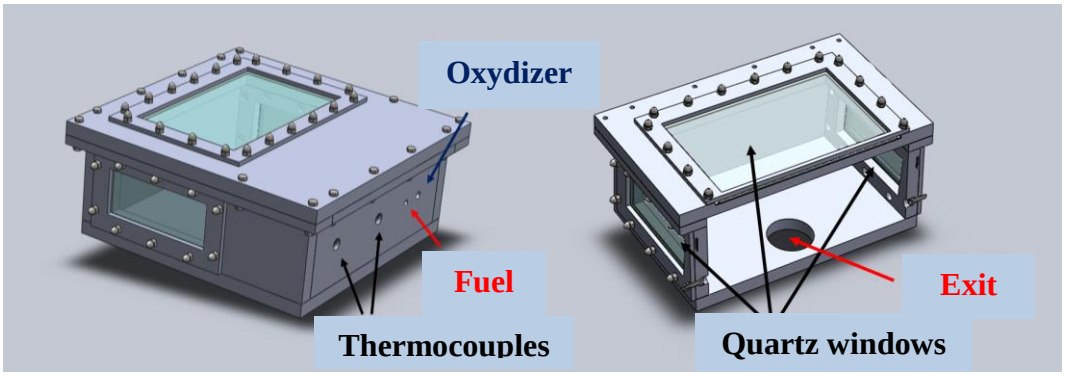

Figure 5.2 Sketch of the new developed steel case for the cyclonic burner

Figure 5.3 Overview of the cyclonic

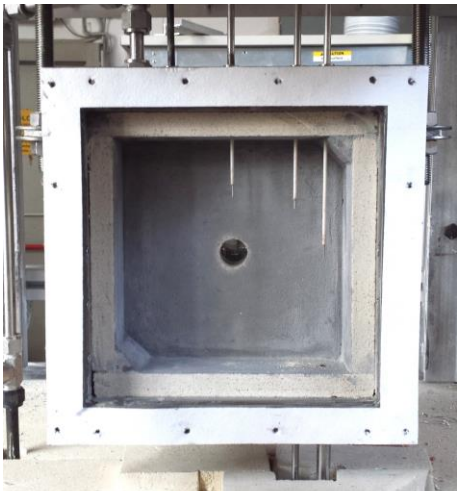

Figure 5.4 Front view of the cyclonic burner

Figure 5.6 shows the cyclonic burner in combustion conditions. The internal case made in vermiculite is used to prevent catalytic effects of the steel. Despite that, the external case made on stainless steel helps to avoid leakage of gases during the operations for safety reasons and to ensure the reliability of the initial conditions of the experimental tests.
On the other hand, the vermiculite is not able to resist at working temperatures higher than 1300°C for continuous operation and was not resistant to thermal shock, as reported before. Therefore, the internal part of the burner can be replaced with Ultraboard®1750/400 when higher temperatures are reached in the combustor.

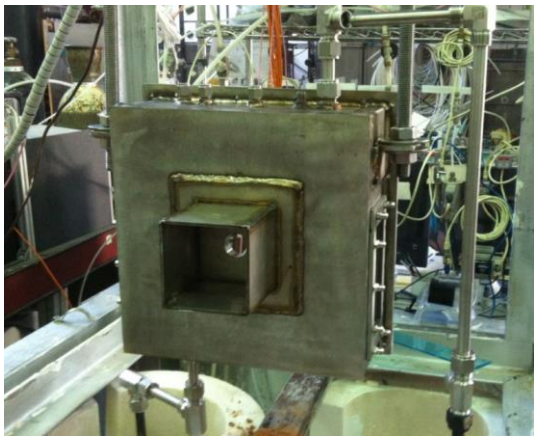

Figure 5.5 The cyclonic burner inside the experimental plant

Figure 5.6 Cyclonic burner in operation inside the experimental plant

As clearly shown in Figure 5.5, a further difference compared to the first configuration is that the new configuration has a vertical combustor position, which facilitates the implementation of the optical diagnostic instruments.
For this reason, the four ovens inside the chamber were placed vertically in the corners of the base of the system, as shown in Figure 5.7.
Figure 5.8 shows a picture of the whole experimental set-up where the cyclonic burner has been operated during the experimental campaign.

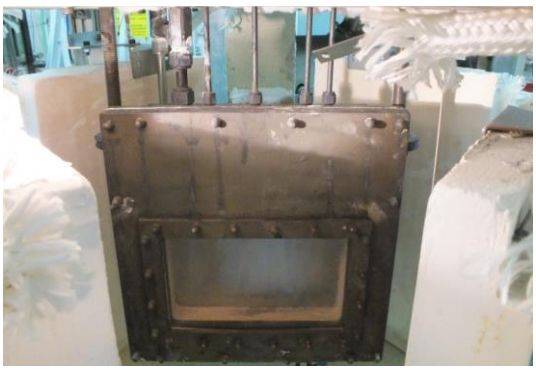

Figure 5.7 Cyclonic burner front view

Figure 5.8 The last configuration of the experimental set-up.

The experimental test rig modifications imposed variations also in the flue gas analysis system. In particular, the water-cooled probe was placed at the exit of the burner coherently with the new configuration.
In such a case, an external case, made in vermiculite, was used to confined the exhaust gases and to insert the probe for flue gas analysis.

5.2 Effect of the Equivalent Ratio for Pre-heated mixtures

The performance evaluation for Air conditions started for preheating conditions in order to evaluate the influence of the equivalence ratio to identify the optimal operational values.
Experimental tests were devoted to characterize the performance of the cyclonic burner in terms of temperature distribution and species emission varying the mixture equivalence ratio for C_3H_8-Air mixtures at a fixed pre-heating temperature. The main flow inlet temperature was fixed equal to T_{in} = 925 K, because, as already discussed, such a value was identified as the minimum auto-ignition temperature for the used mixture.
Figure 5.9 shows the temperatures measured in the mid-plane of the reactor at the three selected stations (T_1, T_2, T_3) as a function of the equivalence ratio Φ for C_3H_8-Air mixtures. The equivalence ratio Φ was changed from ultra-lean conditions (Φ = 0.17) to the stoichiometric one. The curves are parametric in the residence time τ, corresponding to τ = 0.5 s, τ = 1 s and τ = 1.5 s. The figure shows that for any residence time, the temperatures increases with Φ in the investigated range.

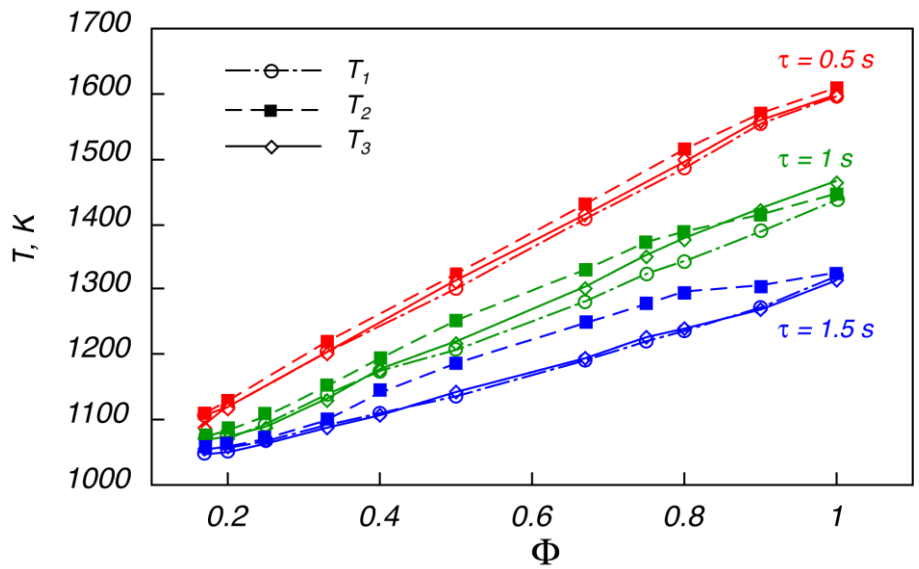

Figure 5.9 Temperature measurements at the three selected stations within the reactor for C_3H_8-Air mixtures as a function of Φ for different τ. T_{in} = 925 K.

In general, as τ decreases, the temperature increases due to an increase of the thermal power of the inlet mixture.

For τ = 1.5 s, the central and the wall-aside temperature are very close to each other, while the T_2 becomes slightly higher for $\Phi > 0.4$. For $\Phi > 0.8$, the temperature difference becomes lower and for the stoichiometric condition all of them become equal.

For τ = 1.0 s, up to $\Phi = 0.4$, the three temperatures are similar, with a maximum difference of 20 K. For $\Phi > 0.4$, the difference among the temperatures increase, and T_2 is the higher one, while T_3 the lowest. For $\Phi > 0.8$, the discrepancies among monitored temperature decrease.

For τ = 0.5 s, the three monitored temperatures are very close to each other, indicating a more uniform temperature field.

Figure 5.10 shows the distribution of unburned gases (CO) and NO_x, for the C_3H_8-Air mixtures as a function of the equivalence ratios, on curves parametric in τ.

The CO concentration is reported in log-scale, while the NO_x one in linear coordinate.

For τ = 0.5 s, the CO diminishes as the equivalence ratio Φ increases, reaches a minimum value at $\Phi = 0.75$ and then increases. The behavior is similar for the other considered residence times but the minimum value occurs at $\Phi = 0.9$.

The concentration of CO becomes lower than 100 ppm, respectively at $\Phi = 0.6$ for τ = 1.5 s, and $\Phi = 0.5$ for τ = 1 s and τ = 0.5 s. These conditions allow to identify the burner temperature equal to 1200 K as noticeable temperature for lowering CO emissions to values compatible with standard emission roles.

It is worth noting that the curves relative to τ = 0.5 s show a CO concentration slightly higher than the case at and τ = 1 s for $\Phi < 0.33$, then values become lower.

This may be attributed to the CO oxidation time. In fact, beneath the temperature of the system for τ = 0.5 s is slightly higher than the one detected for τ = 1 s, the mean residence time within the reactor volume, is not sufficient to insure CO conversion to CO_2.

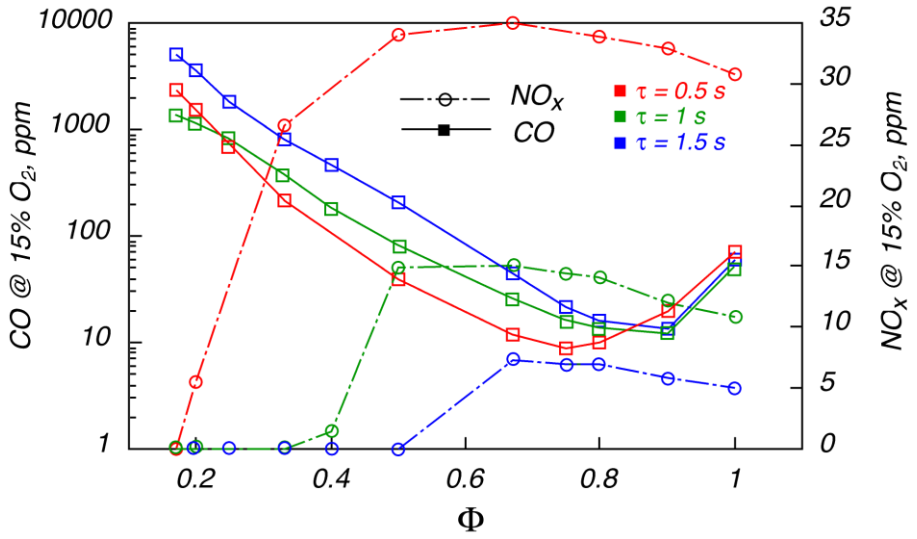

Figure 5.10 CO and NO_x emissions for C_3H_8-Air mixtures as a function of Φ for different τ. T_{in} = 925 K.

Along with the CO concentration, for very lean conditions at low temperatures, some unburned species (CH_4, H_2) have been detected, as shown in Figure 5.11. They completely disappear when the burner temperature exceeds 1200 K. Such a condition occurs at Φ = 0.67 for τ = 1.5 s and at Φ = 0.5 for τ = 1 and 0.5 s, thus in concomitance with CO full consumption.

For any τ value, NO_x concentration increases with Φ, reach a maximum value and then slightly diminishes while the mixture composition moves towards the stoichiometric value. The experimental NO_x values change with the residence time, because it implies different nominal thermal power and thus different system temperatures.

It is worth noting than the NO_x concentration are very low, for τ = 1.5 s they are lower than 10 ppm (the single-digit), for τ = 1 s, the maximum value is 14 ppm, and, for τ = 0.5 s, 34 ppm.

In any case, two noticeable temperatures can be detected: the NO_x concentration start to increase when the system temperature is higher than 1100 K for all the systems, while the maximum value is reached when the system temperature is higher than 1200 K. This may be correlated to the onset of NO reburning chemistry [Alzueta et al., 1998; Zamescu et al. 2001] for temperatures higher than 1200 K.

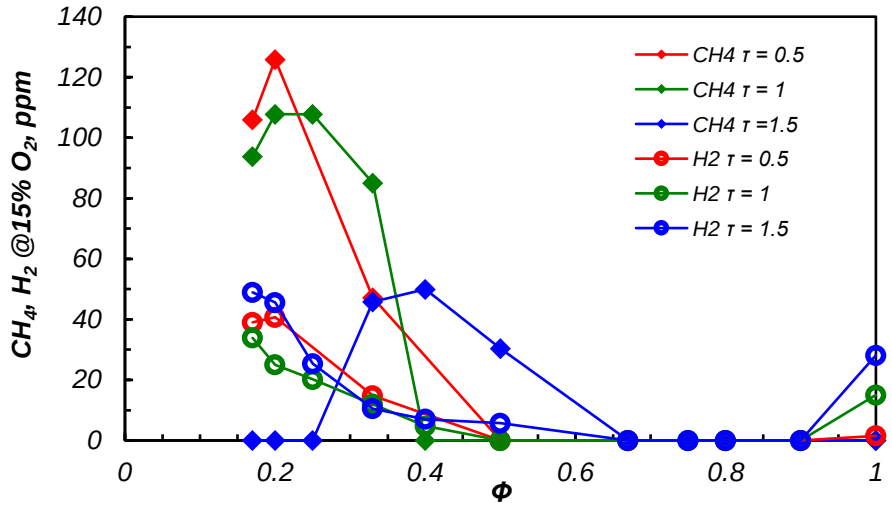

Figure 5.11 CH_4 and H_2 emissions for C_3H_8-Air mixtures as a function of Φ for different τ. T_{in} = 925 K.

The residence time distribution influences the conversion degree of the oxidation reactions, thus the gas expansion due to heat released by reactions and the flow inlet velocities.
In particular, for low system temperatures, the oxidation degree is relatively low with respect to the residence time induced by the cyclonic pattern, as the UHC emissions suggest. When the system exceeds an average temperature of 1100 K, the oxidation kinetic route changes to a faster chemistry, because of the insurgence of high temperature branching reactions, and the maximum heat release is confined in a toroidal area in the proximity of the T_2.
Increasing the mixture equivalence ratio, the heat release area extends radially involving all the reactor volume defining a more uniform condition.
By decreasing the mixture averaged residence time, thus increasing the system thermal power, the system temperature increases thus promoting fast chemistry and realizing a more uniform temperature field.
Thus, it is possible to infer that the optimal operating conditions would by identified for burner temperatures higher than 1200 K and mixtures characterized by a equivalence ratios comprised between $0.7 < \Phi < 0.9$ to minimize UHC emissions.

5.3 Towards lower pre-heating temperature

The previous paragraph permitted to identify the optimal operating conditions in terms of polluting species as a function of the equivalence ratio for preheated conditions.

After the identification of the optimal operating conditions for a C_3H_8-Air, pre-heated at the minimum ignition temperature (T_{in} = 925 K) as a function of the mixture equivalence ratio Φ, the analysis has been continued towards no-preheating conditions, to assess the sustainability of the process. In particular, from burning conditions, the pre-heating temperature has been decreased. As showed in previous works [Sorrentino et al., 2016; de Joannon, 2017], such a strategy allows for extending the operating range of the burner towards pre-heating temperature lower than the minimum auto-ignition one.
The mixture equivalence ratio Φ was fixed to 0.8, because it falls in the optimal equivalence ratio range previously identified. The thermal power was fixed to P = 2 kW and P = 4 kW by adjusting the residence time with the preheating temperature. Figure 5.12 shows that as the preheating temperature is decreased, the system temperatures decrease with a linear trend. The difference between the temperature T_2 and T_1 increase while T_{in}, decreases, suggests that the main heat release is moving towards the inner part of the reactor.

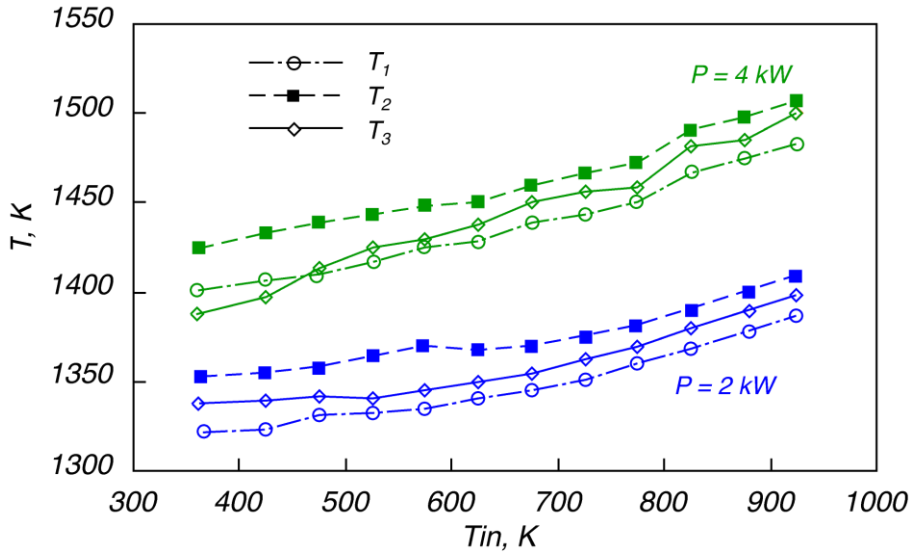

Figure 5.12 Temperature measurements at the three selected stations within the reactor for C_3H_8-Air mixtures as a function of the pre-heating temperature for different thermal power. Φ = 0.8.

The CO emission slightly increases decreasing T_{in}, from 5 ppm to 10 ppm for the P = 2 kW case, while NO_x emission remains almost constant. For the P = 4 kW case, the CO increases from 10 to 15 ppm, and the NO_x decreases from 30 to 24 ppm.
Energy balance between the sensible enthalpy of the inlet mixture and reacting gases suggests that the reactor temperature slightly decreases of a quantity corresponding

to the sensible enthalpy needed to raise the inlet flow temperature to the auto-ignition one.
This analysis shows that it is possible to sustain the oxidation process without a pre-heating strategy while not compromising CO and NO_x emissions. In particular, the system self-stabilizes with the heat released by the oxidation reactions and transported towards fresh incoming reactants by efficient heat exchange mechanisms (convection, diffusion and radiation) promoted by the cyclonic pattern configuration and the vermiculite walls.
Future works can help in identifying the role of radiative heat fluxed from the wall toward the igniting mixture on the stabilization mechanism of the reactive region.

5.4 Effect of the Equivalence Ratio without Pre-heating

Given this background, another analysis has been performed to value the effect of the mixture equivalence ratio on the process stability and emission for C_3H_8-Air mixture without pre-heating. The curves are parametric in the nominal thermal power P that was fixed to respectively 2 kW, 4 kW and 6 kW.
Figure 5.13 shows the temperature profiles obtained as a function of the equivalence ratio Φ for a thermal load equal to P = 2 kW, P = 4 kW and P = 6 kW.

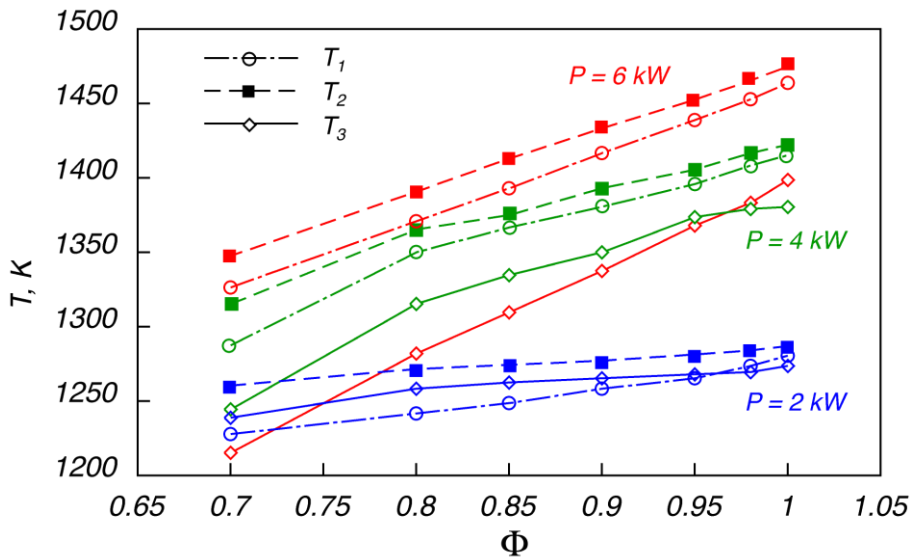

Figure 5.13 Temperature measurements at the three selected stations within the reactor for C_3H_8-Air mixtures as a function of Φ for different P. T_{in} = 345 K.

The equivalence ratio Φ was changed from 0.7 to 1. For the case P = 2 kW, the temperatures T_1, T_2 and T_3 increase with Φ with a maximum difference of 30 K at

the lowest Φ. Increasing Φ, the difference among the thermocouples become less than 10 K, suggesting a more uniform temperature field. For the thermal power equal to 4 kW, the difference between the temperature T_1 and T_2 is 25 K at Φ = 0.7 and then decreases with Φ. It is worth noting that T_3 is the lowest one. As mentioned earlier, T_3 is located at 10 cm from the main nozzle, thus it is directly invested by the main flow. The higher mass and velocity of the main flow with respect to the P = 2 kW case implies that the cold flow needs more time to be pre-heated and auto-ignites. When the thermal power is increased at 6 kW, this trend is confirmed and T_3 is much lower than T_1 and T_2.
Figure 5.14 shows the CO and NO_x emission as a function of Φ for the three thermal loads considered. It is possible to note that in any case the CO slightly diminishes from Φ = 0.7, reaching a minimum value in the range 0.85 < Φ < 0.9. Then, CO emissions increase towards the stoichiometric value.

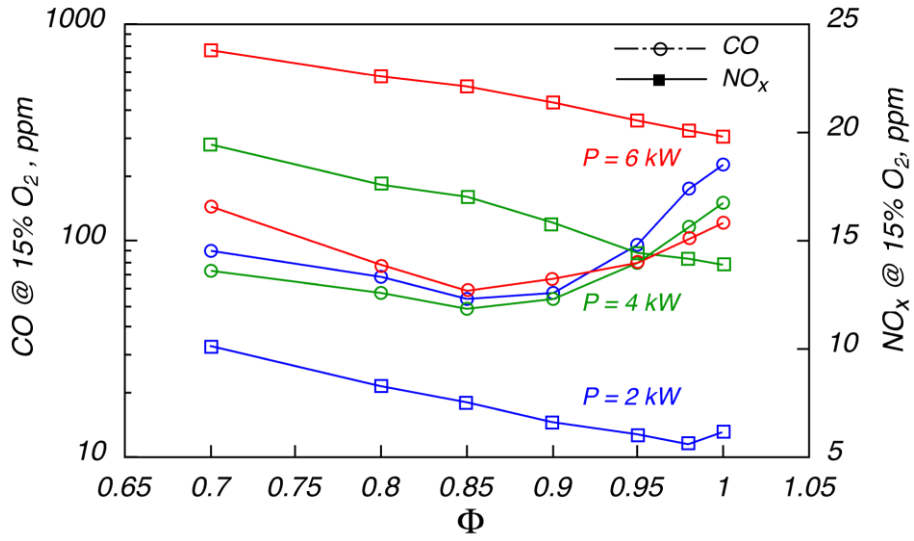

Figure 5.14 CO and NO_x emissions for C_3H_8-Air mixtures as a function of Φ for different P. T_{in} = 345 K.

The higher the thermal power P, the higher the CO emissions are. In any case it is worth noting than for P = 2 kW and P = 4 kW, the CO levels are lower than 100 ppm for 0.7 < Φ < 0.9. For P = 6 kW, such a condition is achieved for 0.8 < Φ < 0.95.
The NO_x slightly diminish with Φ, because of the stoichiometry increases towards fuel rich-conditions. For P = 2 kW their concentration is lower than 10 ppm, while for P = 4 kW, they are in the range 17-13 ppm. In the last case they change from 23 to 19 ppm.

5.5 Identification of the maximum thermal Power

A further analysis has been carried out to value the maximum theoretical thermal power that the burner can sustain without compromising pollutants emission.
Figure 5.15 shows the reference temperatures changing the thermal power of the system from P = 2 kW to P = 8 kW for a mixture of C_3H_8-Air without pre-heating and $\Phi = 0.85$. Such a value has been chosen because, by the previous analysis, the CO emissions present a minimum value.
It is possible to note that as the thermal power increases, the difference between T_1 or T_2 with T_3 increases. In particular, for P > 4 kW, T_3 remains almost constant. The temperatures T_1 and T_2 are close to each other for any P considered.

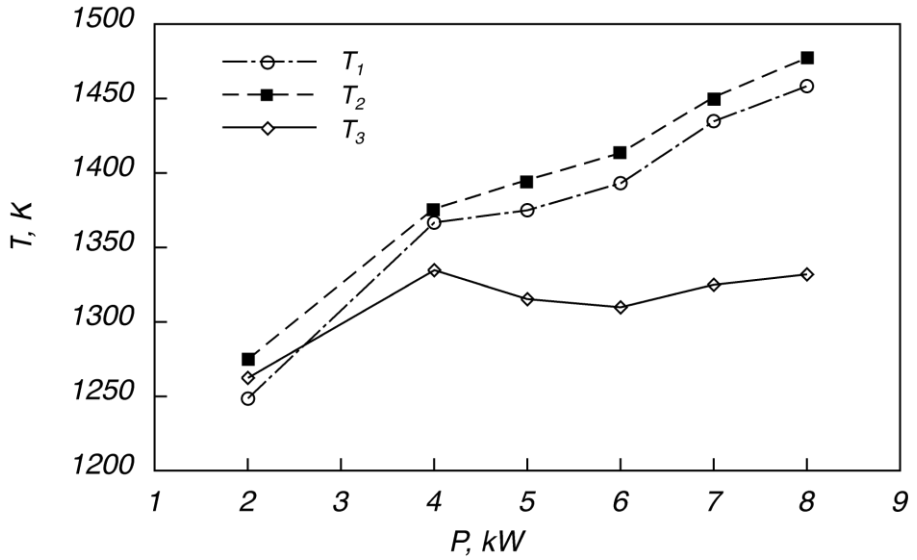

Figure 5.15 Temperature measurements at the three selected stations within the reactor for C_3H_8-Air mixtures as a function of P. $\Phi = 0.85$, $T_{in} = 345$ K.

Figure 5.16 reports the CO and the NO_x emissions for $\Phi = 0.85$. It is possible to note that CO slightly diminishes from P = 2 kW to P = 5 kW, then starts increasing. In any case, the CO emissions are lower than 100 ppm. The NO_x slightly increase with P, passing from 9 ppm for P = 2 kW to 20 ppm to 8 kW.

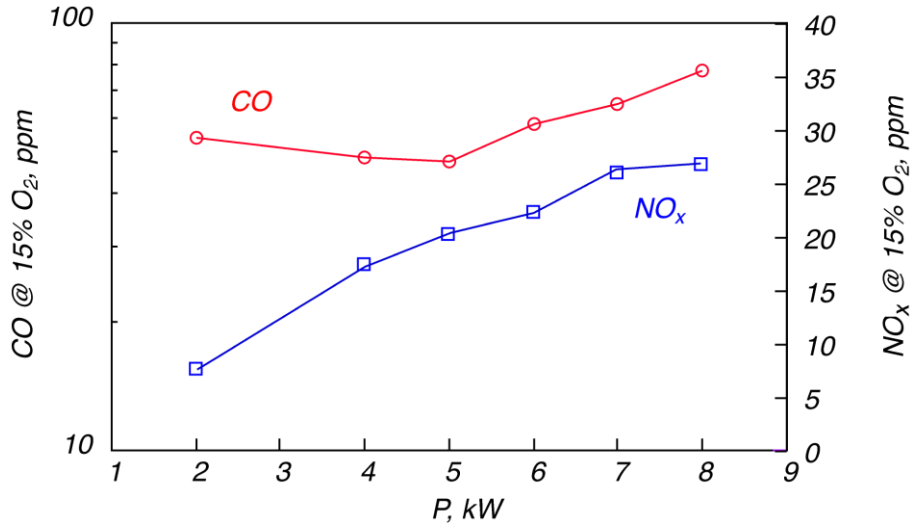

Figure 5.16 CO and NO_x emissions for C_3H_8-Air mixtures as a function of P. Φ = 0.85, T_{in} = 345 K.

5.6 Fuel Flexible Cyclonic Burner

A fundamental aspect concerning the development of the cyclonic burner is to verify the fuel flexibility of the system. In the previous experimental campaign, optimal working conditions was identified as a function of the nominal thermal power. The oxidation process was stable and very low CO and NO_x emissions have been registered for the whole range of the nominal thermal power investigated. In order to verify the fuel flexibility of LUCY burner for small scale applications, partially confirmed by the experimental campaign when the dilution level and the equivalence ratio was varied, further experimental campaigns have been performed with CH_4-Air and Biogas-Air mixtures (60% CH_4, 40% CO_2 [Rasi et al., 2007; Herout et al., 2011]).

5.6.1 Fuel Flexibility: CH_4-Air

Once identified the optimal operating conditions for a C_3H_8-Air mixture, further experimental campaigns have been performed with CH_4-Air mixtures. The same conditions have been reproduced in order to verify the stabilization of the process even for different fuels. Firstly, the cyclonic burner have been operated with a CH_4-Air mixture starting from pre-heated at the minimum ignition temperature (T_{in} = 925 K). As the previous experimental campaigns, when the burner was operated in Propane, the analysis has been continued towards no-preheating conditions, to value

the sustainability of the process. In particular, as shown in Figure 5.17 from burning condition, the pre-heating temperature has been decreased down to T_{in} = 325 K. The mixture equivalence ratio Φ was fixed to 0.9, because it falls in the optimal equivalence ratio range that minimize the CO and NO_x emissions. The thermal power was fixed to P = 4 kW by adjusting the residence time with the preheating temperature. Figure 5.17 shows that as the preheating temperature is decreased, the system temperatures decrease with a linear trend. The difference between the temperature T_3 and T_1 increases decreasing T_{in}, suggesting that even performing the burner with CH_4 the main heat release is moving towards the inner part of the combustion chamber.

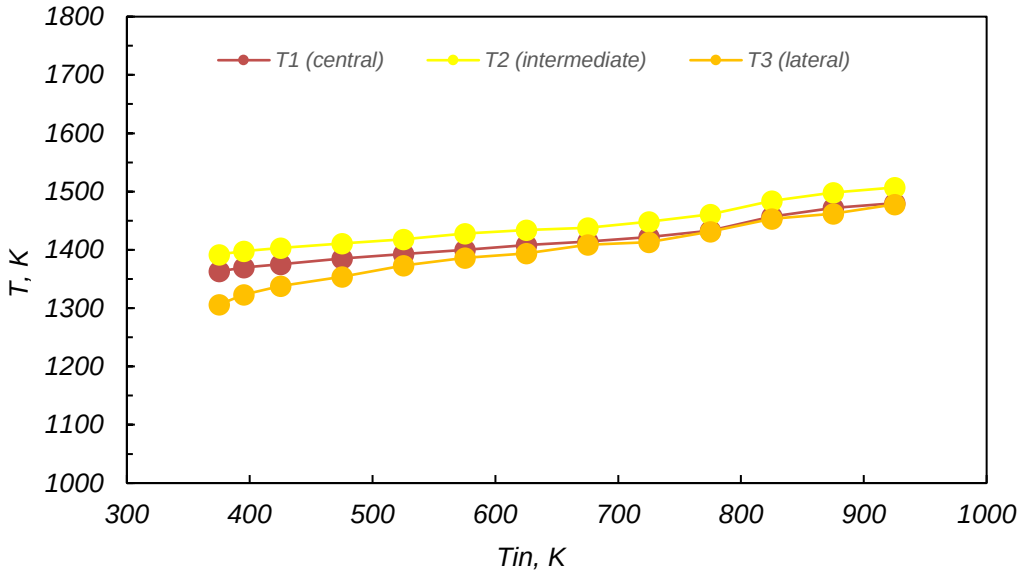

Figure 5.17 Temperature measurements in T_1, T_2, T_3 for CH_4-Air mixtures as a function of the pre-heating temperature for P = 4 kW, Φ = 0.9.

Figure 5.18 show the results of the analysis in terms of CO and NO_x emission as function of the preheating temperature T_{in}. The CO emission is always almost 0 ppm in the whole range of T_{in}, while NO_x emission slightly decrease when there is no preheating of the main flow. In any case NO_x emissions are very low when the cyclonic burner is performed at T_{in} = 325 K. In this case NO_x concentration at the exhaust is 15 ppm.

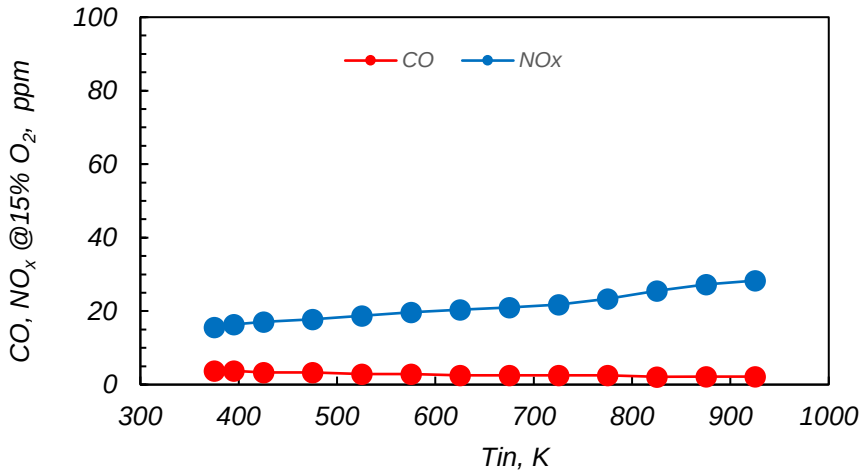

Figure 5.18 CO, NO_x emissions measurements for CH_4-Air mixtures as a function of the pre-heating temperature for P = 4 kW, Φ = 0.8.

This analysis shows that it is possible to sustain the oxidation process without a pre-heating strategy while not compromising CO and NO_x emissions even performing the cyclonic burner with other fuels.

5.6.2 Effect of equivalence ratio without pre-heating: CH_4-Air

A further analysis has been performed to value the effect of the mixture equivalence ratio on the process stability and emission for CH_4-Air mixture without pre-heating. The curves are parametric in the nominal thermal power P that was fixed to respectively 4 kW and 6 kW.
Figure 5.19 shows the temperature profiles obtained as a function of the equivalence ratio Φ for a thermal load equal to P = 4 kW and P = 6 kW.

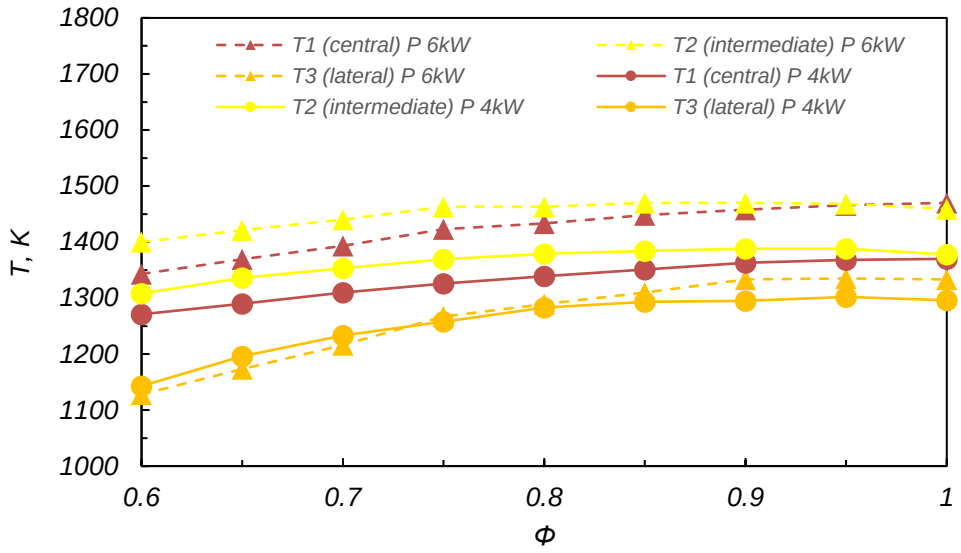

Figure 5.19 Temperature measurements in T_1, T_2, T_3 for CH_4-Air mixtures as a function of Φ for different P. T_{in} = 325 K.

The equivalence ratio Φ was changed from 0.6 to 1. For the case P = 4 kW, the difference between the temperature T_1 and T_2 is 35 K at Φ = 0.6 and then decreases for higher values of Φ. T_3 is the lowest temperature inside the burner. This trend is confirmed even for the case P = 6 kW where T_3 is much lower than T_1 and T_2.
Figure 5.20 shows the CO and NO_x emission as a function of Φ for the thermal loads considered, P = 4 kW and P = 6 kW. For the case P = 4 kW, CO emissions rapidly drop down from Φ = 0.6 (70 ppm), then reach a minimum value in the range 0.8 < Φ < 0.9. They increase towards the stoichiometric value. The same trend is registered for the case P = 6 kW, where CO emissions reach a minimum in the same range of equivalence ratio 0.8 < Φ < 0.9. In any case it is worth noting than for both P = 4 kW and P = 6 kW, the CO levels are lower than 5 ppm for 0.7 < Φ < 0.9.

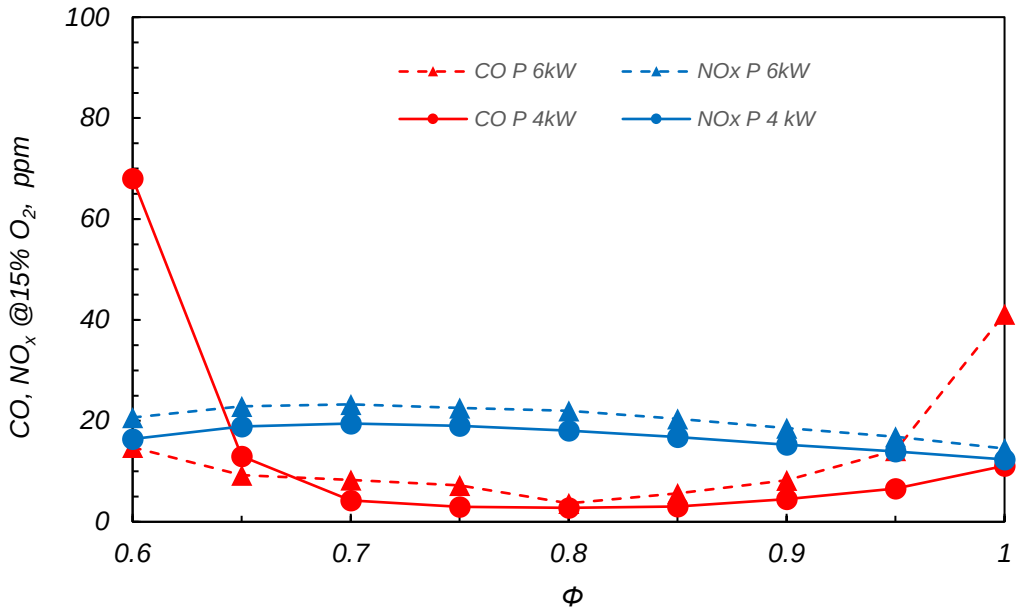

Figure 5.20 CO and NO_x emissions for CH_4-Air mixtures as a function of Φ for different P. T_{in} = 325 K.

The NO_x slightly diminish with Φ, because of the stoichiometry increases towards fuel rich-conditions. For P = 4 kW NO_x concentration varies from 19 ppm to 10 ppm, while for P = 6 kW, they are in the range 21-12 ppm.

5.6.3 Identification of the maximum thermal Power: CH_4-Air

A further analysis for the case CH_4-Air has been carried out to value the maximum theoretical thermal power that the burner can sustain without compromising pollutants emission.
Figure 5.21 shows the reference temperatures changing the thermal power of the system from P = 2 kW up to P = 10 kW for a mixture of CH_4-Air without pre-heating and Φ = 0.8. Such a value has been chosen because, by the previous analysis, the CO emissions present a minimum value.
It is possible to note that as the thermal power increases, the difference between T_1 or T_2 with T_3 increases. In particular, for P > 4 kW, T_3 remains almost constant. The temperatures T_1 and T_2 are close to each other for any P considered.

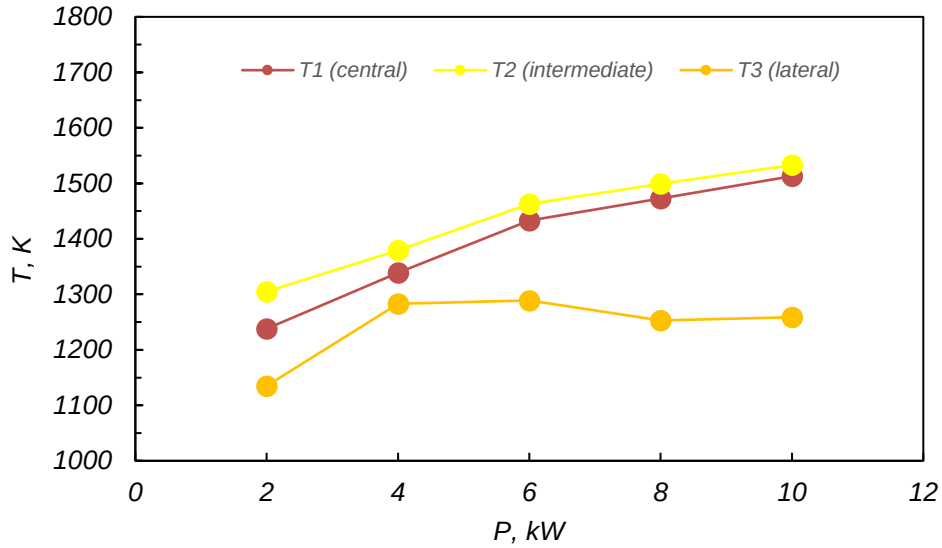

Figure 5.21 Temperature measurements in T_1, T_2, T_3 for CH_4-Air mixtures as a function of P. $\Phi = 0.8$, $T_{in} = 325$ K.

Figure 5.22 reports the CO and the NO_x emissions for $\Phi = 0.8$. It is possible to note that CO slightly diminishes from P = 2 kW to P = 4 kW, then starts increasing. In any case, the CO emissions are lower than 10 ppm. The NO_x slightly increase with P, passing from 10 ppm for P = 2 kW to 25 ppm to 10 kW.

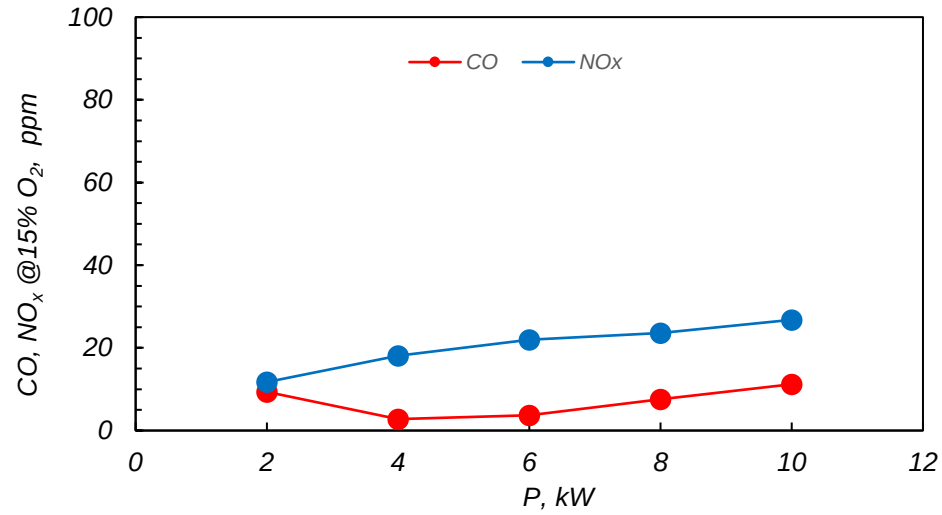

Figure 5.22 CO and NO_x emissions for CH_4-Air mixtures as a function of P. $\Phi = 0.8$, $T_{in} = 325$ K.

5.6.4 Fuel Flexibility: Biogas

The following experimental campaign has the purpose to investigate the possibility to perform the cyclonic burner with lower LHV fuel. In particular, a Biogas (60% CH_4, 40% CO_2) was used as fuel. Firstly, LUCY burner has been operated to value the effect of the mixture equivalence ratio on the process stability and emission for Biogas-Air mixture without pre-heating. The curves are parametric in the nominal thermal power P that was fixed, as already performed in the CH_4-Air case, to respectively 4 kW and 6 kW.
Figure 5.23 shows the temperature profiles obtained as a function of the equivalence ratio Φ for the nominal thermal power equal to P = 4 kW and P = 6 kW.

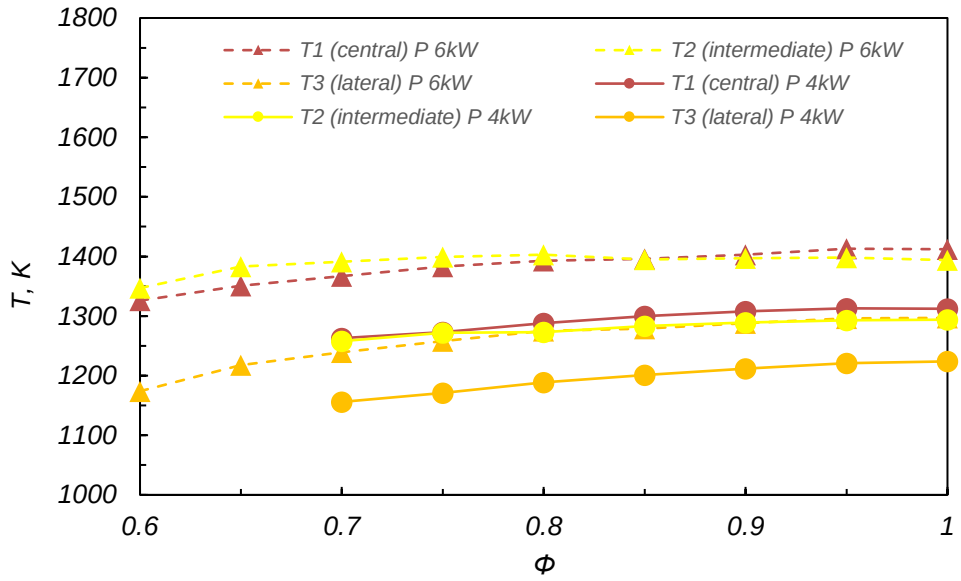

Figure 5.23 Temperature measurements in T_1, T_2, T_3 for Biogas-Air mixtures (60% CH_4, 40% CO_2) as a function of Φ for P = 4 kW, P = 6 kW. T_{in} = 325 K.

The equivalence ratio Φ was changed from 0.6 to 1. For the case P = 4 kW, there is no difference between the temperature T_1 and T_2, while T_3 is the lowest temperature inside the burner. This trend is confirmed even for the case P = 6 kW where T_3 is much lower than T_1 and T_2.
Figure 5.24 shows the CO and NO_x emission as a function of Φ for the thermal loads considered, P = 4 kW and P = 6 kW. For the case P = 4 kW, CO emissions rapidly drop from Φ = 0.7 (250 ppm), then reach a minimum value in the range 0.85 < Φ < 0.95. They increase towards the stoichiometric value. The same trend is registered for the case P = 6 kW, but the minimum range is wider than the case P = 4 kW. CO

emissions reach a minimum in the range of equivalence ratio $0.7 < \Phi < 0.9$, where is almost 0 ppm. In any case it is worth noting than for both P = 4 kW and P = 6 kW, the NO_x emission levels are almost 0 ppm for the whole range of the equivalence ratio Φ here considered.

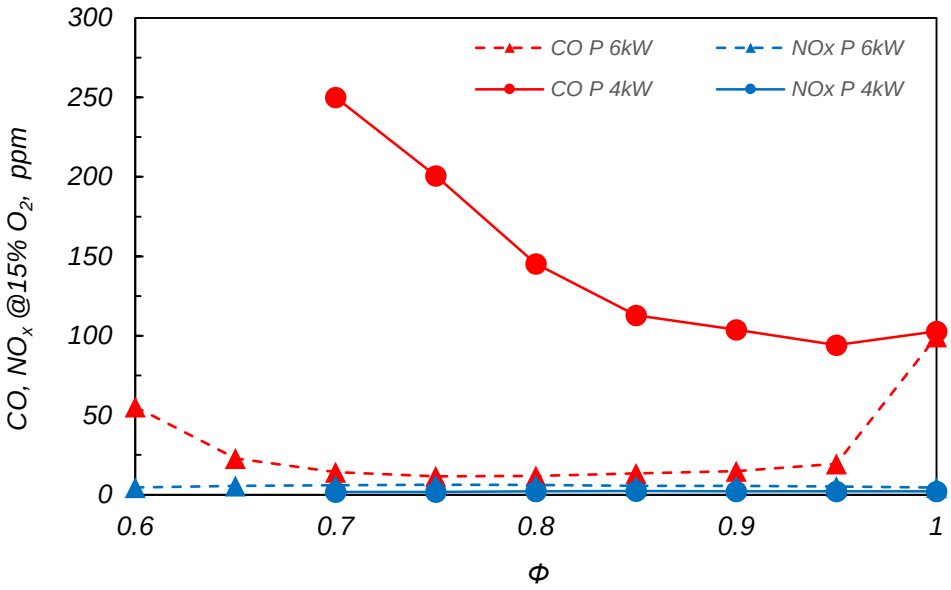

Figure 5.24 CO and NO_x emissions for Biogas-Air mixtures (60% CH_4, 40% CO_2) as a function of Φ for P = 4 kW, P = 6 kW. T_{in} = 325 K.

5.7 Summary

Summarizing the results of the experimental campaigns, the mixtures with equivalent ratios in the range $0.7 < \Phi < 0.9$ show the best performance in terms of CO and NO_x emissions. Temperatures higher than 1200 K have to be reached to insure fuel full conversion with limited CO emissions for the considered residence times and system size. In particular, for $\Phi > 0.4$ emissions are lower than 100 ppm for the most of operative conditions performed during the experimental campaigns.
NO_x emissions show a non-monotonic trend with the equivalence ratio and strongly depend on the working temperatures. In any case analyzed, NO_x emission were lower than 40 ppm with values lower than 10 ppm when temperatures do not exceed 1300 K. When the cyclonic burner was operated with Biogas as fuel, very low NO_x emissions were registered (almost 0 ppm).
Thus, starting from reactive conditions, optimal equivalence ratio Φ (Φ = 0.8 for the pre-heated condition in C_3H_8-Air, Φ = 0.9 for the pre-heated condition in CH_4-Air),

the pre-heating temperature has been diminished, thus moving to not pre-heated condition, to value the sustainability of the process at environmental temperature.
The analysis suggested that the process self-stabilizes by means of the heat released in the oxidation reactions and transported towards the fresh incoming reactants by efficient heat exchange mechanisms promoted by the cyclonic pattern configuration. The system temperatures slightly diminish to pre-heat the cold gases to the auto-ignition temperate without affecting the CO and NO_x emission.
Given these results, a further analysis has been carried out to value the optimal equivalence ratio without pre-heating conditions. The results have suggested that at $\Phi = 0.85$ the emission of CO and NO_x are minimized when C_3H_8 was used as fuel, while the emission of CO and NO_x are minimized at $\Phi = 0.8$ when the system was performed with CH_4. The equivalence ratio $\Phi = 0.9$ is the value that minimizes CO and NO_x emissions when LUCY burner operates with Biogas.
The analysis has suggested that up to P = 10 kW the burner can be exercised with CO emissions compatible with the environmental limits and NO_x lower than 30 ppm. The experimental tests suggested that to limit the NO_x emission to single-digit values, the system working temperature should not exceed 1300 K, while to limit CO emission the temperature should be higher than 1200 K. Finally, the experimental campaigns confirms that the cyclonic flow-field configuration allows to stabilize the oxidation process and to obtain very low CO and NO_x emissions in a wide range of operative conditions, operating with different fuels even in small scale systems.

6. CONCLUSIONS

In the context of academic and industrial research concerning energy production and generation, advanced combustion technologies are used across a broad range of applications. Increasingly, such interest is becoming more sound in its scientific base. There is still a long way to go until they can be important alternatives to renewable sources in the energy transition scenario.
In this context, this thesis improved the understanding of MILD combustion of gaseous fuels through an experimental investigation.
The key outcomes from this investigation are summarized in this chapter.
In particular, an innovative fuel flexible and highly efficient burner for small-scale systems has been developed. In particular, to reach the goal of fuel flexibility and high system efficiency it is usually necessary to operate with different working conditions respect to the traditional ones. As a consequence, the design challenges on the development of innovative systems is to reach the stability of the process. In particular, the oxidation process, reached by means of internal recirculation of mass and enthalpy, becomes more challenging when the size of the system is small (1 - 100 kW).
It has been ensured by means of a cyclonic flow-field configuration of the burner that permits to stabilize the oxidation process and to reach very low pollutants emission (CO, NO_x).
In fact, the cyclonic flow satisfies the following requirements:

- Efficient mixing between the fresh mixture and the burned gases
- Long residence time related to the small scale
- Simple geometry
- Stability of the oxidation process in a wide range of operative conditions

Thus, a small-scale burner has been developed in order to reach both the process stability in a wide range of operative conditions and excellent performance in terms of low pollutants emission.
The Laboratory Unit CYclonic (LUCY) burner has been designed, built and tested in order to characterize the unit and to evaluate its performance.
The cyclonic flow-field allowed to stabilize the oxidation process and it ensured a strong recirculation of the burned gases inside the combustion chamber. In this way, it was possible to operate the burner in MILD combustion conditions with very low pollutant emissions and a high thermal efficiency.
The burner was designed to satisfy the request of stabilization in a wide range of operative conditions. For this purpose, a preliminary experimental campaign was performed to verify the stabilization of the process by means of the cyclonic configuration with strong external dilution. It has been proved that, due to the

cyclonic flow-field configuration, it is possible to operate the burner in a stable way even with high/low diluted and ultra lean/rich mixtures. This is a valuable result in terms of flexibility of the system to be performed in a wide range of operative conditions, which is a requirement for these technologies. In particular, this result is much remarkable when the size of the system is very small.
Several experimental campaigns have been performed in order to characterize the cyclonic burner.

Firstly, a preliminary experimental campaign has been performed and the stabilization of the process has been verified in terms of preheating temperatures required and mixture composition, that lead to the establishment of MILD/flameless combustion in the LUCY burner.
Experiments were performed on C_3H_8/O_2 mixtures strongly diluted in N_2 or CO_2 at 94%. LUCY burner has been tested in strong dilution and extreme lean/reach conditions because they correspond to conservative conditions. Several combustion regimes were identified as functions of the external parameters. In particular, it was possible to identify different working regimes of the system (No Combustion, Low Reactivity and Stable Combustion) and thus the operative conditions corresponding to stable working regime.
It has been observed that when the burner operating in the Stable Combustion regime, MILD combustion conditions occurs.
The experiments showed that MILD combustion can be achieved by means of the cyclonic flow-field configuration, despite the extreme mixture external/internal dilution levels for flow pre-heating temperatures higher than approximately 1000 K for both diluent species. In particular, carbon dioxide slightly increases the operating conditions where the MILD regime is established with respect to the mixture composition.
On the basis of the temperature uniformity within the combustion chamber under MILD operating conditions, chemical simulations were performed under the hypothesis of a perfectly stirred flow reactor. Comparisons between the experimental and numerical results indicated that the combustion chamber could be treated as a well-stirred reactor for a sub-set of operating conditions identified as a part of the MILD combustion region, independently of the diluent species.
Under the MILD combustion regime, the typical flameless conditions along with thermal uniform fields were experimentally observed.
In fact, there was no a visible flame and the luminosity was distributed in the whole volume of the combustion chamber due to a distributed ignition process. This was confirmed by the temperature profile acquired inside the combustion chamber that shows the uniformity of the temperature even changing the inlet conditions.
Furthermore, during the experimental campaigns a hysteresis behavior of the system has been observed and it allows to stabilize the process with two different procedures:

- Upward: Auto-ignition of the mixture increasing T_{in} from non-reactive conditions
- Downward: Auto-ignition of the mixture decreasing T_{in} from reactive conditions

In this way, it was possible to operate the burner in a wider range of operative conditions, even for lower inlet temperatures. The oxidation process was stable until the temperatures inside the chamber was above around 1100K, below that the extinction of the process occurred. The stability was confirmed even for different operative conditions.

Then, a characterization of LUCY burner in terms of pollutants emission have been performed, thus the main operational characteristics of the cyclonic combustion burner were investigated through temperature and exhaust gas emission measurements.
A parametrical investigation has been performed in further experimental campaigns in order to characterize the burner and its stable operative conditions. In fact, the cyclonic burner was designed in such a way to vary independently the operational parameters. Results of the influence of the main external operational parameters, such as equivalence ratio, inlet dilution level and average residence time on the system performance were presented. The appearance of flameless combustion conditions and the thermal fields were used to investigate the stability characteristics. In particular, results showed that MILD Combustion regime was stably achieved for a wide range of external parameters, the working temperatures inside the combustion chamber were reduced and thereby very low NO_x and CO emissions were obtained in a wide operational window.
The critical equivalence ratio above which there is a steep rise in CO emissions was found to be $\Phi = 0.9$ for an inlet dilution level equal to $X_{N2} = 0.88$, whereas NO_x levels increases when the system approaches High-Temperature Combustion conditions, i.e. when the external dilution level is decreased. In this sense the best operational window in order to minimize both the CO and NO_x emissions seems to be in slightly fuel lean conditions and under diluted conditions ($0.82 < XN_2 < 0.86$).
The impact of the average residence time (that is strongly related to the nominal thermal power) on pollutants emissions is instead twofold. Such dependency is strongly influenced, among other parameters, on entrainment (recirculation) of reactive species, injection velocity, air and fuel injection configuration, fluid-dynamics stabilized structures and residence time distribution of fluid particles. The role of oxidizer injection velocity on the CO emissions is directly related to the establishment of toroidal vortex flows inside the chamber due to the cyclonic flow motion. In particular, the recirculation and the stirring/mixing phenomena between the jets are strongly dependent on the intensity of such vortex structures. In particular, the jointly CO and NO_x emissions reach a minimum value for $1 < \tau < 2$ s

where the residence times are enough long to permit the complete oxidation of the diluted mixtures.
Finally, the residence time distribution (RTD) suggests that one can have benefit on emissions by tailoring the flow field in a proper way. Specifically, scaling of the combustor for higher heat intensity render the system very complex and make its implementation highly challenging.

The emissions in terms of CO and NO_x are still very low in the whole range of the operative conditions, when both the dilution and the equivalence ratio were varied, considered even lower than 10 ppm, thus performing in single digit in some cases.
Thus, the preliminary experimental campaigns:

- Allowed to verify and to establish how to obtain a stable process by means of the cyclonic configuration.
- It was observed that the downward operational procedure allows to stabilize the oxidation process in a wide range of operating condition
- Permitted to observe very low CO and NO_x emissions in a wide ramnge of operative conditions

Then, further experimental campaigns have been operated in order to verify the performance of LUCY burner and to optimize it in terms of low pollutants emission in the usual working conditions:

- Without external dilution of the mixture
- Without external preheating of the inlet flows

Furthermore, the performance of the cyclonic burner have been evaluated in terms of working temperatures and pollutant emission with respect to mixture equivalence ratio, pre-heating temperature and thermal power.
The downward procedure has been performed from the optimal conditions in preheated inlet Air to the conditions in absence of external preheating. It has been observed that the process, due to the cyclonic configuration, can self-stabilize by means of heat transport phenomena. Thus, the burned gases are able to preheat the inlet flows up to the auto-ignition temperature.
In particular, the first analysis has been performed for C_3H_8/Air mixtures considering a pre-heating temperature equal to the minimum auto-ignition temperature, for different residence times. The analysis suggested that mixtures with an equivalent ratio in the range $0.7 < \Phi < 0.9$ show the best performance in terms of CO and NO_x emissions. Temperatures higher than 1200 K have to be reached to insure fuel full conversion with limited CO emissions for the considered residence times and system size. In particular, for $\Phi > 0.4$ emissions are lower than 100 ppm.
The NO_x emissions show a non-monotonic trend with the equivalence ratio and strongly depend on the working temperatures. In any case analyzed, NO_x emission

were lower than 40 ppm with values lower than 10 ppm when temperatures do not exceed 1300 K.
Following, starting from system burner conditions and $\Phi = 0.8$ (optimal value for the analyzed pre-heated condition), the pre-heating temperature has been diminished, thus moving to not pre-heated condition, to prove the sustainability of the process at environmental temperature. The analysis suggested that the self-stabilization process is sustained by the heat released from the oxidation reactions and transported towards fresh incoming reactants with an efficient heat exchange mechanisms promoted by the cyclonic pattern configuration. The system temperatures slightly diminish to pre-heat the cold gases to the auto-ignition temperature without affecting the CO and NO_x emissions.
Given such results, a further analysis has been carried out to evaluate the optimal equivalence ratio without pre-heating conditions. The results suggested that at $\Phi = 0.85$ the emission of CO and NO_x are minimized.
Under this conditions, it was possible to exploit the maximum thermal power that could be reached considering the size of the burner. The analysis has suggested that up to P = 8 kW the burner can be performed with very low pollutant emissions: CO emissions are compatible with the environmental limits and NO_x are lower than 30 ppm.
The experimental tests suggested that to limit the NO_x emission to single-digit values, the system working temperature should not exceed 1300 K, while to limit CO emission the temperature should be higher than 1200 K when the burner is performed C_3H_8/Air.

Therefore, the cyclonic burner performance without external preheating for different thermal power have been evaluated. Promising values of CO and NO_x have been obtained, confirming the excellent choice of the cyclonic flow-field configuration as a strategy to both stabilize the process and lowering the pollutants emission for the whole range of thermal power explored.

Moreover, the experimental campaigns have been replied in the same conditions even adopting different fuels, in order to verify the expected fuel flexibility of the system. For this purpose, a further analysis has been carried out to value the optimal equivalence ratio without pre-heating conditions when the cyclonic burner was performed with CH_4-Air and Biogas-Air mixtures.
The results suggested that the best operative window to perform the cyclonic burner is at an equivalence ratio $0.7 < \Phi < 0.9$, where the emission of CO and NO_x are minimized independently from the fuel nature.
Under these conditions, it was possible to exploit the maximum thermal power that could be reached considering the size of the burner. The analysis has suggested that up to P = 10 kW the burner can be exercised with CO emissions compatible with the environmental limits and NO_x lower than 30 ppm.

The best results in terms of low pollutant emissions have been obtained performing the cyclonic burner with CH_4, where CO and NO_x emissions are very low in the whole range of P considered. Promising results have been obtained even when the system was operated in Biogas as fuel.
Thus, when operating LUCY burner using CH_4 and Biogas the performance have been resulting very low, confirming the fuel flexibility of the system.

Results suggest that LUCY burner is a promising system for energy production at small scale.
Finally, it is possible to summarize that:

- The cyclonic flow configuration allows to reach MILD combustion conditions
- The stability of the oxidation process has been verified in a wide range of operative conditions
- The cyclonic burner can be operated without external Pre-Heating and without external Dilution
- Remarkable performance in terms of low pollutant emissions (CO, NO_x) have been obtained
- Fuel flexibility has been confirmed for several values of the Thermal Power

REFERENCES

Abtahizadeh, E., van Oijen, J., & de Goey, P. (2012). Numerical study of mild combustion with entrainment of burned gas into oxidizer and/or fuel streams. Combustion and Flame, 159(6), 2155-2165.

Agafonov, G. L., Smirnov, V. N., & Vlasov, P. A. (2011). Shock tube and modeling study of soot formation during the pyrolysis and oxidation of a number of aliphatic and aromatic hydrocarbons. Proceedings of the Combustion Institute, 33(1), 625-632.

Alzueta, M. U., Bilbao, R., Millera, A., Glarborg, P., Østberg, M., & Dam-Johansen, K. (1998). Modeling low-temperature gas reburning. NO x reduction potential and effects of mixing. Energy & Fuels, 12(2), 329-338.

Aminian, J., Galletti, C., Shahhosseini, S., & Tognotti, L. (2012). Numerical investigation of a MILD combustion burner: analysis of mixing field, chemical kinetics and turbulence-chemistry interaction. Flow, turbulence and combustion, 88(4), 597-623.

Arghode, V. K., & Gupta, A. K. (2010). Effect of flow field for colorless distributed combustion (CDC) for gas turbine combustion. Applied Energy, 87(5), 1631-1640.

Arghode, V. K., & Gupta, A. K. (2011). Development of high intensity CDC combustor for gas turbine engines. Applied Energy, 88(3), 963-973.

Arghode, V. K., & Gupta, A. K. (2013). Role of thermal intensity on operational characteristics of ultra-low emission colorless distributed combustion. Applied energy, 111, 930-956.

Arghode, V. K., Gupta, A. K., & Bryden, K. M. (2012). High intensity colorless distributed combustion for ultra low emissions and enhanced performance. Applied energy, 92, 822-830.

Arrieta, C. E., & Amell, A. A. (2014). Highly flexible burner concept for research on combustion technologies with recirculation of hot combustion products. Applied Thermal Engineering, 63(2), 559-564.

Baukal, C.E., Schwartz, R.E. (2001) The John Zink Combustion Handbook. Tulsa: CRC Press.

Baukal, C.E. (Ed.). (2010). Industrial combustion testing. CRC Press.

Beer, J. M., & Lee, K. B. (1965). The effect of the residence time distribution on the performance and efficiency of combustors. In Symposium (International) on Combustion (Vol. 10, No. 1, pp. 1187-1202). Elsevier.

Bianchi, M., De Pascale, A., & Spina, P. R. (2012). Guidelines for residential micro-CHP systems design. Applied Energy, 97, 673-685.

Bobba, M. K., Gopalakrishnan, P., Periagaram, K., & Seitzman, J. M. (2008). Flame structure and stabilization mechanisms in a stagnation-point reverse-flow combustor. Journal of Engineering for Gas Turbines and Power, 130(3), 031505.

Bolshova, T. A., Bunev, V. A., Knyazkov, D. A., Korobeinichev, O. P., Chernov, A. A., Shmakov, A. G., & Yakimov, S. A. (2012). Dependence of the lower flammability limit on the initial temperature. Combustion, Explosion, and Shock Waves, 48(2), 125-129.

Bolz, S., & Gupta, A. K. (1998). Effect of air preheat temperature and oxygen concentration on flame structure and emission. Univ. of Maryland, College Park, MD (US).

Bowman, C. T. (1992, January). Control of combustion-generated nitrogen oxide emissions: technology driven by regulation. In Symposium (International) on Combustion (Vol. 24, No. 1, pp. 859-878). Elsevier.

Bykov, V., & Maas, U. (2007). The extension of the ILDM concept to reaction–diffusion manifolds. Combustion Theory and Modelling, 11(6), 839-862.

Cao, S., Zou, C., Han, Q., Liu, Y., Wu, D., & Zheng, C. (2015). Numerical and experimental studies of NO formation mechanisms under methane moderate or intense low-oxygen dilution (MILD) combustion without heated air. Energy & Fuels, 29(3), 1987-1996.

Cavaliere, A., & de Joannon, M. (2000). Detailed chemical kinetics in the reactor design for diluted high temperature combustion of air/paraffin mixtures. In Crest—

Third International Symposium on High Temperature Air Combustion and Gasification, Yokohama, Japan.

Cavaliere, A., & de Joannon, M. (2004). Mild combustion. Progress in Energy and Combustion science, 30(4), 329-366.

Cavigiolo, A., Galbiati, M. A., Effuggi, A., Gelosa, D., & Rota, R. (2003). Mild combustion in a laboratory-scale apparatus. Combustion Science and Technology, 175(8), 1347-1367.

Christo, F. C., & Dally, B. B. (2005). Modeling turbulent reacting jets issuing into a hot and diluted coflow. Combustion and flame, 142(1-2), 117-129.

Coelho, P. J., & Peters, N. (2001). Numerical simulation of a mild combustion burner. Combustion and flame, 124(3), 503-518.

Colorado, A. F., Herrera, B. A., & Amell, A. A. (2010). Performance of a flameless combustion furnace using biogas and natural gas. Bioresource Technology, 101(7), 2443-2449.

Coriton, B., Frank, J. H., & Gomez, A. (2013). Effects of strain rate, turbulence, reactant stoichiometry and heat losses on the interaction of turbulent premixed flames with stoichiometric counterflowing combustion products. Combustion and Flame, 160(11), 2442-2456.

Cresci, E., & Milani, (2012) A recent developments and applications of flameless oxidation, IRFR report, available at http://www.flox.com/documents/09%20IFRF2012.pdf

Dally, B. B., Karpetis, A. N., & Barlow, R. S. (2002). Structure of turbulent non-premixed jet flames in a diluted hot coflow. Proceedings of the combustion institute, 29(1), 1147-1154.

Dally, B. B., Riesmeier, E., & Peters, N. (2004). Effect of fuel mixture on moderate and intense low oxygen dilution combustion. Combustion and flame, 137(4), 418-431.

de Azevedo, C. G., de Andrade, J. C., & de Souza Costa, F. (2015). Flameless compact combustion system for burning hydrous ethanol. Energy, 89, 158-167.

de Joannon, M., Cavaliere, A., Faravelli, T., Ranzi, E., Sabia, P., & Tregrossi, A. (2005). Analysis of process parameters for steady operations in methane mild combustion technology. Proceedings of the Combustion Institute, 30(2), 2605-2612.

de Joannon, M., Langella, G., Beretta, F., Cavaliere, A., & Noviello, C. (2000). Mild combustion: Process features and technological constrains. Combustion science and technology, 153(1), 33-50.

de Joannon, M., Sabia, P., Sorrentino, G., Bozza, P., & Ragucci, R. (2017). Small size burner combustion stabilization by means of strong cyclonic recirculation. Proceedings of the Combustion Institute, 36(3), 3361-3369.

de Joannon, M., Sabia, P., Tregrossi, A., & Cavaliere, A. (2004). Dynamic behavior of methane oxidation in premixed flow reactor. Combustion science and technology, 176(5-6), 769-783.

de Joannon, M., Sorrentino, G., & Cavaliere, A. (2012). MILD combustion in diffusion-controlled regimes of hot diluted fuel. Combustion and Flame, 159(5), 1832-1839.

de Swart, J. A., Bastiaans, R. J., van Oijen, J. A., de Goey, L. P. H., & Cant, R. S. (2010). Inclusion of preferential diffusion in simulations of premixed combustion of hydrogen/methane mixtures with flamelet generated manifolds. Flow, turbulence and combustion, 85(3), 473-511.

Derudi, M., Villani, A., & Rota, R. (2007). Mild combustion of industrial hydrogen-containing byproducts. Industrial & Engineering Chemistry Research, 46(21), 6806-6811.

Derudi, M., Villani, A., & Rota, R. (2007). Sustainability of mild combustion of hydrogen-containing hybrid fuels. Proceedings of the Combustion Institute, 31(2), 3393-3400.

Doost, A. S., Ries, F., Becker, L. G., Bürkle, S., Wagner, S., Ebert, V., Dreizler, A., di Mare, F., Sadiki, A., & Janicka, J. (2016). Residence time calculations for complex swirling flow in a combustion chamber using large-eddy simulations. Chemical Engineering Science, 156, 97-114.

Duan, F., Liu, J., Chyang, C. S., Hu, C. H., & Tso, J. (2013). Combustion behavior and pollutant emission characteristics of RDF (refuse derived fuel) and sawdust in a vortexing fluidized bed combustor. Energy, 57, 421-426.

Dunn-Rankin, D. (Ed.). (2011). Lean combustion: technology and control. Academic Press.

Duwig, C., Li, B., Li, Z. S., & Aldén, M. (2012). High resolution imaging of flameless and distributed turbulent combustion. Combustion and Flame, 159(1), 306-316.

Duwig, C., Stankovic, D., Fuchs, L., Li, G., & Gutmark, E. (2007). Experimental and numerical study of flameless combustion in a model gas turbine combustor. Combustion Science and Technology, 180(2), 279-295.

Effuggi, A., Gelosa, D., Derudi, M., & Rota, R. (2008). Mild combustion of methane-derived fuel mixtures: natural gas and biogas. Combustion Science and Technology, 180(3), 481-493.

Flamme, M., & Kremer, H. (1991). NOx output from industrial burners using preheated air and NOx control techniques. Gas, Wärme international, 40(11), 502-506.

Galletti, C., Parente, A., & Tognotti, L. (2007). Numerical and experimental investigation of a mild combustion burner. Combustion and flame, 151(4), 649-664.

Galletti, C., Parente, A., Derudi, M., Rota, R., & Tognotti, L. (2009). Numerical and experimental analysis of NO emissions from a lab-scale burner fed with hydrogen-enriched fuels and operating in MILD combustion. International journal of hydrogen energy, 34(19), 8339-8351.

Gaydon, A. G., Moore, N. P. W., & Simonson, J. R. (1955). Chemical and spectroscopic studies of blue flames in the auto-ignition of methane. Proceedings of the Royal Society of London. Series A, Mathematical and Physical Sciences, 1-19.

Gicquel, O., Darabiha, N., & Thévenin, D. (2000). Liminar premixed hydrogen/air counterflow flame simulations using flame prolongation of ILDM with differential diffusion. Proceedings of the Combustion Institute, 28(2), 1901-1908.

Gupta, A. K. (2000). Flame characteristics and challenges with high temperature air combustion. In Proceedings of the International Joint Power Generation Conference (pp. 23-26).

Gupta, A. K. (2004). Thermal characteristics of gaseous fuel flames using high temperature air. Transactions-American Society of Mechanical Engineers Journal of Engineering for Gas Turbines and Power, 126(1), 9-19.

Gupta, A. K., Lilley, D. G., & Syred, N. (1984). Swirl flows. Tunbridge Wells, Kent, England, Abacus Press, 1984, 488 p.

Hardesty, D. R., & Weinberg, F. J. (1973). Burners producing large excess enthalpies. Combustion Science and Technology, 8(5-6), 201-214.

Hasan, A. E. E. K. (2013). Investigation of Colorless Distributed Combustion (CDC) with Swirl for Gas Turbine Application (Doctoral dissertation, University of Maryland, College Park).

Haworth, D. C. (2010). Progress in probability density function methods for turbulent reacting flows. Progress in Energy and Combustion Science, 36(2), 168-259.

He, Y. (2008). Flameless combustion of natural gas in the SJ/WJ furnace (Doctoral dissertation).

He, Y., Zou, C., Song, Y., Liu, Y., & Zheng, C. (2016). Numerical study of characteristics on NO formation in methane MILD combustion with simultaneously hot and diluted oxidant and fuel (HDO/HDF). Energy, 112, 1024-1035.

Herout, M., Malatak, J., Kucera, L., & Dlabaja, T. (2011). Biogas composition depending on the type of plant biomass used. Res. Agric. Eng, 57(4), 137.

Hosseini S. E., Bagheri G., Khaleghi M., & Wahid M. A. (2015). Study on the characteristics of hydrogen-enriched biogas co-flow flameless combustion, Recent Advantages in Mechanics and Mechanical Engineering.

Hosseini, S. E., & Wahid, M. A. (2014). Development of biogas combustion in combined heat and power generation. Renewable and Sustainable Energy Reviews, 40, 868-875.

Hsu, K. Y., Goss, L. P., & Roquemore, W. M. (1998). Characteristics of a trapped-vortex combustor. Journal of Propulsion and Power,14(1), 57-65.

Ihme, M., & See, Y. C. (2011). LES flamelet modeling of a three-stream MILD combustor: Analysis of flame sensitivity to scalar inflow conditions. Proceedings of the Combustion Institute, 33(1), 1309-1317.

Ihme, M., Cha, C. M., & Pitsch, H. (2005). Prediction of local extinction and re-ignition effects in non-premixed turbulent combustion using a flamelet/progress variable approach. Proceedings of the Combustion Institute, 30(1), 793-800.

Isaac, B. J., Parente, A., Galletti, C., Thornock, J. N., Smith, P. J., & Tognotti, L. (2013). A novel methodology for chemical time scale evaluation with detailed chemical reaction kinetics. Energy & fuels, 27(4), 2255-2265.

Jones, R., Goldmeer, J., & Monetti, B. (2011). Addressing Gas Turbine Fuel Flexibility. GE Energy Report GER4601 rev. B, October, 29, 2012.

Katsuki, M., & Hasegawa, T. (1998, January). The science and technology of combustion in highly preheated air. In Symposium (International) on combustion (Vol. 27, No. 2, pp. 3135-3146). Elsevier.

Khalil, A. E., & Gupta, A. K. (2011). Distributed swirl combustion for gas turbine application. Applied energy, 88(12), 4898-4907.

Khalil, A. E., & Gupta, A. K. (2015). Impact of internal entrainment on high intensity distributed combustion. Applied Energy, 156, 241-250.

Khalil, A. E., & Gupta, A. K. (2015). Toward ultra-low emission distributed combustion with fuel air dilution. Applied Energy, 148, 187-195.

Khidr, K. I., Eldrainy, Y. A., & EL-Kassaby, M. M. (2017). Towards lower gas turbine emissions: Flameless distributed combustion. Renewable and Sustainable Energy Reviews, 67, 1237-1266.

Khosravy el_Hossaini, M. (2013). Review of the new combustion technologies in modern gas turbines. In Progress in Gas Turbine Performance. InTech.

Krishnamurthy, N., Paul, P. J., & Blasiak, W. (2009). Studies on low-intensity oxy-fuel burner. Proceedings of the Combustion Institute, 32(2), 3139-3146.

Kruse, S., Kerschgens, B., Berger, L., Varea, E., & Pitsch, H. (2015). Experimental and numerical study of MILD combustion for gas turbine applications. Applied Energy, 148, 456-465.

Kumar, S., Paul, P. J., & Mukunda, H. S. (2002). Studies on a new high-intensity low-emission burner. Proceedings of the combustion institute, 29(1), 1131-1137.

Kumar, S., Paul, P. J., & Mukunda, H. S. (2005). Investigations of the scaling criteria for a mild combustion burner. Proceedings of the combustion institute, 30(2), 2613-2621.

Kwiatkowski, K., & Mastorakos, E. (2016). Regimes of Nonpremixed Combustion of Hot Low-Calorific-Value Gases Derived from Biomass Gasification. Energy & Fuels, 30(6), 4386-4397.

Lammel, O., Schütz, H., Schmitz, G., Lückerath, R., Stöhr, M., Noll, B., Aigner, M., Hase, & Krebs, W. (2010). FLOX® combustion at high power density and high flame temperatures. Journal of Engineering for Gas Turbines and Power, 132(12), 121503.

Lamouroux, J., Ihme, M., Fiorina, B., & Gicquel, O. (2014). Tabulated chemistry approach for diluted combustion regimes with internal recirculation and heat losses. Combustion and flame, 161(8), 2120-2136.

Li, P., Mi, J., Dally, B. B., Wang, F., Wang, L., Liu, Z., Chen, S., & Zheng, C. (2011). Progress and recent trend in MILD combustion. Science China Technological Sciences, 54(2), 255-269.

Li, P., Wang, F., Mi, J., Dally, B. B., & Mei, Z. (2014). MILD combustion under different premixing patterns and characteristics of the reaction regime. Energy & Fuels, 28(3), 2211-2226.

Lückerath, R., Meier, W., & Aigner, M. (2008). FLOX® combustion at high pressure with different fuel compositions. Journal of Engineering for Gas Turbines and Power, 130(1), 011505.

Magnussen, B. F., & Hjertager, B. W. (1981). On the structure of turbulence and a generalized eddy dissipation concept for chemical reaction in turbulent flow. In 19th AIAA aerospace meeting, St. Louis, USA (Vol. 198, No. 1).

Maraver, D., Sin, A., Royo, J., & Sebastián, F. (2013). Assessment of CCHP systems based on biomass combustion for small-scale applications through a review of the technology and analysis of energy efficiency parameters. Applied energy, 102, 1303-1313.

Masunaga, A. (2001). Application of regenerative burner for forging furnace. In Proceedings of the Forum on High-Temperature Air Combustion Technology (p. 109).

Medwell, P. R., Kalt, P. A., & Dally, B. B. (2007). Simultaneous imaging of OH, formaldehyde, and temperature of turbulent nonpremixed jet flames in a heated and diluted coflow. Combustion and Flame, 148(1), 48-61.

Melo, M. J., Sousa, J. M. M., Costa, M., & Levy, Y. (2009). Experimental investigation of a novel combustor model for gas turbines. Journal of Propulsion and Power, 25(3), 609.

Mi, J., Li, P., Dally, B. B., & Craig, R. A. (2009). Importance of initial momentum rate and air-fuel premixing on moderate or intense low oxygen dilution (MILD) combustion in a recuperative furnace. Energy & Fuels, 23(11), 5349-5356.

Milani, A., & Saponaro, A. (2001). Diluted combustion technologies. IFRF Combustion Journal, 1, 1-32.

Minamoto, Y., & Swaminathan, N. (2015). Subgrid scale modelling for MILD combustion. Proceedings of the Combustion Institute, 35(3), 3529-3536.

Oldenhof, E., Tummers, M. J., Van Veen, E. H., & Roekaerts, D. J. E. M. (2011). Role of entrainment in the stabilisation of jet-in-hot-coflow flames. Combustion and Flame, 158(8), 1553-1563.

Orsino, S., Weber, R., & Bollettini, U. (2001). Numerical simulation of combustion of natural gas with high-temperature air. Combustion Science and Technology, 170(1), 1-34.

Özdemir, I. B., & Peters, N. (2001). Characteristics of the reaction zone in a combustor operating at mild combustion. Experiments in Fluids, 30(6), 683-695.

Parente, A., Galletti, C., & Tognotti, L. (2008). Effect of the combustion model and kinetic mechanism on the MILD combustion in an industrial burner fed with

hydrogen enriched fuels. International Journal of Hydrogen Energy, 33(24), 7553-7564.

Parente, A., Galletti, C., & Tognotti, L. (2011). A simplified approach for predicting NO formation in MILD combustion of CH 4–H 2 mixtures. Proceedings of the Combustion Institute, 33(2), 3343-3350.

Parente, A., Galletti, C., Riccardi, J., Schiavetti, M., & Tognotti, L. (2012). Experimental and numerical investigation of a micro-CHP flameless unit. Applied energy, 89(1), 203-214.

Parente, A., Sutherland, J. C., Dally, B. B., Tognotti, L., & Smith, P. J. (2011). Investigation of the MILD combustion regime via principal component analysis. Proceedings of the Combustion Institute, 33(2), 3333-3341.

Peters, N. (1984). Laminar diffusion flamelet models in non-premixed turbulent combustion. Progress in energy and combustion science, 10(3), 319-339.

Pilavachi, P. A. (2002). Mini-and micro-gas turbines for combined heat and power. Applied thermal engineering, 22(18), 2003-2014.

Plessing, T., Peters, N., & Wünning, J. G. (1998). Laseroptical investigation of highly preheated combustion with strong exhaust gas recirculation. In Symposium (International) on Combustion (Vol. 27, No. 2, pp. 3197-3204). Elsevier.

Pope, S. B. (1985). PDF methods for turbulent reactive flows. Progress in Energy and Combustion Science, 11(2), 119-192.

Rafidi, N., & Blasiak, W. (2006). Heat transfer characteristics of HiTAC heating furnace using regenerative burners. Applied Thermal Engineering, 26(16), 2027-2034.

Ranzi, E., Frassoldati, A., Grana, R., Cuoci, A., Faravelli, T., Kelley, A. P., & Law, C. K. (2012). Hierarchical and comparative kinetic modeling of laminar flame speeds of hydrocarbon and oxygenated fuels. Progress in Energy and Combustion Science, 38(4), 468-501.

Rasi, S., Veijanen, A., & Rintala, J. (2007). Trace compounds of biogas from different biogas production plants. Energy, 32(8), 1375-1380.

Rebola, A., Costa, M., & Coelho, P. J. (2013). Experimental evaluation of the performance of a flameless combustor. Applied Thermal Engineering, 50(1), 805-815.

Reddy, V. M., Sawant, D., Trivedi, D., & Kumar, S. (2013). Studies on a liquid fuel based two stage flameless combustor. Proceedings of the Combustion Institute, 34(2), 3319-3326.

Rosato, A., Sibilio, S., & Ciampi, G. (2013). Energy, environmental and economic dynamic performance assessment of different micro-cogeneration systems in a residential application. Applied Thermal Engineering, 59(1), 599-617.

Rottier, C., Lacour, C., Godard, G., Taupin, B., Porcheron, L., Hauguel, R., Carpentier S., Boukhalfa A. M., & Honoré, D. (2009). On the effect of air temperature on mild flameless combustion regime of high temperature furnace. In Proceedings of the European Combustion Meeting. Wien, Austria.

Rupley, F.M., Kee, R.J., Miller, J.A., Coltrin, M.E., Grcar, J.F., Meeks, E., Moffat, H.K., Lutz, A.E., Dixon-Lewis, G., Smooke, M.D., Warnatz, J., Evans, G.H., Larson, R.S., Mitchell, R.E., Petzold, L.R., Reynolds, W.C., Caracotsios, M., Stewart, W.E., Glarborg, P., Wang, C., Adigun, O., Houf, W.G., Chou, C.P., Miller, S.F. (2003). Reaction Design, San Diego

Sabia, P., de Joannon, M., Lavadera, M. L., Giudicianni, P., & Ragucci, R. (2014). Autoignition delay times of propane mixtures under MILD conditions at atmospheric pressure. Combustion and flame, 161(12), 3022-3030.

Sabia, P., de Joannon, M., Picarelli, A., & Ragucci, R. (2013). Methane auto-ignition delay times and oxidation regimes in MILD combustion at atmospheric pressure. Combustion and Flame, 160(1), 47-55.

Sabia, P., de Joannon, M., Sorrentino, G., Giudicianni, P., & Ragucci, R. (2015). Effects of mixture composition, dilution level and pressure on auto-ignition delay times of propane mixtures. Chemical Engineering Journal, 277, 324-333.

Sabia, P., Lavadera, M. L., Giudicianni, P., Sorrentino, G., Ragucci, R., & de Joannon, M. (2015). CO2 and H2O effect on propane auto-ignition delay times under mild combustion operative conditions. Combustion and flame, 162(3), 533-543.

Sabia, P., Sorrentino, G., Chinnici, A., Cavaliere, A., & Ragucci, R. (2015). Dynamic behaviors in methane MILD and oxy-fuel combustion. Chemical effect of CO2. Energy & Fuels, 29(3), 1978-1986.

Saponaro A. Combustion & Environment Research Centre - Ansaldo Caldaie, 2009.

Sato J. Combustion in High Temperature Air, 1997, p. 286-289

Shimo, N. (2000). Fundamental research of oil combustion with highly preheated air. In Proceedings of the 2nd International Seminar on High Temperature Combustion in Industrial Furnaces.

Shuman, T. R. (2000). NOx and CO formation for lean-premixed methane-air combustion in a jet-stirred reactor operated at elevated pressure (Doctoral dissertation, University of Washington).

Sidey, J., Mastorakos, E., & Gordon, R. L. (2014). Simulations of autoignition and laminar premixed flames in methane/air mixtures diluted with hot products. Combustion Science and Technology, 186(4-5), 453-465.

Sobiesiak, A., Rahbar, S., & Becker, H. A. (1998). Performance characteristics of the novel low-NO x CGRI burner for use with high air preheat. Combustion and flame, 115(1), 93-125.

Sorrentino, G., Sabia, P., Bozza, P., Ragucci, R., & de Joannon, M. (2017). Impact of external operating parameters on the performance of a cyclonic burner with high level of internal recirculation under MILD Combustion conditions. Energy.

Sorrentino, G., Sabia, P., de Joannon, M., Cavaliere, A., & Ragucci, R. (2015). Design and Development of a Lab-Scale Burner for MILD/Flameless Combustion. Chemical engineering transactions, 43.

Sorrentino, G., Sabia, P., de Joannon, M., Cavaliere, A., & Ragucci, R. (2016). The effect of diluent on the sustainability of MILD combustion in a cyclonic burner. Flow, Turbulence and Combustion, 96(2), 449-468.

Sorrentino, G., Sabia, P., de Joannon, M., Ragucci, R., Cavaliere, A., Göktolga, U., van Oijen, J., & de Goey, P. (2015). Development of a novel cyclonic flow combustion chamber for achieving MILD/flameless combustion. Energy Procedia, 66, 141-144.

Sorrentino, G., Scarpa, D., & Cavaliere, A. (2013). Transient inception of MILD combustion in hot diluted diffusion ignition (HDDI) regime: A numerical study. Proceedings of the Combustion Institute, 34(2), 3239-3247.

Stadler, H., Toporov, D., Förster, M., & Kneer, R. (2009). On the influence of the char gasification reactions on NO formation in flameless coal combustion. Combustion and Flame, 156(9), 1755-1763.

Straub, D. L., Casleton, K. H., Lewis, R. E., Sidwell, T. G., Maloney, D. J., & Richards, G. A. (2005). Assessment of rich-burn, quick-mix, lean-burn trapped vortex combustor for stationary gas turbines.Journal of engineering for gas turbines and power, 127(1), 36-41.

Szegö, G. G., Dally, B. B., & Nathan, G. J. (2009). Operational characteristics of a parallel jet MILD combustion burner system.Combustion and Flame, 156(2), 429-438.

Tsuji, H., Gupta, A. K., Hasegawa, T., Katsuki, M., Kishimoto, K., & Morita, M. (2002). High temperature air combustion: from energy conservation to pollution reduction. CRC press.

Turns, S. R. (1995). Understanding NOx formation in nonpremixed flames: experiments and modeling. Progress in Energy and Combustion Science, 21(5), 361-385.

Van Der Lans, R. P., Glarborg, P., Dam-Johansen, K., & Larsen, P. S. (1997). Residence time distributions in a cold, confined swirl flow: implications for chemical engineering combustion modelling. Chemical engineering science, 52(16), 2743-2756.

van Oijen, J. A. (2013). Direct numerical simulation of autoigniting mixing layers in MILD combustion. Proceedings of the Combustion Institute, 34(1), 1163-1171.

van Oijen, J., & Goey, L. D. (2000). Modelling of premixed laminar flames using flamelet-generated manifolds. Combustion Science and Technology, 161(1), 113-137.

Vandervort, C. L. (2001). 9 ppm NOx/CO combustion system for F class industrial gas turbines. Transactions of the ASME-A-Engineering for Gas Turbines and Power, 123(2), 317-321.

Veríssimo, A. S., Rocha, A. M. A., & Costa, M. (2011). Operational, combustion, and emission characteristics of a small-scale combustor. Energy & Fuels, 25(6), 2469-2480.

Veríssimo, A. S., Rocha, A. M. A., & Costa, M. (2013). Experimental study on the influence of the thermal input on the reaction zone under flameless oxidation conditions. Fuel processing technology, 106, 423-428.

Veríssimo, A. S., Rocha, A. M. A., & Costa, M. (2013). Importance of the inlet air velocity on the establishment of flameless combustion in a laboratory combustor. Experimental thermal and fluid science, 44, 75-81.

Vondál, J., & Hájek, J. (2012). Swirling flow prediction in model combustor with axial guide vane swirler. Chemical Engineering, 29(2), 1069-1074.

Wang, F., Li, P., Mei, Z., Zhang, J., & Mi, J. (2014). Combustion of CH4/O2/N2 in a well stirred reactor. Energy, 72, 242-253.

Wang, F., Mi, J., & Li, P. (2013). Combustion regimes of a jet diffusion flame in hot co-flow. Energy & Fuels, 27(6), 3488-3498.

Weber, R., Orsino, S., Lallemant, N., & Verlaan, A. D. (2000). Combustion of natural gas with high-temperature air and large quantities of flue gas. Proceedings of the Combustion Institute, 28(1), 1315-1321.

Weber, R., Smart, J. P., & vd Kamp, W. (2005). On the (MILD) combustion of gaseous, liquid, and solid fuels in high temperature preheated air. Proceedings of the Combustion Institute, 30(2), 2623-2629.

Weinberg, F. J. (1971). Combustion temperatures: the future?. Nature, 233(5317), 239-241.

Weinberg, F. J. (1986). Combustion in heat recirculating burners, Chap. 3 in Advanced Combustion Methods, F. Academic Press, London.

Wu, S. R., Chang, W. C., & Chiao, J. (2007). Low NOx heavy fuel oil combustion with high temperature air. Fuel, 86(5), 820-828.

Wünning, J. A., & Wünning, J. G. (1997). Flameless oxidation to reduce thermal NO-formation. Progress in energy and combustion science, 23(1), 81-94.

Wünning, J. G., & Milani, A. (2012). Handbook of Burner Technologies for Industrial Furnaces: Fundamentals-Burner Technologies-Applications. Oldenbourg Industrieverlag.

Xing, X. J., Wang, B., & Lin, Q. (2007). Structure of reaction zone of normal temperature air flameless combustion in a 2 ton/h coal-fired boiler furnace. Proceedings of the Institution of Mechanical Engineers, Part A: Journal of Power and Energy, 221(4), 473-480.

Yasuda, T. (1999, January). Dissemination project of high performance industrial furnace with use of high temperature air combustion technology. In Proc of Second International High Temperature Air Combustion Symposium, Taiwan (p. B3).

Yetter, R. A., Glassman, I., & Gabler, H. C. (2000). Asymmetric whirl combustion: a new low NOx approach. Proceedings of the combustion institute, 28(1), 1265-1272.

Yoshikawa, K. (2000, March). Recent progress and future prospect of the CREST MEET Project. In Crest—Third International Symposium on High Temperature Air Combustion and Gasification, Yokohama, Japan A (Vol. 1).

Yu, Y., Gaofeng, W., Qizhao, L., Chengbiao, M., & Xianjun, X. (2010). Flameless combustion for hydrogen containing fuels. international journal of hydrogen energy, 35(7), 2694-2697.

Zabetakis, M. G. (1965). Flammability characteristics of combustible gases and vapors (No. BULL-627). Bureau of Mines Washington DC.

Zarnescu, V., & Pisupati, S. V. (2001). The effect of mixing model and mixing characteristics on NO x reduction during reburning. Energy & fuels, 15(2), 363-371.

Zhang, C., Ishii, T., Hino, Y., & Sugiyama, S. (2000). The numerical and experimental study of non-premixed combustion flames in regenerative furnaces. TRANSACTIONS-AMERICAN SOCIETY OF MECHANICAL ENGINEERS JOURNAL OF HEAT TRANSFER, 122(2), 287-293.

Zhang, H., Yue, G., Lu, J., Jia, Z., Mao, J., Fujimori, T., Toshiyuki, S., & Kiga, T. (2007). Development of high temperature air combustion technology in pulverized fossil fuel fired boilers. Proceedings of the Combustion Institute, 31(2), 2779-2785.

Zhou, J., Adrian, R. J., Balachandar, S., & Kendall, T. M. (1999). Mechanisms for generating coherent packets of hairpin vortices in channel flow. Journal of fluid mechanics, 387, 353-396.